

Optical Properties and Photochemical Response of Colored Dissolved Organic Matter (CDOM) at Jobos Bay National Estuarine Research Reserve (JOBANERR),

Puerto Rico

by

Suhey Ortiz Rosa

A thesis submitted in fulfillment of the requirements for the degree of
MASTER OF SCIENCE
in

MARINE SCIENCES
(Chemical Oceanography)

UNIVERSITY OF PUERTO RICO
MAYAGÜEZ CAMPUS
2010

Approved by:

Julio Morell, M.S.
Member, Graduate Committee

Date

José M. López, Ph.D.
Member, Graduate Committee

Date

Jorge E. Corredor, Ph.D.
President, Graduate Committee

Date

Kurt Gove, Ph.D.
Representative of Graduate Studies

Date

Nilda E. Aponte, Ph.D.
Chairperson of the Department

Date

COPYRIGHT

In presenting this dissertation in partial fulfillment of the requirements for a Master in Marine Sciences degree at the University of Puerto Rico, I agree that the library shall make its copies freely available for inspection. I therefore authorize the Library of the University of Puerto Rico at Mayagüez to copy my MS Thesis totally or partially. Each copy must include the title page. I further agree that extensive copying of this dissertation is allowable only for scholarly purposes. It is understood, however, that any copying or publication of this dissertation for commercial purposes, or for financial gain, shall not be allowed without my written permission.

Signed: Suhey Ortiz Rosa

Date: December 17, 2010

ABSTRACT

The study evaluated the optical properties and dynamics of CDOM in JOBANERR. CDOM absorption coefficient spectrum (a_{CDOM}), Slope (S), excitation emission matrix (EEM) fluorescence and Parallel Factor Analysis (PARAFAC) were used to characterize sources of CDOM. S values varied from 0.014–0.034 nm^{-1} and a_{CDOM} ranged from 0.11 m^{-1} to 11 m^{-1} . Mar Negro presented a strong terrestrial source of CDOM while Mar Blanco is a transitional area combining terrestrial and marine CDOM sources. Barca presented a strong marine source and it is influenced by terrestrial sources in wet months. Spatial differences were observed between mangrove semi-enclosed areas and open areas of the bay. Significant differences were found on DOC, salinity and slope parameters seasonally between the study sites. Dissolved Organic Carbon (DOC), a_{CDOM} and fluorescence intensity of the main fluorophores (C, M, A, H) were related to salinity, chlorophyll, and UV dose. DOC and a_{CDOM} presented a low correlation ($R^2 = 0.16$). UV dose correlated with a_{CDOM} (Pearson coefficient = -0.98) in an exponential decay. Chlorophyll correlated with a_{CDOM} (Pearson coefficient = 0.73). PARAFAC showed seven components in samples exposed to sunlight described as humic-like, protein-like, degradation or microbial substances. Two principal processes transform CDOM: photodegradation and dilution. The high variability of CDOM signatures in Jobos waters are explained by chemical transformations of CDOM.

RESUMEN

Se estudiaron las propiedades ópticas y la dinámica de MODC en JOBANERR. La caracterización de MODC se realizó por análisis de absorción (a_{MODC}) y pendiente (S) espectral, fluorescencia por matrices de Excitación-Emisión (EEM) y Análisis “Parallel Factor” (PARAFAC por sus siglas en ingles). Los valores de S varían de 0.014-0.034 nm^{-1} y a_{MODC} de 0.11 m^{-1} a 11 m^{-1} . Mar Negro presentó una señal fuerte de MODC terrestre, Mar Blanco presentó señales terrestres y marinas y Barca una señal marina influenciada por fuentes terrestres durante periodos de lluvia. Diferencias espaciales y temporales entre las áreas de manglar y las aguas fuera de la bahía fueron determinadas. Medidas de carbono orgánico disuelto (DOC), a_{MODC} , y la intensidad de fluorescencia de los fluoróforos principales (C, M, A, H) fueron relacionadas con medidas de salinidad, clorofila y dosis de luz UV. DOC and a_{CDOM} presentaron una correlación positiva baja ($R^2 = 0.16$). Se observó una correlación significativa entre UV y a_{MODC} la cual mostró decaimiento exponencial (Coeficiente Pearson = -0.98). La clorofila presentó una correlación positiva con a_{CDOM} (Coeficiente Pearson = 0.73). A través de PARAFAC, siete componentes se identificaron en las muestras expuestas a la luz. Estos se encuentran representados por material húmico, proteínas, materia derivada de la degradación microbiana y productos de fotólisis. La alta variabilidad en las señales de MODC en JOBANERR puede ser explicada principalmente por fotodegradación, con una influencia menor por dilución.

Dedicada a mis padres que con su apoyo, ayuda y esfuerzo me han acompañado, dirigido y motivado a cultivar mi pasión por el mar.

Dedicada a Kai Bajari por ser mi norte y fortaleza de vida.

A ellos que siempre están presentes.

ACKNOWLEDGMENTS

This research was conducted in the National Estuarine Research Reserve System under award no. NA07NOS4200049 from the Estuarine Reserves Division, Office of Ocean and Coastal Resource Management, NOAA.

I would like to express my gratitude for all the support received from the people who in way one or another made possible this project.

- I would like to express my gratitude to my advisor Dr. Corredor for the help, support, guidance and patience.
- To Professor Morell for comments and suggestions to complete the study.
- To Dr. López for the support and guidance.
- This work would not be possible without the advice, discussions and support from Dr. Ramón López, for his technical and field assistance, motivation, friendship and helpfully comments trough this study.
- Ángel Dieppa for field and research logistic.
- Dr. Youhei Yamashita for training on EEM's and PARAFAC and helpfully comments in photodegradation and fluorescence analysis.
- Dr. Rudolf Jaffe for laboratory facilities and equipment at FIU to fluorescence analysis and helpfully comments in fluorescence and photodegradation manuscript.
- Dr. Roy Armstrong and Dr. Yasmín Detrés for bio-optics laboratory facilities and equipment to photodegradation experiments.
- Juan González and Carlos Anselmi for technical support and training on Matlab Software and Damian Osorio for technical support.
- Dr. Jorge Ortiz for DOC and TDN lab equipment.
- Dr. Meléndez for fluorescence spectrophotometer.
- José Vera for fluorescence training.
- Val Hensley for CDOM and NH_4^+ analysis training.
- Don Claudio for field support.
- Mariano Solórzano for GIS maps and graphs assistance.
- Rafael Benítez for DOC and TDN analyses, statistical analyses, motivation, and technical support.
- Thanks to Brenda, Carmen, Chino, Daniel, Koralys, Juan, Carlos, Belitza, Rosa Linda, Ori, Yari, Brandy, Kat, Stacy, Katie, Ramón, Marla, Milton, Dihalia, Mónica, Ivone, Diana, Santos, Melissa, Duane and Héctor for share their lives with me and Kai into Magueyes journey.
- Thanks to Magueyes Island personnel especially to Vitamina, Godo, Negrito, Lili and Zulma, Taty, Nan and Marcos.
- Thanks to Dr. Sherman and Dr. Otero for the research assitanships.
- To Dr. Ernesto Otero for laboratory facilities.
- Specially thanks to Brenda, Chino, Carmen, Dannisse, Alex, and Daniel for unconditional support.
- To my friends and family that support me with love.

Table of Contents

COPYRIGHT	II
ABSTRACT	III
RESUMEN	IV
ACKNOWLEDGMENTS	VI
TABLE OF CONTENTS	VIII
LIST OF TABLES	X
LIST OF FIGURES	XI
LIST OF APPENDIXES	XIII
INTRODUCTION	1
MATERIALS AND METHODS	5
Site Description	5
Samples Collection	8
Optical CDOM Characterization	8
Absorption Spectroscopy	9
Fluorescence spectroscopy.....	9
Photodegradation Experiment.....	10
Salinity, DOC and Chlorophyll	13
Ammonium (NH₄⁺)	13
Statistical Analysis	14
RESULTS	14
Seasonal and Spatial Variability	14
Salinity	14
Absorption Coefficient.....	17
Slope	20
Chlorophyll	22
DOC	23
Fluorescence: Seasonal and Spatial Variability	26
Photodegradation	36

DOC	36
Absorption Coefficient.....	37
Slope Ratio.....	39
Fluorescence Index	39
Fluorescence: EEM's and PARAFAC	42
Nitrogen products	52
DISCUSSION	54
Absorption Coefficient.....	54
Slope	55
Chlorophyll	57
Photobleaching.....	58
DOC	58
Fluorescence, Photodegradation and PARAFAC	59
NH ₄ ⁺ and TDN	63
CONCLUSION	64
LITERATURE CITED	66
APPENDIX 1 Site description.....	71
APPENDIX 2 Data by sampling site and sampling date.....	73
APPENDIX 3 Table with characteristics of the seven components derived from photodegradation experiment by Parallel Factor Analysis (PARAFAC).....	78
APPENDIX 4 Excitation Emmission Matrices (EEM) for Barca - Ba, Canal - Ca, Mar Blanco - MB, Mar Negro - MN and Site 20 – St20 for 4 months (December 2007, March 2008, June 2008 and September 2008) identified with the main fluorophores named by Coble (1996). The color scale is in Quinine Sulfate Units (QSU)	81
APPENDIX 5 Spatial and seasonal distribution of CDOM in Jobos Bay National Estuarine Research Reserve (JOBANERR).....	86

LIST OF TABLES

Table 1 Transmittance percentage at discrete wavelengths12

Table 2 Linear fit regression of Salinity vs. $a_{(412,254,355)}$ 19

Table 3 Linear Fit Regression for DOC vs. $a_{(412,254,355)}$ 25

Table 4 Non-Linear Regression for Salinity vs. F_{max} 29

Table 5 Chlorophyll vs. F_{max} (Linear Fit) regression by site29

Table 6 DOC vs F_{max} (Linear Fit) regression by site29

Table 7 Perason’s correlation between fluorophores regions and salinity, chlorophyll, DOC,
 a_{350} 31

Table 8 First order kinetic for UV dose vs. PARAFAC component.....50

Table 9 Differences between components identified by PARAFAC.....51

LIST OF FIGURES

Figure 1 Location of Jobos Bay in Puerto Rico and its watershed area.....	7
Figure 2 a) Sampling sites and b) Mar Negro in JOBANERR, Puerto Rico	7
Figure 3 Example of CDOM spectral curve for sampling sites at Jobos Bay	10
Figure 4 Tedlar bag transmittance	12
Figure 5 Salinity changes for the sampling period (July 2007- September 2008).....	16
Figure 6 Monthly values of absorption coefficients at all sampling sites.....	18
Figure 7 a) Salinity vs. Absorption coefficient at 412 nm and b) Salinity vs. Slope parameter...20	
Figure 8 Slopes (250-550 nm) calculated by Natural Log transformation (Non-Linear Fit)	22
Figure 9 Chlorophyll vs. Absorption and Slope parameters	23
Figure 10 DOC vs. Absorption Coefficients at 412, 254 and 355 nm.....	25
Figure 11 SUVA ₂₅₄ spatial dynamic for Jobos Bay	26
Figure 12 Salinity vs. Fluorescence Maximum (F_{max}) at four sampling sites (Mar Negro, Barca, Canal, Mar Blanco) in four months around the year (December 2007, March 2008, June 2008 and September 2008)	30
Figure 13 Seasonal and Spatial Variability in Fluorescence Intensity (F_{max}) (QSU) for JOBANERR in specific sampling areas (Barca, Canal, Mar Negro, Mar Blanco).	32
Figure 14 Fluorescence Intensity in quinine sulfate units (QSU) for C region (Excitation 350 nm / Emission 429-447) for sampling sites by 4 months (December 2007- March, June and September 2008)	34
Figure 15 Fluorescence Intensity (QSU) for Proteins (B/T) region (Excitation 280 nm / Emission 315/451) for sampling sites by 4 months (December 2007- March, June and September 2008)..	34
Figure 16 Fluorescence Intensity (QSU) for region H (Excitation 295-330 / Emission 337-443) for sampling sites by 4 months (December 2007- March, June and September 2008)	35
Figure 17 Fluorescence Intensity (QSU) for region A (Excitation 240-260 nm / Emission 321-429) for sampling sites by 4 months (December 2007- March, June and September 2008).....	35

Figure 18 DOC changes on samples exposed to sunlight (light) and kept in the dark during 96 hours of natural sunlight exposure (8 days or 12963 KJ.m ⁻² UV dose).....	38
Figure 19 Absorption coefficient (350 nm) vs. Dissolved Organic Carbon (Standard Deviation Bars) exposed to natural sunlight)	38
Figure 20 UV dose with natural sunlight vs. absorption coefficient at 350 nm. Exponential decay (first order kinetic)	39
Figure 21 UV dose vs. Slope Ratio (Helms <i>et al.</i> , 2008) for dark and light samples.....	40
Figure 22 Fluorescence Index vs. DOC; Absorption coefficients at 350 nm vs. Fluorescence Index; Slope Ratio vs. Fluorescence Index; UV dose vs. Fluorescence Index.....	41
Figure 23 EEM's of the components identified by PARAFAC and their excitation and emission peaks	43-44
Figure 24 UV dose vs. Fluorescence Intensity of components identified by PARAFAC (a) Dark samples (b) irradiated samples.....	47
Figure 25 EEM's Average for dark samples in the top left (a) 0hr and top right (b) 96 hr Fluorescence Intensity in Quinine Sulfate Units (QSU) and EEM for Standard Deviation in the bottom left (c) stdev 0hr bottom right (d) stdev 96hr	48
Figure 26 EEM's Average for light samples in the top left (a) 0hr and top right (b) 96 hr Fluorescence Intensity in Quinine Sulfate Units (QSU) and EEM for Standard Deviation in the bottom left(c) stdev 0hr bottom right (d) stdev 96hr	49
Figure 27 Fluorescence intensity of the main fluorophores (named by Coble 1996) at zero UV dose and (96hr) 8203 UV dose (KJ.m ⁻²). D = dark, L = light.....	51
Figure 28 UV dose exposures vs. Total Dissolved Nitrogen.....	52
Figure 29 UV dose vs. NH ₄ ⁺ exposed to natural sunlight	53

LIST OF APPENDICES

APPENDIX 1 Site description.....	71
APPENDIX 2 Data by sampling site and sampling date.....	73
APPENDIX 3 Table with characteristics of the seven components derived from photodegradation experiment by Parallel Factor Analysis (PARAFAC).....	78
APPENDIX 4 Excitation Emmission Matrices (EEM) for Barca - Ba, Canal - Ca, Mar Blanco - MB, Mar Negro - MN and Site 20 – St20 for 4 months (December 2007, March 2008, June 2008 and September 2008) identified with the main fluorophores named by Coble (1996). The color scale is in Quinine Sulfate Units (QSU).	81
APPENDIX 5 Spatial and seasonal distribution of CDOM in Jobos Bay National Estuarine Research Reserve (JOBANERR).....	86

INTRODUCTION

The photochemistry and photobiology of chromophoric dissolved organic matter (CDOM) in marine environments has been well studied over the last 20 years, principally at continental margins influenced by large rivers around the world. CDOM constitutes an important but variable fraction of the total dissolved organic matter (DOM) in the oceans. CDOM is the primary sunlight-absorbing constituent of natural waters (Brinkmann *et al.*, 2003; Kowalczyk *et al.*, 2005) and a major factor controlling light penetration in the water column (Kowalczyk *et al.*, 2003). The sunlight absorbed by CDOM is responsible for the formation of photochemical intermediates with consequences that include alteration in the biological availability of some metals, the production of trace gases (Blough and Del Vecchio, 2002) and the photochemical release of ammonium (Morell and Corredor, 2001). At increasing levels, CDOM absorption can affect primary productivity and ecosystem structure by reducing the amount and quality of photosynthetic active radiation (PAR) available to phytoplankton (Bidigare *et al.*, 1993 in Keith *et al.*, 2001). In addition, the chlorophyll signal in ocean color is confused with CDOM, overestimating the chlorophyll values obtained by satellite measurements. Therefore, the study of CDOM absorption is an important tool for the calibration and validation of satellite measurements (Del Vecchio and Subramaniam, 2004), and can be correlated with benthic habitat changes and phytoplankton dynamics.

Although, CDOM can be found in oceanic waters, the highest concentrations of CDOM are observed in coastal areas and in semi-enclosed seas closer to direct sources of terrestrial

organic matter (Kowalczyk *et al.*, 2005). In coastal regions like estuaries, the development of marine organisms can be influenced by CDOM in shallow areas. The source and dynamics of CDOM are influenced by hydrology, geomorphology, land use, biogeochemical processes and vegetation cover at the area (Maie *et al.*, 2006). In estuaries, CDOM concentrations are controlled by river inputs, porewater re-suspension, production and degradation of vascular plants and algae, as well as anthropogenic sources (Bianchi, 2007). Mangroves provide a significant input of DOM to tropical estuarine regions (Jaffé *et al.*, 2004) and other coastal ecosystems but there is a lack of information regarding its production, fate and effects. Dittmar *et al.* (2001) have carried out some of the few studies on mangrove derived DOM and recognize that the exported organic material has a recognizable effect on the food webs in coastal water ecosystems. About 50% of the net primary production in mangroves is exported as organic matter to the ocean (Dittmar *et al.*, 2006). Tannin comprises as much as 20% of a mangrove leaf (Benner *et al.*, 1990; in Hernes *et al.*, 2001) and is an important component of chromophoric dissolved organic matter (CDOM). It is a highly colored and reactive substance (Hernes *et al.*, 2001).

CDOM typically displays a light absorption spectrum of exponential decrease with increasing wavelength. A commonly used expression that defines the absorption parameter (a), an inherent optical property that depends on the substances present in water, is

$$a(\lambda) = a(\lambda_0) e^{-S(\lambda-\lambda_0)} \quad (1)$$

where (λ_0) = 412 nm reference wave length, S = curve slope, and $a(\lambda)$ = absorption measured in m^{-1} . When determined instrumentally using a spectrophotometer, the absorption coefficients are calculated from the relation

$$a(\lambda) = 2.303 A(\lambda)/r \quad (2)$$

where A is the optical density (absorbance) and r is the path length of the cell.

The slope parameter (S in equation 1 above) defines how rapidly the absorption decreases with increasing wavelength (Blough and Del Vecchio, 2002). Moreover, S defines the spectral dependence of CDOM and provides information about its sources. S varies with the source of CDOM, showing a range from as low as $\sim 0.01 \text{ nm}^{-1}$ for terrestrial humic acids, to as high as 0.02 to 0.03 nm^{-1} for oligotrophic waters (Blough and Del Vecchio, 2002; Del Vecchio and Subramaniam, 2004; Wurl, 2009). Other slope calculation (slope ratio) was integrated to the analysis to provide information about CDOM sources. The slope ratio (S_R), is the ratio of spectral slopes calculated for two discrete wavelength regions, i.e., 275-295 nm ($S_{(275-295)}$) and 350-450 nm ($S_{(350-400)}$) (Helms *et al.*, 2008). This ratio is a useful indicator of molecular weight and photobleaching of CDOM.

Another useful feature for characterizing CDOM is its inherent fluorescence. CDOM in natural waters is comprised of a mixture of individual chromophoric compounds containing discrete fluorophores that can be identified using the excitation emission matrix (EEM) (Kowalczyk *et al.*, 2005). Parallel factor analysis (PARAFAC) is a valuable data analysis tool for characterizing and quantifying changes in DOM fluorescence in natural environments (Cory and McKnight, 2005; Hall *et al.*, 2005; Stedmon and Markager, 2005a,b; Murphy *et al.*, 2006; and references there in Stedmon and Bro, 2008). It provides both a quantitative and qualitative model of DOM values and separates the complex signal measured into its individual underlying fluorescent phenomena with specific excitation and emission (EEM) spectra (Stedmon and Bro,

2008). EEM spectra can be used to follow changes in CDOM resulting from biological or physical processing of the material, or to trace CDOM from different sources (Kowalczuck *et al.*, 2005; Stedmon and Markager, 2005 a,b; Murphy *et al.*, 2006; Yamashita and Jaffe, 2008).

In estuarine areas the principal fluorophores are represented by peaks A (humic like), M (marine humic like), C (humic like), B (tyrosine like) and T (tryptophan like) as named by Coble (1996). M and C peaks have been proposed as water mass tracers (E. Parlanti *et al.*, 2000). Del Castillo *et al.* (1999) described the peaks A, M and C for tropical water in the Orinoco River plume and Maie *et al.* (2006) for Florida Coastal Everglades.

This study was undertaken to characterize the optical properties and photodegradation dynamics of CDOM in the waters of Jobos Bay, a NOAA National Estuarine Research Reserve (JOBANERR), located on the south coast of Puerto Rico. Jobos Bay is the second largest estuary in Puerto Rico and has more than three times the shoreline of any other estuary in the island (Zitello *et al.*, 2008). It comprises important marine communities such as seagrass beds and coral reefs. It is influenced mostly by groundwater, runoff and a small river input. Mangrove is the dominant habitat at Jobos Bay.

Specific goals were to characterize CDOM absorption and fluorescence in the Bay, describe its temporal and spatial distribution, and to parameterize its photochemical diagenesis under natural irradiance. The spatial and seasonal variations of CDOM were correlated with Dissolved Organic Carbon (DOC), salinity and chlorophyll data to identify the processes that drive CDOM dynamics in the bay, including photodegradation and/or dilution. The absorption

coefficient was used to create an absorbance map for the JOBANERR area. Our study aims at understanding the role of mangrove-derived CDOM in tropical waters and will provide a useful tool for water mass tracing for the management of JOBANERR.

MATERIALS AND METHODS

Site Description

Jobos Bay is a coastal embayment on the Caribbean coast of Puerto Rico with high salinity and low river influences known for its extensive mangrove cover (Figure 1). The waters within the bay contain large amounts of CDOM due mainly to mangrove decomposition. Jobos Bay watershed covers 137 km² in the South Coastal Plain of Puerto Rico, and drains surface and ground water directly to Jobos Bay via aquifers, runoff and Rio Seco river (Figure 1). The watershed is a rural area with vegetated lands, including grassland, forest and shrub, covering 70% of the landscape (Appendix 1, Figure 1) (Zitello *et al.*, 2008). It sits a number of industrial facilities, including two electric power plants, an oil refinery, and several major chemical and pharmaceutical factories. Two groundwater units discharge in the coastal zone; a shallow aquifer at 3 m that supplies the mangrove complex at the watershed's coastal margins and a 23 m deep aquifer that provide freshwater to the offshore mangrove islands that form Jobos Bay's southern boundary (Zitello *et al.*, 2008) (Appendix 1, Figure 2). Tides at Jobos are mixed, but chiefly diurnal, showing a mean of 17.3, ranging from 17.0 cm to 36.0 cm (Lugo *et al.*, 1987 in Robles *et al.*, 2002). The tide dynamic of Jobos Bay conforms to the USFWS criteria (1979)

of an intertidal estuarine system dominated by seagrass bed and coral reefs (Robles *et al.*, 2002).

The total rainfall in Jobos watershed was 1278.7 mm for the entire year sampled. September 2007 and 2008 were recorded as the wettest months with a total precipitation of 90.9 mm and 339.8 mm respectively; on the contrary March was the driest month, with an average rainfall of 10.0 mm (NASA, Tropical Rainfall Measuring Mission (TRMM)). (Figure 3, Appendix 1).

Eight sites were sampled at JOBANERR along a gradient from shore to offshore (Figure 2a).

Samples were collected from:

1. The innermost part of the Bay is known as Mar Negro (MN). The area is surrounded by mangroves and houses, which suggests it is directly influenced by human activities. Water depth in Mar Negro averages 2 meters and the bottom is frequently covered with cyanobacterial mats. These waters are deeply tinted with CDOM “tannin”; which gives the area its Spanish name which translates as “Black Sea” (Figure 2b).
2. Site 9 is an active water quality monitoring station which sits next to a seasonal lagoon whose water levels are influenced by tides and rainfall. The water is “black”, average depth is 1 meter and the bottom is composed of clay and silt.
3. Site 10 is a mangrove-enclosed area. Water and bottom present similar characteristics to those at site 9.
4. Mar Blanco (MB) is a region in the middle of the bay, with generally “green” waters; the average depth at this site is approximately 8 meters.

5. Site 19 is an area ~1m depth with seagrasses and clear water.
6. Site 20 is the only active JOBANERR station with real time data access. The site depths fluctuate around ~1m , has clear waters with seagrasses.
7. Navigation Channel (Canal) is ~9 m deep with green waters exiting the bay.
8. Barca (Ba) is an offshore site with “blue” waters and ~17 m depth.

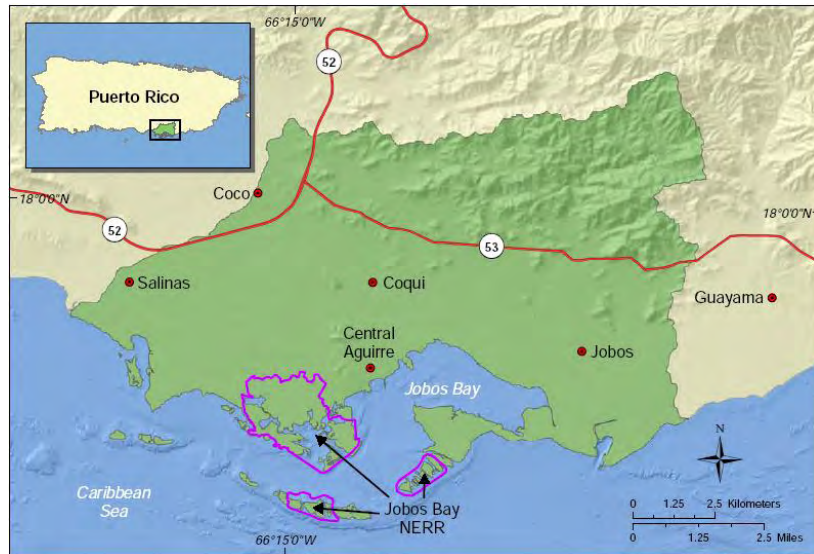


Figure 1 Location of Jobos Bay and its watershed area in Puerto Rico (Zitello *et al.*, 2008).



Figure 2 a) Sampling sites and b) Mar Negro in JOBANERR, Puerto Rico (Images from Google Earth ©)

Sample collection

An intensive sampling effort was conducted during a 14-month period (July 2007 to September 2008) in Jobos Bay National Estuarine Research Reserve, shared by Salinas and Guayama municipalities, located in the southern region of Puerto Rico. Sampling was conducted on a monthly basis and included water samples and ancillary data collection at 12 stations. However, sampling from only 8 stations has been considered here. In the other 4 stations the sampling effort was irregular during the sampling period. Water samples were collected directly from the sea surface (~ 0.25 meter), with 1 L amber glass bottles and kept in the dark at ~4°C for a maximum of 24 hours until absorbance analysis was performed. Also, 19 L water samples were collected in plastic buckets for photodegradation experiments. The bottles and buckets were previously washed with 10% HCl, rinsed with 2M NaOH and then rinsed with distilled water 3 times (Ciotti and Bricaud, 2006). All storage bottles were precombusted at 450°C for 8 hours. Water was filtered through Whatman GF/F filters (precombusted 450°C/24 hr) and then through 0.2 µm membrane filters. The first 250 ml of each sample were used to rinse the filtration materials and then discarded (Ciotti and Bricaud, 2006).

Optical CDOM Characterization

Optical CDOM characterization included determination of absorption coefficient ($a \text{ m}^{-1}$), Spectral Slope ($S \text{ nm}^{-1}$), the Slope Ratio (S_R), EEM fluorescence and PARAFAC analysis.

Absorption Spectroscopy

Spectrophotometric analysis was carried out using a Shimadzu 1601-UV instrument. Samples were analyzed in 10 cm path length quartz cells over a wavelength range of 200 to 700 nm. Milli-Q water absorbance was subtracted from the sample data and subsequently the value at 700 nm was subtracted from the entire spectrum (Miller *et al.*, 2002). The absorbance values were converted to absorption coefficients, a (λ , m^{-1}), and absorption coefficients at 350 nm (a_{350}) and 412 nm (a_{412}) (m^{-1}) were reported as quantitative parameter of CDOM (Figure 3). The data was analyzed from 250 to 550 nm using equation 1. Slope ratio (S_R) was determined according to Helms *et al.* (2008) to estimate molecular weight and to address the source of CDOM.

Fluorescence Spectroscopy

EEM fluorescence was determined with a Horiba Jovin Yvon Spex Fluoromax 3 spectrofluorometer according to Yamashita and Jaffé (2008) and Santin *et al.* (2009). The post-acquisition corrections were carried out as follows; 1) inner filter corrections were carried out using UV-Vis absorbance data (McKnight *et al.*, 2001), 2) EEM of Milli-Q water were subtracted from sample EEM's for removing mainly Raman scatter, 3) instrument excitation/emission corrections were carried out according to the procedure provided by the manufacturer, 4) fluorescence intensities were corrected to the area under the water Raman peak (excitation = 350 nm) and analyzed daily (Cory and McKnight, 2005). Fluorescence intensities were converted to quinine sulfate unit (QSU) using a calibration with quinine sulfate monohydrate (Yamashita and Tanoue, 2003).

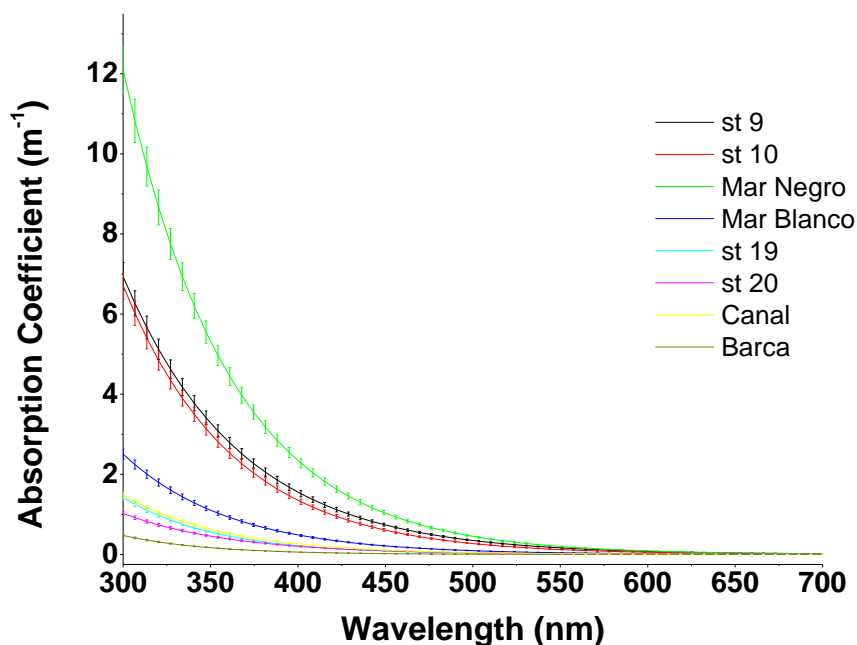


Figure 3 Example of CDOM spectral curve for sampled sites at Jobos Bay.

The fluorescence index was calculated as the ratio of fluorescence emission intensities at 470 nm and 520 nm at 370 nm excitation according to Cory and McKnight (2005) and Maie *et al.* (2006). PARAFAC modeling was conducted with 56 samples, product of a photodegradation experiment, using the DOMFluor toolbox on Matlab Software (Stedmon and Bro, 2008). The wavelength range used for PARAFAC was 240-455 nm and 250-700 nm for excitation and emission, respectively. The correct number of components was determined by two validation methods, i.e., split half analysis and random initialization (Stedmon and Bro, 2008).

Photodegradation Experiment

In order to characterize photodegradation kinetics of Mar Negro waters, UV-Visible absorbance, and EEM fluorescence spectra were determined. The experiment was conducted at

UPRM Marine Sciences Department field station on Magueyes Island. The samples were exposed to natural sunlight in 2 L Tedlar (polivinyfluoride) bags for 96 hours (8 days or 12963 KJ.m⁻²), together with dark controls double wrapped with aluminum foil. The bags were previously washed with 10% HCl and rinsed 3 times with distilled water. The filtered samples were injected into Tedlar bags and incubated in direct sunlight at ~0.25 m depth off the Magueyes field station dock. Samples were obtained every 4 hours during the first 12 hours of sunlight exposure, and then every 12 hours, from 3 different bags, UV-Vis absorbance, and EEM fluorescence were determined. The samples for DOC and fluorescence analysis were frozen until analysis. Dissolved organic carbon levels were determined by the Tropical Limnology Laboratory at University of Puerto Rico-Rio Piedras Campus using high-temperature combustion with a Teledyne Tekmar Apollo 9000 instrument.

Figure 4 shows the spectral transmission for Tedlar bags and table 1 shows the discrete values at specific wavelength with high transmittance throughout the visible (75%) and UV (65%) spectra (Loiselle *et al.* 2009; Twardowski and Donaghay, 2002). Loiselle and collaborators (2009) examined the bags for potential release of CDOM using MilliQ water and conclude that Tedlar bags do not contribute to CDOM absorption or sample bias.

Surface irradiance measurements were obtained with a Biospherical Instruments Inc. GUV-511 radiometer permanently installed at Magueyes Island, which records data at four narrow bandwidths of UV (305, 320, 340, and 380 nm) and a broadband sensor for PAR (400-700 nm). The irradiation dose was integrated according to Detrés *et al.*, (2001). Spectral irradiance measurement at surface, out of the water, and underwater (0.25m) were conducted

using an Optronic OL-754 high resolution spectroradiometer (Optronic Laboratories) (Detrés *et al.*, 2001) to correct irradiance measurements at 0.25m depth by the attenuation coefficient (K_d).

This instrument acquired scans from 280-700 nm every 2 nm.

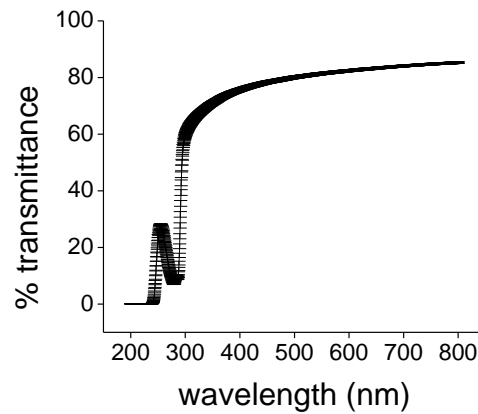


Figure 4 Tedlar bag transmittance.

Table 1 Transmittance percentage at discrete wavelengths.

<i>Wavelength (nm)</i>	<i>% T</i>
800	85.3
700	84.1
600	82.4
500	80.1
400	75.7
300	59.7
200	0.1

Salinity, DOC and Chlorophyll

Practical Salinity values were obtained in situ by CTD (SBE-25) from surface water at all sampling sites. In addition samples were analyzed for DOC and chlorophyll concentration. Dissolved organic carbon was determined by high-temperature combustion with a Shimadzu TOC-5000A analyzer conducted by the Ecology and Stable Isotope Laboratory at Georgia University and with a Teledyne Tekmar Apollo 9000 instrument at University of Puerto Rico by the Tropical Limnology Laboratory. To determine chlorophyll concentration, 1L of water was filtered through 0.7 μm Whatman GF/F filters, which were then frozen immediately. The filters were soaked in 90% acetone for 24 hours and refrigerated in darkness at 4 °C. Chlorophyll *a* concentration was measured with a Turner-Design 10 fluorometer (J. Zhao *et al.*, 2009).

Ammonium (NH_4^+)

To assess production or loss of NH_4^+ during photodegradation 25 mL quartz tubes were filled with 20 mL of sample water. The tubes were placed horizontally in a black grid at 0.25m depth, exposed to natural sunlight. Dark controls were double wrapped with aluminum foil. Samples were obtained every 4 hr for the first 12hr of exposure and then every 12 hours for 8 days and analyzed for ammonium using the o-phthaldialdehyde (OPA) fluorescence method of Holmes *et al.* (1999).

Total Nitrogen (TN) concentration was determined by chemiluminescence method using the Teledyne Tekmar Apollo 9000 instrument. TN concentrations are the mean of triplicate analyses performed on each of the three experimental and control samples.

Statistical Analysis

Statistical analyses were carried out with Minitab 15 statistical package. Normality test was established and in those cases where the data was not normally distributed it was transformed by Box-Cox or Johnson transformation to normalize the data (e.g. Salinity, DOC, SUVA, Chl). One way ANOVA was applied to determine the significant differences between sampling areas. To determine SUVA and salinity differences between sampling sites a multiple comparisons test (Tukey) was applied. Non-Parametric test (Kruskal-Wallis) was applied to establish seasonal and spatial differences on absorption coefficient and slope parameters. Pearson's correlation was applied to Chlorophyll, Salinity, $a_{412+350}$, Slope, $\text{TN}_{\text{light} + \text{dark}}$, $\text{NH}_4^+_{\text{light} + \text{dark}}$, $\text{DOC}_{\text{light} + \text{dark}}$.

RESULTS

Seasonal and Spatial Variability

Salinity

Practical Salinity decreased from July 2007 to October 2007, increased from October 2007 to June 2008 and decreased again from July 2008 to September 2008 (Figure 5). Mar

Negro presented broad salinity range with values fluctuating from 8.52 (September 2008) to 45.78 (July 2007). The salinity average for MN was 38.3 excluding the low outlying value observed in September 2008 (8.52).

The sites in the open area presented smaller ranges of salinity. The highest salinity values were reported between March 2008 to June 2008 and the minimum values in September 2008. At Mar Blanco the minimum value observed was 24.98 (July 2007) and the maximum 36.98 (March 2008). In the navigation channel the maximum salinity value observed was 36.6 (March 2008) and the minimum 32.05 (September 2008). At the offshore site, Barca, the maximum was 37.07 (June 2008) and the minimum 33.47 (August 2008).

Salinity showed no significant differences (one way-ANOVA) between sampling sites and significant differences seasonally ($F = 9.77$, $P = 0.000$). To identify seasonal differences in salinity Tukey's test was applied. July (highest value) differs with August and September; December and August differ from March and June; March and June presented similar values; January, March and June differ from September values.

Even though low salinity values coincided with the high CDOM absorption values, a negative tendency with CDOM ($R = -0.19$, $SD = 1.42$, $n = 116$, $P = 0.04$) was observed when considering the totality of the data (Figure 7) (Table 2). In addition, relationships between salinity and a_{254} and a_{355} showed a negative tendency and higher standard deviations of the data. Considering monthly regressions between a_{412} and salinity the data showed positive correlations December 2007, January, March and September 2007 showed an $R^2 > 0.90$. July and September

2008 presented $R^2 \leq 0.50$ and April, May, June and August 2008 showed $R^2 \geq 0.50-0.90$. October and December 3, 2007 showed the lowest correlation $R^2 \leq 0.10$. Furthermore, the Slope parameter (S) showed low relation with salinity ($R = -0.07$, $SD = 0.01$, $n = 117$, $P = 0.07$).

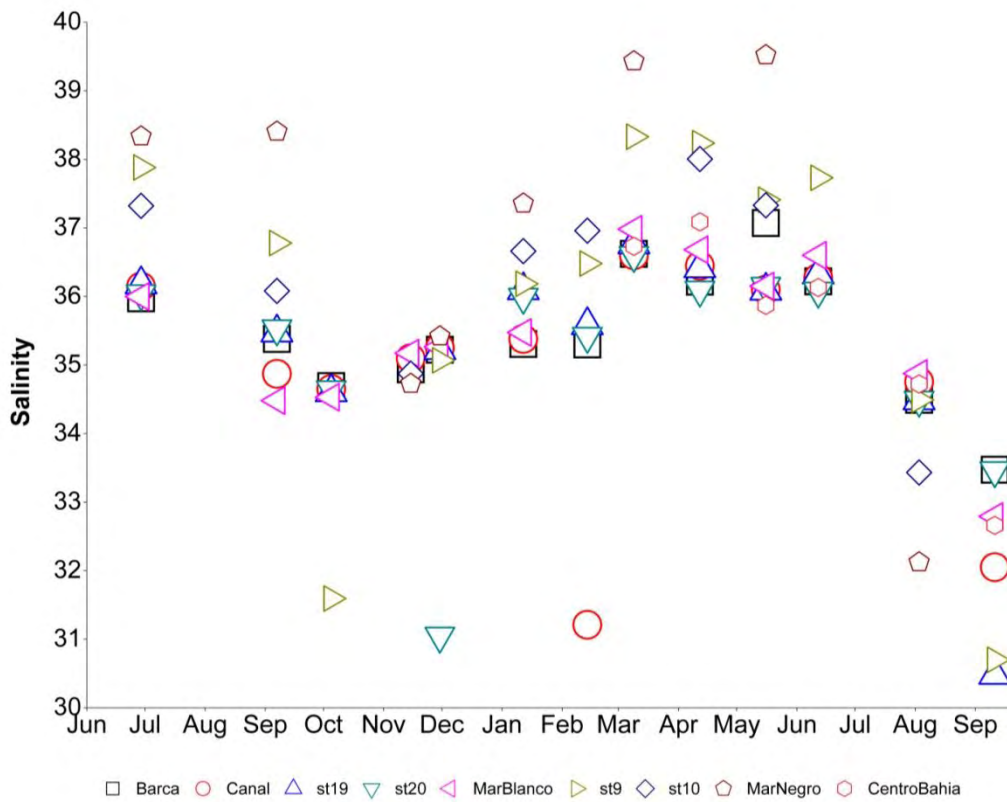


Figure 5 Salinity changes for the sampling period (July 2007- September 2008).

Absorption Coefficient (a_{412})

Based on absorption parameter (a_{412}), Jobos Bay can be divided in two zones: Inner/mangrove area and outer/open area. In the mangrove area, Mar Negro (MN) presented the highest absorption coefficient ($a_{412} \text{ m}^{-1}$) values. This is followed by Site 9, Site 10 and finally Mar Blanco (MB) ($\text{MN} > 9 > 10 > \text{MB}$) (Figure 6). In December 2007 Site 10 had higher values than Site 9. In September 2007, absorption was higher at MB (1.66 m^{-1}) than at Site 10 (0.115 m^{-1}). From March to June the absorption values were reduced to less than 2 m^{-1} . For the same period Site 9 and MN presented similar absorption values and Site 10 values were low. Mar Blanco, maintained constant values with minimal variation from October 2007 to September 2008. The absorption value varied significantly only in September 2007 at this station. Significant variation at Mar Blanco was only observed in September 2007. At Mar Blanco, the highest value was observed on September 2007 (1.68 m^{-1}) and the lowest on December 2007 (0.235 m^{-1}). The maximum value for Mar Negro was observed in September 2007 (11.48 m^{-1}) and the minimum (1.21 m^{-1}) in March. During the dry period, from March to June this site did not present significant changes. At Site 9 the highest value was observed in September 2007 (6.11 m^{-1}) and the lowest in July 2007 (1.28 m^{-1}). Site 10 presented the maximum in December 2007 (3.07 m^{-1}) and the minimum in September 2007 (0.11 m^{-1}). In general for all sampling sites the absorption values were lower than 5 m^{-1} , excluding September samples, which reached values as high as 11.48 m^{-1} . The highest values were observed in September 2007 and 2008 at Mar Negro.

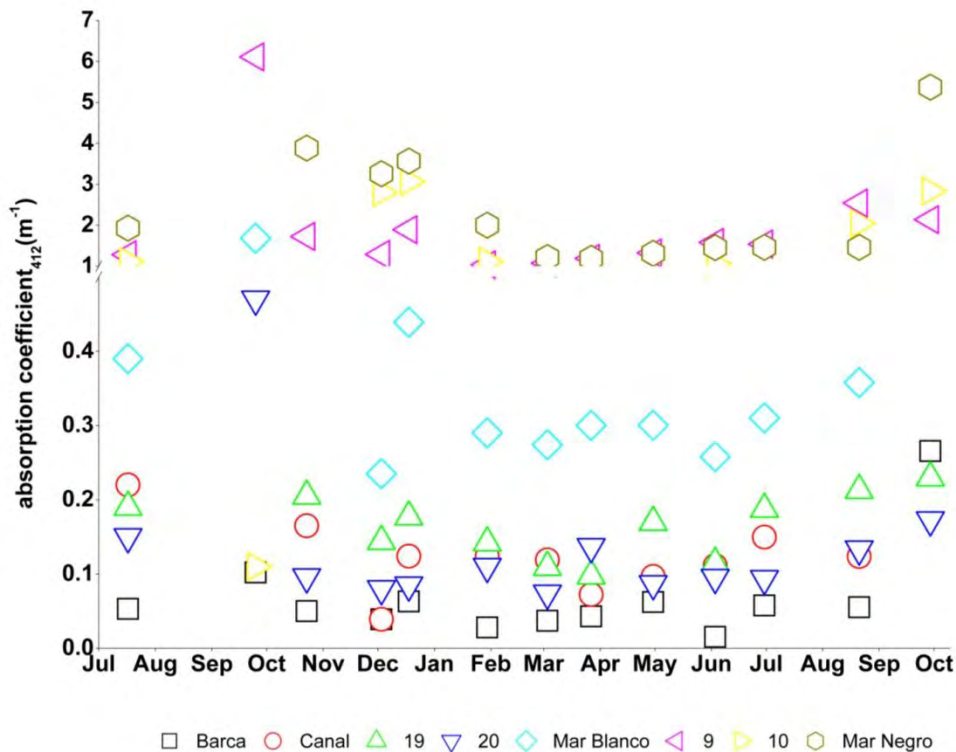


Figure 6 Monthly values of absorption coefficients at all sampling sites.

In the open area, the highest values observed in September 2007 and 2008, were similar to the mangrove area (Figure 6). The highest values were observed at Site 19 followed by Canal, Site 20 and Barca ($19 > Ca > 20 > Ba$). Excluding September 2007 and 2008 all absorption values in the 1-year period were lower than 0.3 m^{-1} . The outer stations exhibited less temporal variability. The highest value at Site 19 was 0.7 m^{-1} and was observed in September 2007, and the lowest was 0.09 m^{-1} on March 28, 2008. At Canal the highest value was 0.75 m^{-1} in September 2007 also, and the lowest value 0.07 m^{-1} in November 2007. The maximum value (0.47 m^{-1}) at Site 20 occurred in September 2007 and the minimum (0.074 m^{-1}) in March 2008. At Barca the highest value (0.265 m^{-1}) was observed in September 2008 and the lowest value (0.015 m^{-1}) on June 3, 2008 with an average yearly value of $< 0.1 \text{ m}^{-1}$. Absorption coefficient at 412 nm did not present a seasonal pattern but presented spatially significant differences

(Kruskal-Wallis $H = 62.02$, $P = 0.000$). Mar Negro, st9 and st10 are different from Barca, Canal and st20; Station 19 is different from Mar Negro and station 9; Mar Blanco is different from Barca.

A negative correlation was observed between a_{412} and salinity (range 8–47) ($R = -0.19$) (Figure 7, Table 2). Excluding the lowest salinity value (8) and using a range from 30 to 40 there is a weak positive, but not significant, correlation ($R = 0.15$, $n = 103$, $P = 0.12$, $SD = 1.39$). Monthly linear fit regressions between salinity and a_{412} presented positive and significant differences (Jul 2007 $R^2 = 0.47$, Sep 2007 $R^2 = 0.5$, Oct 2007 $R^2 = 0.08$, Dec 2007 $R^2 = 0.1$, Dec 2007 $R^2 = 0.98$, Jan 2008 $R^2 = 0.9$, Mar 2008 $R^2 = 0.98$, Mar 2008 $R^2 = 0.92$, Apr 2008 $R^2 = 0.84$, Jun 2008 $R^2 = 0.59$, Jun 2008 $R^2 = 0.66$, Aug 2008 $R^2 = 0.29$, Sep 2008 $R^2 = 0.89$). Also, a strong positive correlation was found between a_{412} and chlorophyll ($R = 0.78$, $n = 40$, $P < 0.0001$, $SD = 0.955$).

Table 2 Linear fit regression of Salinity vs. $a_{(412,254,355)}$

nm	R	R^2	SD	N	P
412	-0.19	0.036	1.42	116	0.04
254	-0.32	0.102	11.86	116	3.8E-4
355	-0.19	0.036	3.45	116	0.039

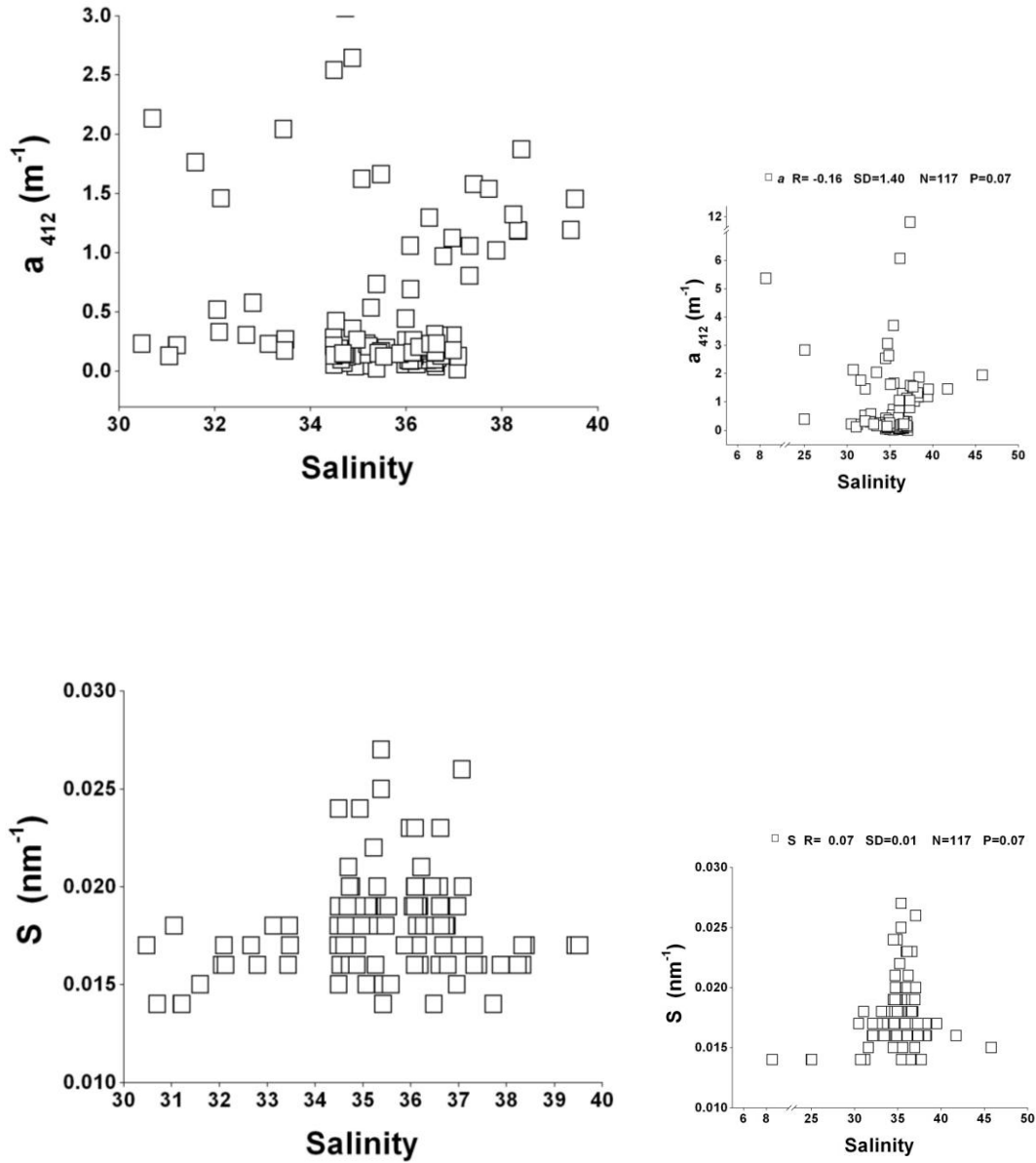


Figure 7 a) Salinity vs. Absorption coefficient at 412 nm and b) Salinity vs. Slope parameter.

Slope

Average slope values can be organized from highest to lowest as follows: Ba > Ca \geq 20 > 19 > MB > MN > 10 > 9 (Figure 8). Slope values in September 2007 for Site 10 and Barca were

outliers for the data sampled, with values of 0.08 and 0.102 nm⁻¹, respectively (Figure 8). If September 2007 data is excluded, all slope values are lower than 0.03 nm⁻¹. Even excluding the September 2007 value (0.102 nm⁻¹), Barca had the highest slopes which ranged from 0.017 nm⁻¹ (September 2008) to 0.026 nm⁻¹ (June 2008). At Canal the range of values was between 0.014 nm⁻¹ (July 2007) and 0.027 nm⁻¹ (September 2007). Site 20 presented a broad range of slopes with values ranging between 0.014 (July 2007) and 0.034 nm⁻¹ (September 2007). Site 19 values fluctuated between 0.015-0.023 nm⁻¹ with the maximum and minimum values occurring in the same months than those of Site 20. Mar Blanco presented an average of 0.017 nm⁻¹ with a range between 0.014-0.019 nm⁻¹. The other three sites at the inner part of mangroves (10 [with the exception of the September 2007 outlier], MN and 9) presented lower averages (values) (0.014-0.016 nm⁻¹) with the highest values between January and June 2008.

Slope do not presented spatial significant differences (H = 11.02, P = 0.138) but presented seasonal significant differences (Kruskal-Wallis H = 31.07, P = 0.000). July values are different to September 2007, January and June values; September 2007 differs with June and September 2008. Pearson's correlation coefficient showed a positive correlation (R = 0.159, P = 0.086) between salinity and slope parameters, but the test were not significant.

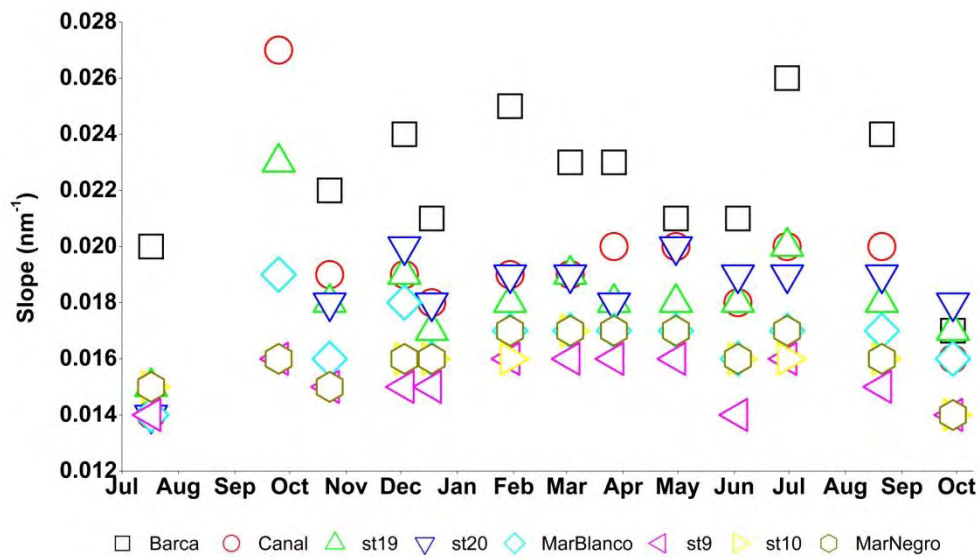
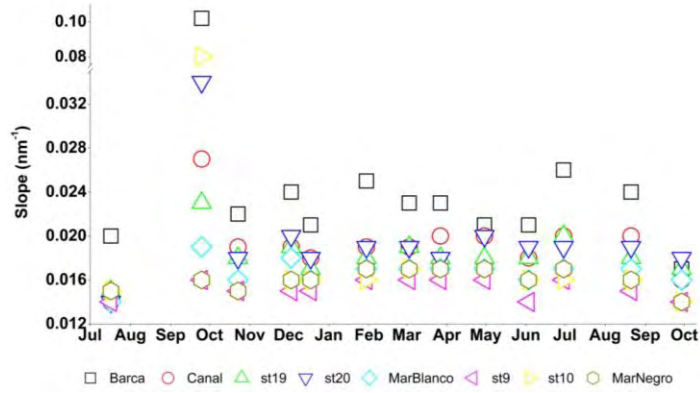


Figure 8 Slopes (250-550 nm) calculated by Natural Log transformation (Non-Linear Fit) and zoom to slope scale.

Chlorophyll

In most study sites the highest chlorophyll values were observed in September 2008 and correspond with a period of heavy rain. The only exception was Site 9 with a chlorophyll peak on March 28, 2008 (11.6 µg/L). The lowest values varied by site and season. In general the

chlorophyll values can be organized in descending order as follows: 9 > MN > 10 > Mar Blanco > Canal > 19 > Barca > 20. The average value for Mar Negro was 4.78 $\mu\text{g/L}$ while the average at Barca was 0.52 $\mu\text{g/L}$ and 1.38 $\mu\text{g/L}$ at Mar Blanco. A positive correlation was established between chlorophyll and a_{355} ($R = 0.71$, $SD = 1.72$, $n = 112$, $P < 0.0001$) and with a_{412} ($R = 0.73$, $SD = 0.65$, $n = 113$, $P < 0.0001$). A linear fit showed a negative relation between the S parameter and chlorophyll ($R = -0.38$, $SD = 0.002$, $n = 97$, $P < 0.0001$) (Figure 9). Pearson's coefficient showed a negative and significant correlation between Chlorophyll and Slope ($R = -0.416$, $P = 0.000$). The Johnson transformation was used to normalize chlorophyll data. Subsequently, one way ANOVA was applied to recognize seasonal and spatial differences. Significant seasonal differences were observed ($F = 2.41$, $P = 0.021$). September 2008 differs from Dec 3, Jan, Mar 3, Jun 3 and Jun 30. In addition, significant spatial differences were present ($F = 5.19$, $P = 0.000$). Mar Negro and st9 differ with Barca, Canal and st20; st9 differs with st19.

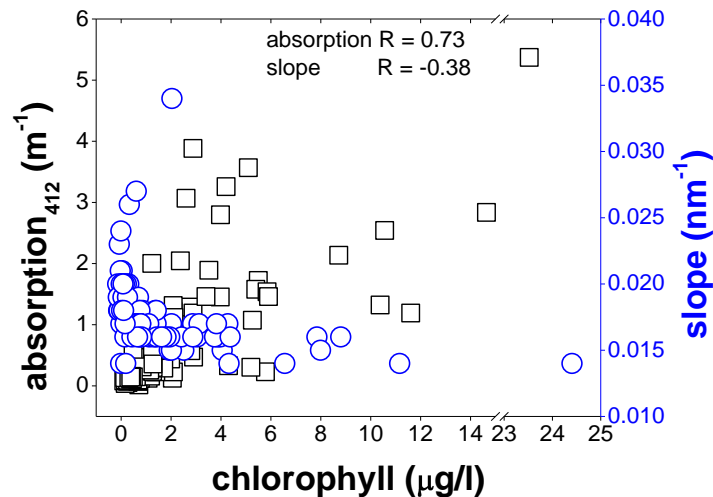


Figure 9 Chlorophyll vs. Absorption and Slope parameters.

Dissolved Organic Carbon (DOC)

DOC values at Jobos Bay varied from 907 μM in the mangrove zone, to 116 μM at the center of the bay. DOC values were also lower in the shallow seagrass areas. The highest value was observed in December 2007 at Mar Negro (907 μM). These values for Mar Negro ranged from 252 to 907 μM with an average of 512 μM for the one year sampling period. DOC values at the most offshore water, site (Barca), with, ranged between 138 to 729 μM , and averaged 298 μM . The DOC values at Site 20 ranged from 123 to 649 μM , and averaged 286 μM . Site 20 is a shallow seagrass area on the bay. Although, the DOC had a broad range of values, those for a_{412} , a_{254} and a_{355} presented a narrow range. For instance, at Site 20, a_{355} ranged from 0.46 to 0.21 m^{-1} , excluding the value observed in September 2007 (1.63 m^{-1}), a period of heavy rain. Mar Negro values ranged from 3.04 to 9.05 m^{-1} , excluding rainy periods in September 2007 and 2008 that do not necessarily match with the highest DOC values. Barca presented a similar trend, with values ranging from 0.11 to 0.16 m^{-1} excluding September 2007 and 2008. A linear regression between DOC and a_{355} shows a weak, positive relation ($R = 0.4$, $SD = 2.29$, $n = 80$, $P = 2.25\text{E}^{-4}$), a_{254} ($R = 0.37$, $SD = 10.35$, $n = 80$, $P = 7.67\text{E}^{-4}$) and also a weak, positive relation with a_{412} ($R = 0.37$, $SD = 0.91$, $n = 80$, $P = 6.83\text{E}^{-4}$) (Figure 10). If seagrass areas are excluded (st19 and st20) the relation between DOC and a_{412} is slightly higher ($R = 0.46$, $SD = 2.41$, $n = 61$, $P = 1.65\text{E}^{-4}$) (Table 3). Seasonal significant differences ($F = 5.24$, $P = 0.002$) were observed on DOC values. December 3 differed from March 3 and August 2008. Values didn't show significant spatial differences.

Specific UV Absorbance at 254 nm ($SUVA_{254}$) was calculated to identify the recalcitrance of DOC in Jobos Bay. September 2008 showed the highest $SUVA$ values followed by October 2007 and April 2008. This parameter presented a similar spatial pattern to DOC. The highest values were observed in mangrove areas (MN, st9, st10) decreasing seaward (Figure 11). The lowest $SUVA$ values were observed in Barca, st19 and st20.

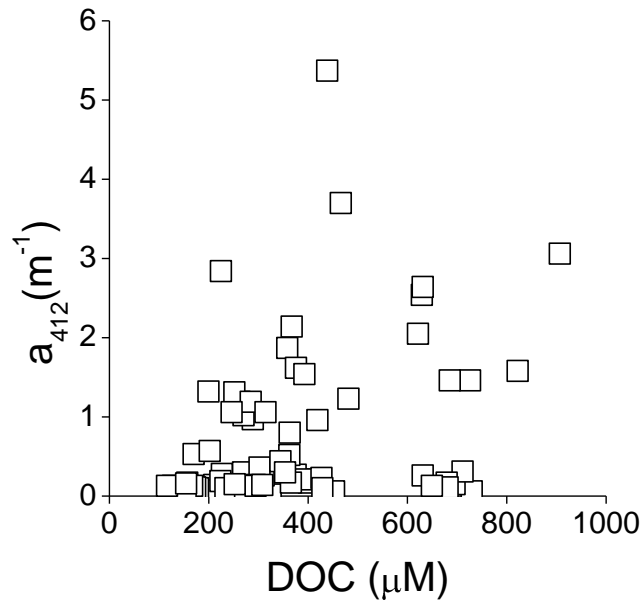


Figure 10 DOC vs. Absorption Coefficients at 412, 254 and 355 nm.

Table 3 Linear Fit Regression for DOC vs. $a_{(412,254,355)}$

nm	R	R ²	SD	N	P
412	0.37	0.14	0.91	80	6.84E-4
254	0.36	0.13	10.39	80	7.67E-4
355	0.40	0.16	2.29	80	2.25E-4

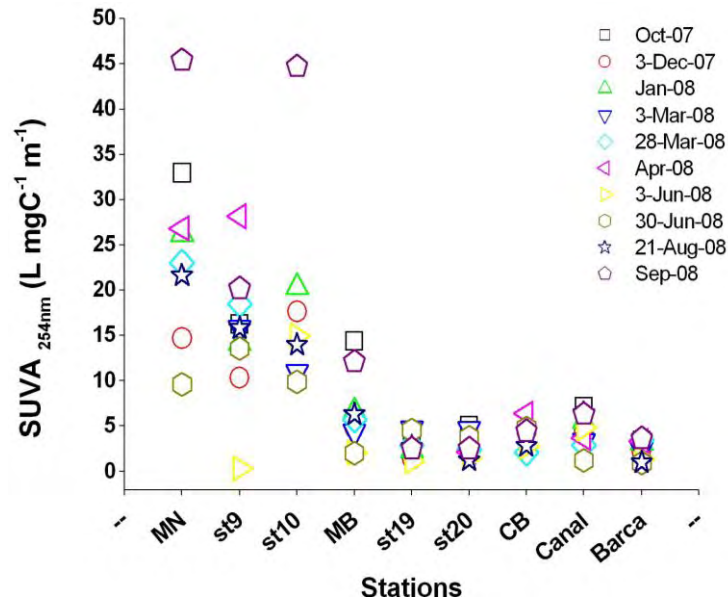


Figure 11 SUVA₂₅₄ spatial dynamic for Jobos Bay.

Fluorescence: Spatial and Seasonal Distribution

In general, there was a significant, negative correlation between salinity and the main fluorophores (Table 4). The strongest correlation was with region Tyrosine/Tryptophan like (B/T) and the weakest with region C (humic like) (Figure 12). A and B/T peaks showed the highest fluorescence (F_{max}) values in most cases. F_{max} varied from 13-230 QSU at MN, 2-17 QSU at MB, 1-42 QSU at Canal and 1-91 QSU at Barca.

At Barca, the protein region (B/T) was the dominant fluorescence peak, except in September when region A dominated. Region C showed the lowest fluorescence intensity.

Regions C and H viewed an increased fluorescence during the rainy period (September), which was higher than that of March but not the one in December. Peaks A and B/T presented maximum fluorescence in December when levels were 8 times greater than in March, which had the next highest values, followed by September and June (Figure 12). Regions A and B/T were 3 times higher in March than in June. Region H was 3 times higher in December than in June. A significant difference was presented between June and December ($F = 3.81$, $P = 0.039$) for Barca and Canal.

At Canal the highest fluorescence regions were B/T and A in June, followed by September, March and December. March represented the main peak in region H. Mar Blanco presented the main peak A in December and September followed by March and then June. However, the greatest fluorescence was observed in region H and B/T, in March and December, respectively. The maximum value for B/T region (December) was twice the March F_{\max} .

At Mar Negro, the main fluorophores were situated in the protein region followed by region A. The fluorescence intensity at this site was twice that found at Barca. September showed the highest fluorescence followed by June, December and finally March. Mar Negro showed the highest values for all fluorophores for all sampling sites (Figure 12). Peak C at MN presented the lowest fluorescence values compared with the other fluorophores, but, was approximately 10 times greater than in the other sampling sites.

In general, the main fluorophores presented a positive correlation with chlorophyll (Table 5). The highest correlation was observed with B/T region. At Barca a higher correlation with

chlorophyll was related to the protein region. Meanwhile, at Canal a higher correlation was established with peak C; at Mar Blanco with peak A and at Mar Negro with B/T and A regions.

Dissolved organic carbon presented no significant correlation in comparison with significant correlation presented by chlorophyll with the main fluorophores (Table 7). In Barca, a linear fit regression showed a higher relationship with the proteins; in Canal with H region; in MB with C and A region associated to humic terrestrial sources. Very low relationship was established considering all samples together.

Spatially, MN had the highest fluorescence intensity (FI) on peak C (42.13) as expected. Seasonally, the values can be organized in the following order: June > September > December > March. Site 20 showed the lowest FI for all sampling sites, with the highest value in September (2.38) and the lowest in June (0.607) (Figure 13). At Mar Blanco, the highest FI was in March (6.71) and the lowest in June (2.48), and values were similar for September and December. The highest FI at Canal was in June (6.31) and the lowest was in December (1.38). Barca had the lowest value in June (0.98) and the highest in December (3.69). Peak C did not present a strong seasonal pattern (Figure 14) but presented significant spatial differences. Mar Negro differed with Barca, Canal and st20 but it did not differ with Mar Blanco ($F = 8.91$, $P = 0.001$). At Barca and Site 20, the highest values were observed in September and December, but Canal and MN had their highest values in June while MB peaked in March. Barca and Site 20 showed the maximum values in December and September.

Table 4 Non-Linear Regression for Salinity vs. highest fluorescence (F_{\max}) (Mar Negro + Canal + Mar Blanco + Barca)

Region	R	R ²	SD	N	P
C	-0.47	0.22	13.47	16	0.065
H	-0.59	0.34	20.88	16	0.014
A	-0.69	0.47	40.92	16	0.002
B/T	-0.72	0.51	44.83	16	0.001

Table 5 Chlorophyll vs. F_{\max} (Linear Fit) regression by site.

Site	Barca	Canal	MB	MN	All
Region	R ²				
C	0.06	0.22	0.03	0.16	0.47
H	0.0007	0.13	0.01	0.41	0.57
A	0.08	0.06	0.33	0.76	0.67
B/T	0.10	0.10	0.02	0.81	0.71

Table 6 DOC vs F_{\max} (Linear Fit) regression by site.

Site	Barca	Canal	MB	MN	All
Region	R ²				
C	0.13	0.09	0.73	-	0.06
H	0.19	0.89	0.50	-	0.03
A	0.39	0.0009	0.71	-	0.05
B/T	0.69	0.014	0.55	-	0.06

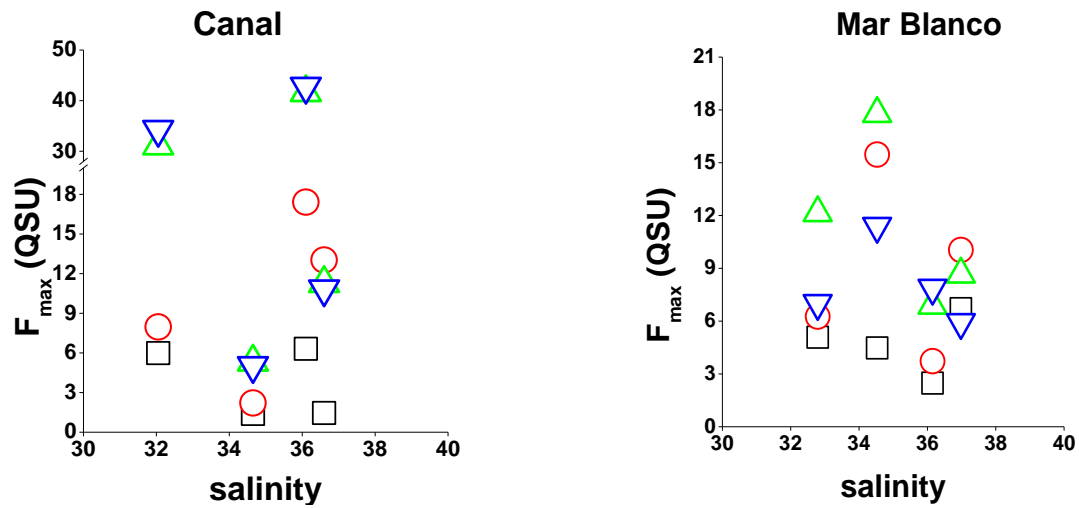
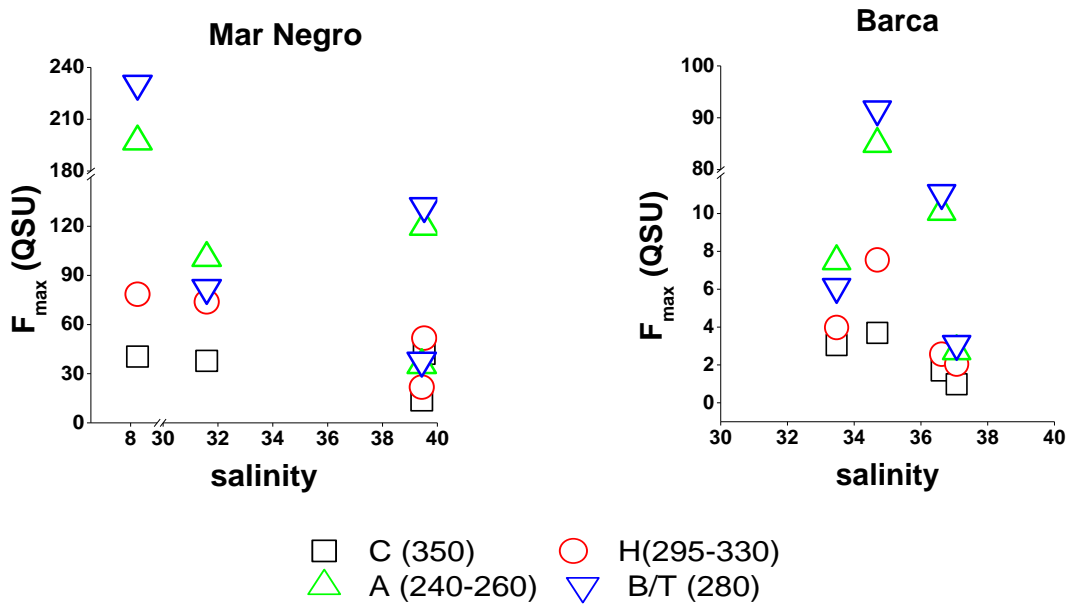


Figure 12 Salinity vs. Fluorescence Maximum (F_{max}) at four sampling sites (Mar Negro, Barca, Canal, Mar Blanco) in four months of the year (December 2007, March 2008, June 2008 and September 2008).

Table 7 Pearson's correlation between fluorophores regions and salinity, chlorophyll, DOC, a_{350} .

	Region H (295-330)	Region A (240-260)	Region C (350)	Region B/T (280)
Salinity	R= -0.667 P = 0.003	R= -0.7 P = 0.002	R = -0.496 P = 0.043	R = -0.715 P = 0.001
Chlorophyll	R= 0.763 P = 0.000	R= 0.827 P = 0.000	R= 0.697 P = 0.001	R = 0.852 P = 0.000
DOC	R= 0.138 P = 0.669	R = 0.183 P = 0.570	R = 0.186 P = 0.563	R= 0.203 P = 0.528
a_{350}	R= 0.940 P = 0.000	R= 0.759 P = 0.000	R= 0.914 P = 0.000	R = 0.688 P = 0.002

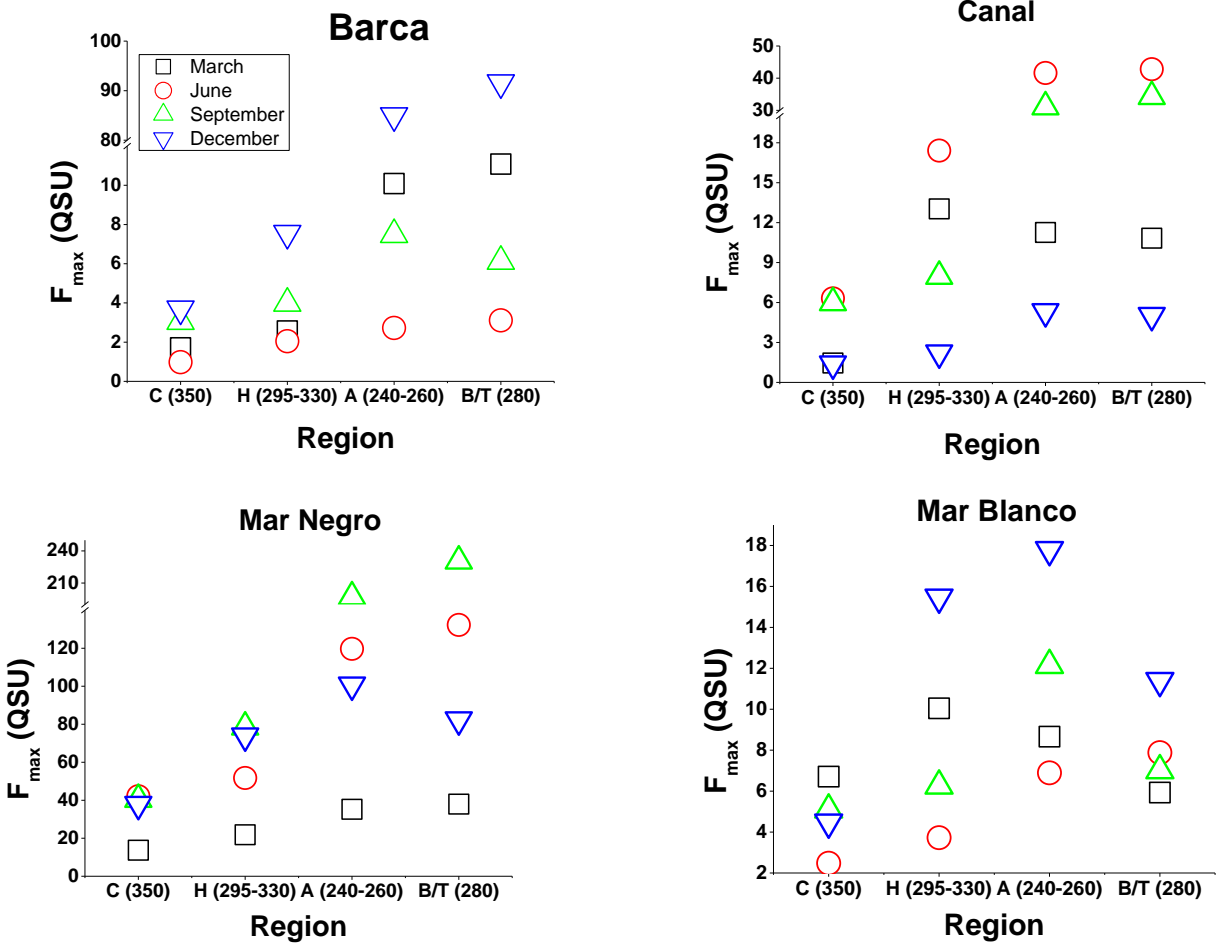


Figure 13 Seasonal and Spatial Variability in Fluorescence Intensity (F_{max}) (QSU) for JOBANERR in specific sampling areas (Barca, Canal, Mar Negro, Mar Blanco).

In general, the protein region (B/T) with excitation at 280 nm presented the highest values for all sampling sites. The highest value was recorded at Mar Negro in September (230.54) (Figure 15). June had the second highest value (132.29) at this site followed by December (82.33) and finally March (37.97). In December, Barca had the highest value (91.61) of all sites, but the other values for Barca were among the lowest recorded. Canal had its highest value in June (42.80) followed by September (34.28), March (10.83) and December (5.03). Mar Blanco showed low fluorescence in the protein region, with the highest value being 11.39 QSU in December. The lowest value at Site 20 occurred in June (1.35) and the highest was in September (20.37). The protein region did not present a seasonal pattern. MN and Site 20 had their maximum values in September, but MB and Ba showed the maximum values in December. The only site with maximum fluorescence in June was Canal. Spatially, the significant differences on region B/T were between MN, MB and st20 ($F = 4.37$, $P = 0.017$).

Region H showed a similar trend than that of Region C . The highest values were observed at MN where the highest F_{\max} was found in September (78.53) followed by December (73.85) > June (51.71) > March (21.83) (Figure 16). These values were six times higher than at Canal, the site with the second highest fluorescence. Fluorescence intensity was similar at Canal and MB but peaks were at different times. Barca and Site 20 had very low values at region H with the lowest value (0.95) for all sampling sites found in June at Site 20. On region H, significant differences were observed between MN and the other sites ($F = 12.9$, $P = 0.000$).

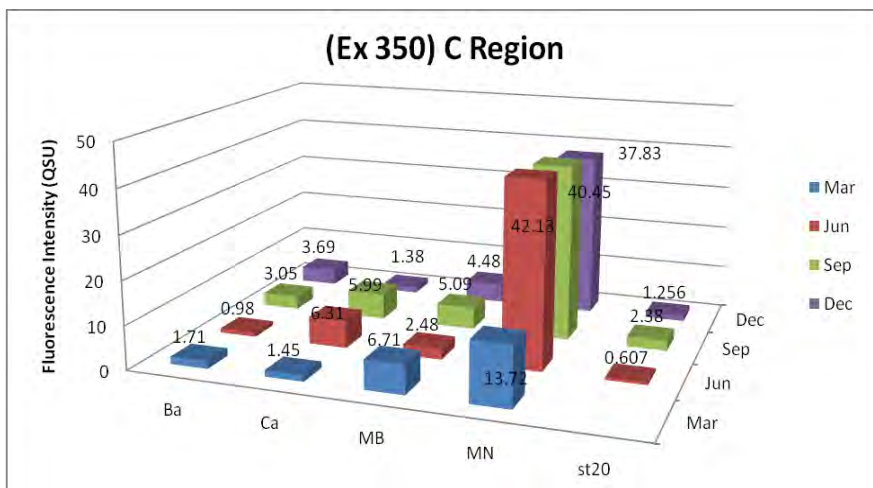


Figure 14 Fluorescence Intensity in quinine sulfate units (QSU) for C region (Excitation 350 nm / Emission 429-447) for sampling sites by 4 months (December 2007- March, June and September 2008)

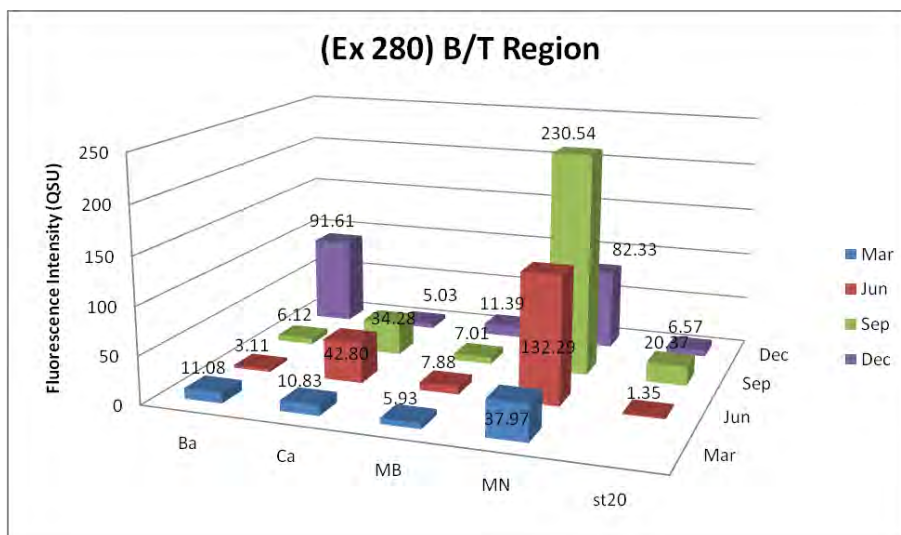


Figure 15 Fluorescence Intensity (QSU) for Proteins (B/T) region (Excitation 280 nm / Emission 315/451) for sampling sites in 4 months (December 2007- March, June and September 2008).

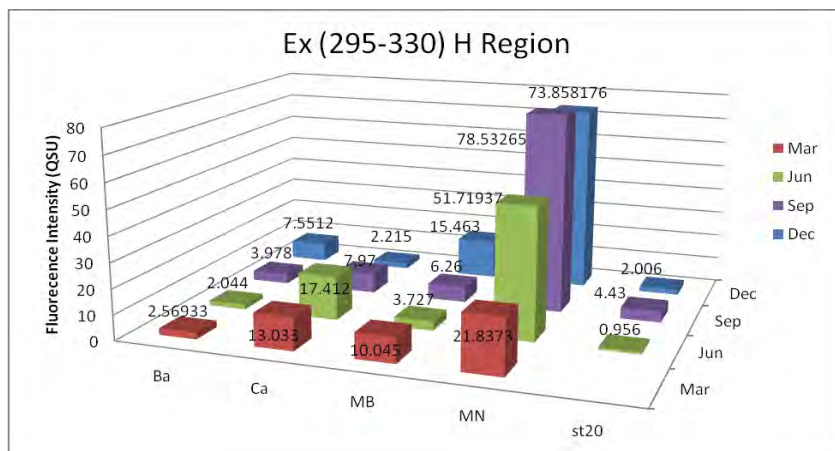


Figure 16 Fluorescence Intensity (QSU) for region H (Excitation 295-330 / Emission 337-443) for sampling sites in 4 months (December 2007- March, June and September 2008).

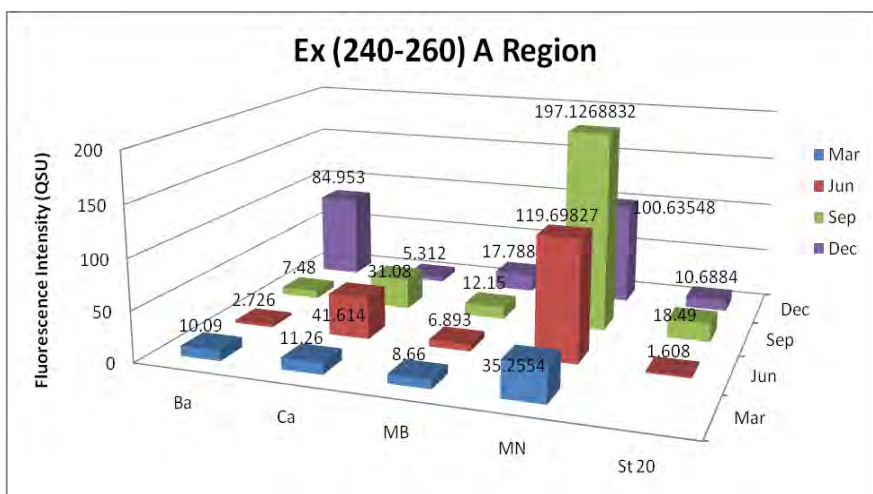


Figure 17 Fluorescence Intensity (QSU) for region A (Excitation 240-260 nm / Emission 321-429) for sampling sites in 4 months (December 2007- March, June and September 2008).

At Mar Negro, F_{\max} for region A was highest in September (197.12) and lowest in March (35.25) (Figure 17). Besides MN, the second to highest value was found at Canal in June (41.61) which is 4.5 times lower than that at MN for the same month; the lowest value at Canal was recorded in December (5.31). The highest value at Barca occurred in December (84.95), a value similar to MN for the same month, and the lowest value was observed in June (2.72). MB and Site 20 presented the lowest values for region A. The lowest value was observed at Site 20 in June (1.60). This region did not present a seasonal pattern. Region A presented significant differences on spatial scale. MN differed from MB and st20 ($F = 4.23$, $P = 0.019$).

In general, the main fluorophores did not display a seasonal pattern but presented spatial differences depending on fluorescence region. The highest values were generally found at MN with clear spatial pattern. There was high variability of fluorescence values between Canal and MB. The same variability was found between Barca and Site 20, although Site 20 consistently had some of the lowest values for the main fluorophores.

Photodegradation

Dissolved Organic Carbon

DOC values decreased exponentially with sunlight exposure ($R^2 = 0.90$) (Figure 18). DOC increased from 417.6 μM to 441.8 μM in the first 4 hr and then decreased exponentially reaching 342.1 μM after 96 hours (12963 KJ.m^{-2}). The final value represents an 18% loss of DOC over 8 days. In addition, DOC loss conformed well to a_{350} loss with $R^2 = 0.75$ by linear fit

regression (Figure 19). DOC concentration in dark samples increased in the first 4 hours from 427.1 μM to 433.8 μM , decreased for the following 12 hours (350 μM), and increased again reaching a higher value (375.2 μM) than samples exposed to sunlight. Pearson's correlation showed a significant negative correlation for DOC and UV dose under light exposure ($R = -0.872$, $P = 0.002$) and negative no significant correlation on dark conditions ($R = -0.564$, $P = 0.114$). Similar results were observed between DOC and a_{350} . Positive significant correlation on light conditions ($R = 0.871$, $P = 0.002$) and negative no significant correlation on dark samples ($R = -0.366$, $P = 0.333$).

Absorption Coefficient (a_{350})

Sunlight exposure caused significant changes in the optical properties of Mar Negro seawater. After 96 hours (12963 $\text{KJ}\cdot\text{m}^{-2}$) of sunlight exposure, the absorption coefficient (a_{350}) decreased from 5.11 to 2.03 m^{-1} , with no significant change observed in dark samples (5.25 to 5.12 m^{-1}). Absorption loss conformed well to an exponential decay model with $R^2 = 0.98$ ($f = a \cdot \exp(-b \cdot x)$) (Figure 20). Pearson's test showed negative significant correlation between a_{350} and UV dose (light, $R = -0.981$, $P = 0.002$; dark, $R = 0.365$, $P = 0.334$).

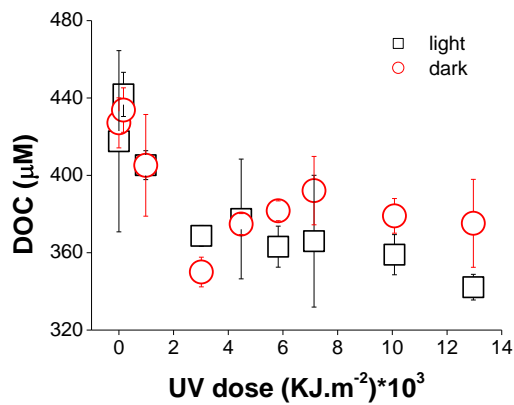


Figure 18 DOC changes on samples exposed to sunlight (light) and kept in the dark during 96 hours of natural sunlight exposure (8 days or 12963 KJ.m⁻² UV dose).

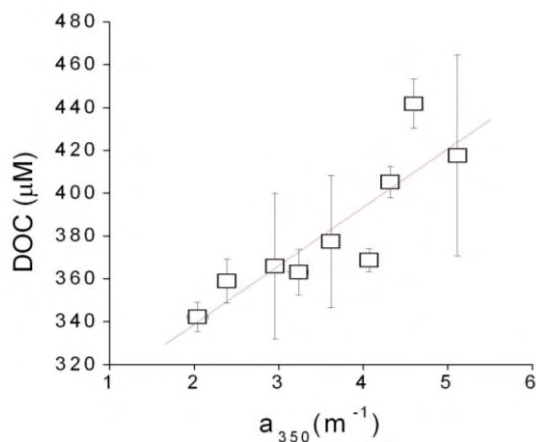


Figure 19 Absorption coefficient (350 nm) vs. Dissolved Organic Carbon (Standard Deviation Bars) exposed to natural sunlight.

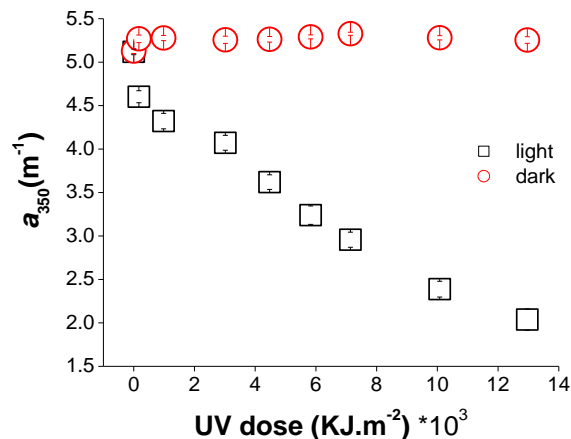


Figure 20 UV dose with natural sunlight vs. absorption coefficient at 350 nm. Exponential decay (first order kinetic).

Slope Ratio (S_R)

The S_R had a narrow range from 1.18 to 1.15 in samples without exposure to sunlight, and 1.64 to 1.15 in those with exposure (Figure 21). S_R increased over time with sunlight exposure and correlated positively (Linear Fit) with irradiance ($R^2 = 0.96$). S_R vs. FI showed an exponential decrease ($R^2 = 0.60$) (Figure 22). S_R showed negative significant correlation with DOC ($R = -0.824$, $P = 0.006$).

Fluorescence Index (FI)

In this study, FI ranged from 1.31 to 1.46, possibly related to terrestrial sources (McKnight *et al.*, 2001) of CDOM. FI correlated positively with the absorption coefficient at 350 nm ($R^2 = 0.53$) and DOC ($R^2 = 0.50$) (Figure 22). The Fluorescence Index correlated positively with UV Irradiance in a first order exponential decay ($R^2 = 0.69$) and with Linear Fit Regression ($R^2 = 0.49$) (Figure 22), but did not correlate with dark samples ($R^2 = 0.10$).

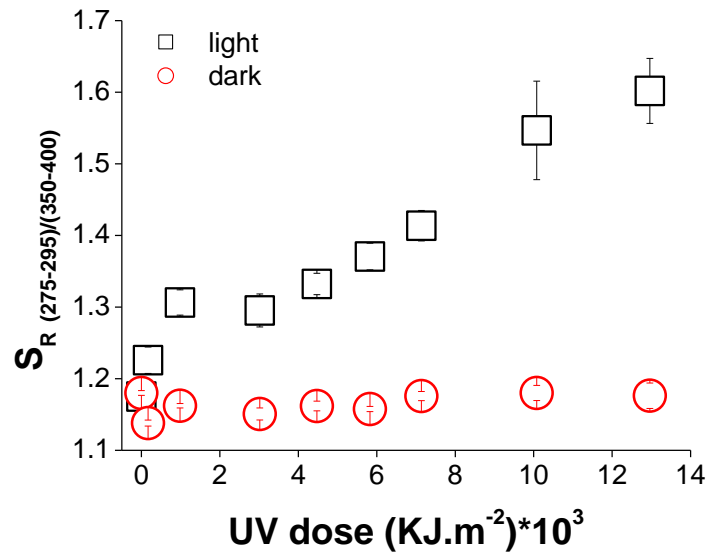


Figure 21 UV dose vs. Slope Ratio (Helms *et al.*, 2008) for dark and light samples.

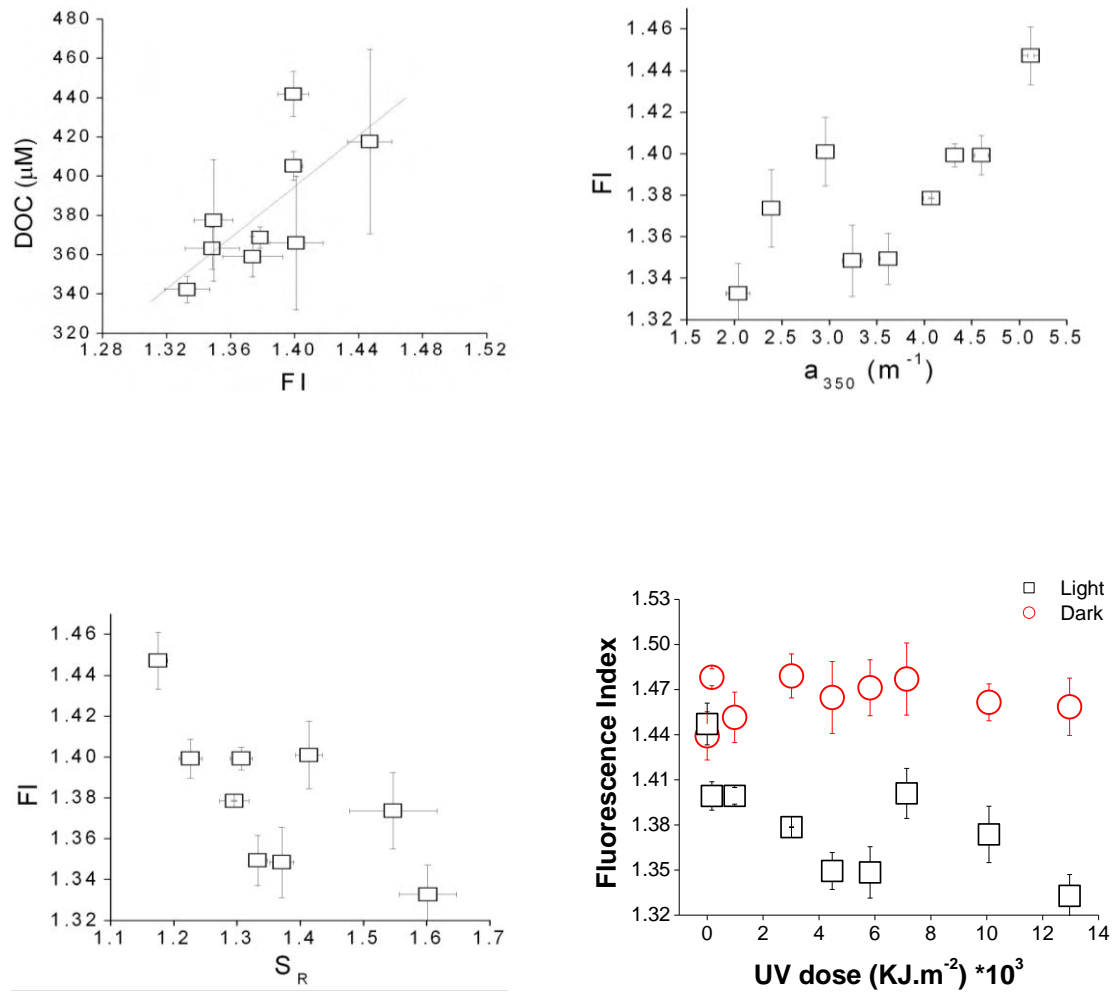


Figure 22 Fluorescence Index vs. DOC; Absorption coefficients at 350 nm vs. Fluorescence Index; Slope Ratio vs. Fluorescence Index; UV dose vs. Fluorescence Index.

Fluorescence: EEM's and PARAFAC

To identify the fluorescent components, Excitation-Emission Matrix (EEM) techniques were applied to photodegradation data combined with a PARAFAC model. Seven components were identified with PARAFAC. They are similar to the components reported in the literature. Component 1 has two excitation (Ex) peaks, the main peak at 295 and a secondary peak at < 250 nm with a spread emission (Em) at 382-450 nm (Figure 23). This component was similar to the traditionally assigned marine humic-like peak M (Coble, 1996). The peak position of this component was also similar to PARAFAC components previously reported, i.e., terrestrial/autochthonous humic-like C3 by Stedmon and Markager (2005), terrestrial humic-like C1 by Yamashita and Jaffé (2008) and marine humic-like C6 in Yamashita *et al.* (2008). Thus, this component can be categorized as a ubiquitous terrestrial humic-like component.

Component 2 presented peaks at Ex = 265 (365) nm and Em = 463 nm (Figure 23), and can be categorized as traditional terrestrial humic-like peaks A and C (Coble, 1996). PARAFAC components similar to component 2 in this study are reported as microbial humic-like C5 that is abundant in Florida Coastal Everglades (Yamashita and Jaffe, 2008) and as microbial reduced quinone-like component (SQ2) by Cory and McKnight (2005). The PARAFAC component found in an open ocean sample (C1, Yamashita *et al.*, 2010) was also similar to this component. Thus, this component might be produced during microbial reworking of organic matter.

Component 3 peaked at Ex < 250 nm and Em = 464 nm and was categorized as terrestrial humic-like peak A (Coble, 1996). In the PARAFAC studies, similar components are determined as terrestrial humic-like C1 by Yamashita *et al.* (2008), photo-oxidized product (C3) in Stedmon

et al. (2007) and exported by agricultural catchments by Stedmon and Markager (2005). Thus, this component has terrestrial origin but might be produced during the process of photodegradation.

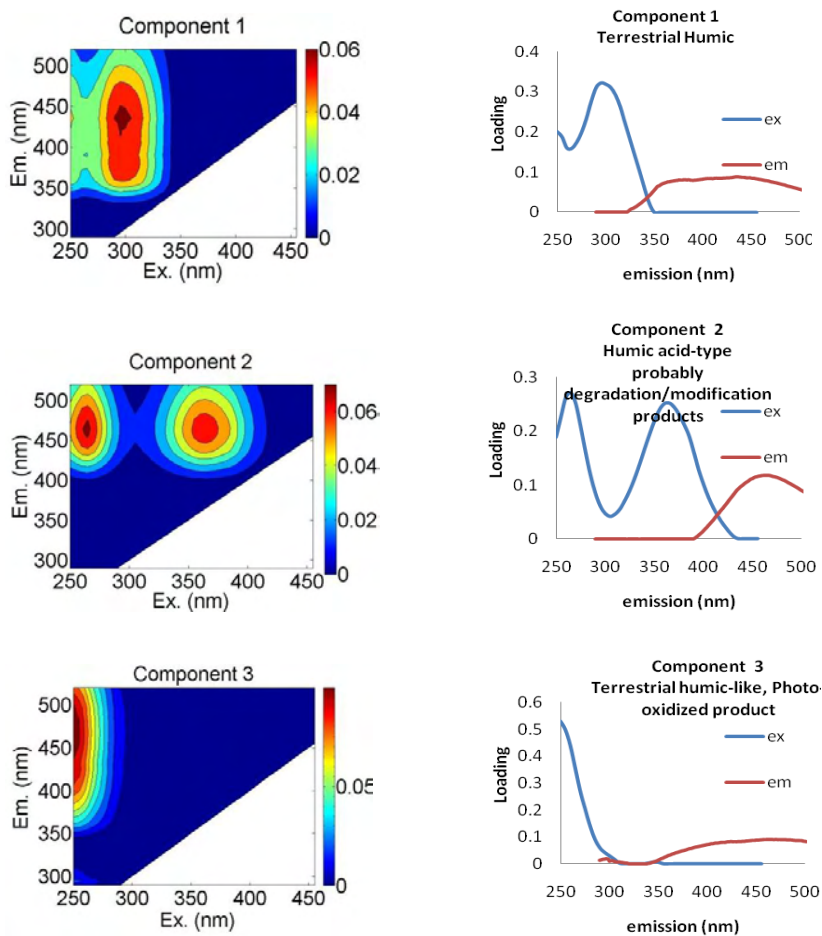
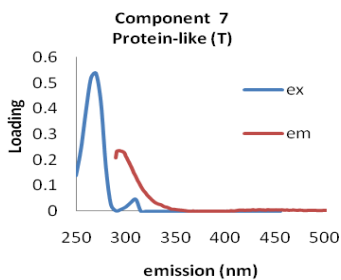
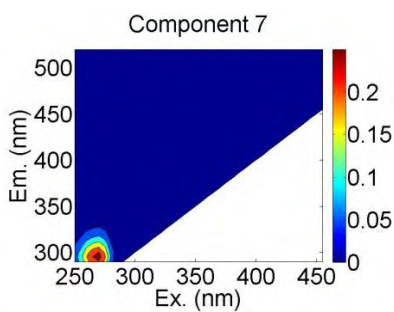
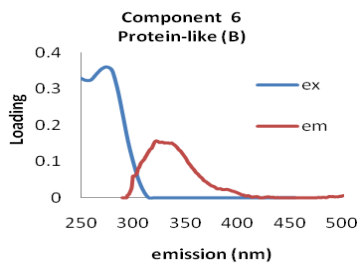
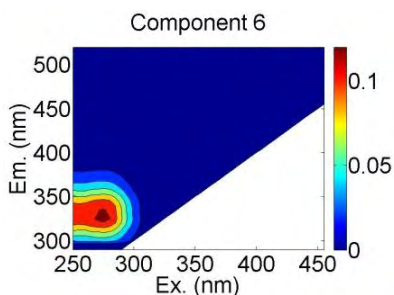
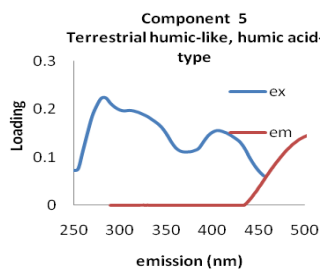
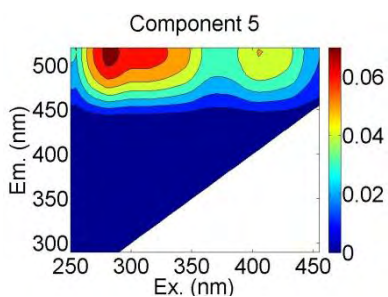
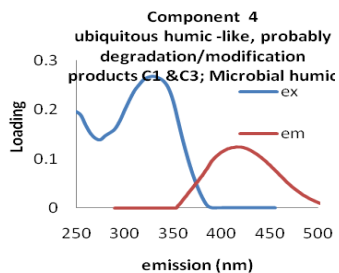
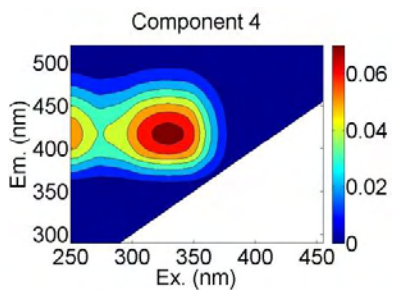


Figure 23 EEM's of the components identified by PARAFAC and their excitation and emission peaks.



Cont. Figure 23 EEM's of the components identified by PARAFAC and their excitation and emission peaks.

Component 4 peaked at $\text{Ex} = 330$ (250) nm and $\text{Em} = 415$ nm (Figure 23). It has been identified as similar to traditional humic-like peak C or marine humic-like peak M (Coble, 1996). Similar components were also assigned as microbial humic-like by Stedmon and Markager (2005) and ubiquitous humic-like and were probably degradation/modification products C1 and C3 for Florida Coastal Everglades by PARAFAC.

Component 5 showed a broad range of Ex loadings and peaked at $\text{Ex} = 285$ (405) nm and $\text{Em} = 515$ nm. This component showed characteristics associated with high molecular weight and aromatic organic compounds (Kowalczyk *et al.*, 2009; McKnight *et al.*, 2001; Stedmon *et al.*, 2003). Similar components are reported in the literature as terrestrial humic-like C2 by Yamashita and Jaffe (2008), terrestrial reduced quinone-like SQ1 by Cory and McKnight (2005), and humic acid-type C2 by Santin *et al.* (2010).

The components 6 and 7 in this study showed peak maxima in the protein-like fluorophores region. They represent tryptophan-like and tyrosine-like fluorophores, respectively (Coble, 1996; Yamashita and Tanoue, 2003). Stedmon and Markager (2005) described their origin as an autochthonous microbial source. The fluorescence characteristics of these components are comparable to spectral characteristic of polyphenols such as gallic acids and tannins (Maie *et al.*, 2008). The spectral properties of both protein-like components may represent the binding of their organic molecules having a complex effect on fluorescence (Kowalczyk *et al.*, 2009).

Significant difference was identified between components showed by PARAFAC (light, One way ANOVA $F = 6.72$, $P = 0.000$; dark, Kruskal Wallis $H = 57.81$, $P = 0.000$) (Table 9). The differences were showed between component 1 and 3 (light + dark) and 7 (dark) with no differences between component 1 and components 2, 3, 4, 5 and 6. Component 2 differs from component 3 (light) and components 5, 6 and 7 (dark). Component 3 was different to components 4 (light), 5, 6 and 7 (light + dark). Component 4 was different to components 5 and 7 (dark).

Visual analysis of EEM's showed the maximum fluorescence intensity (F_{\max}) on peak A. F_{\max} decreased from 22 QSU, at the beginning of the experiment, to 10 QSU, after 96 hours of sunlight exposure (Figure 24). Peak M began at 16 QSU at time zero and decreased to 10 QSU at the end of the experiment. Visually, this peak is not very well defined and differs by approximately 3 QSU from the PARAFAC model component. Peak C was also not very well defined with a broad Ex/Em (325-400/400-500) range and F_{\max} ranging from 16 to 7 QSU at time zero, and from 10 to 4 after 96 hours of exposure. A well-defined peak, B/T appears at 9 hours with a value of 7 QSU and disappears when exposure increases. On other hand, the PARAFAC model identified 7 components with similar F_{\max} . The model identified 3 additional components compared to the visual analysis (EEM) technique (Figure 25-26).

The maximum fluorescence (F_{\max}) for components 1 and 2 (M and A/C peak; Coble 1996) were similar in samples exposed to light, starting with 13 and ending with 4 QSU. At zero light exposure, Component 3 (Region A) had the highest F_{\max} , which decreased from 22 to 10 QSU during the course of the experiment.

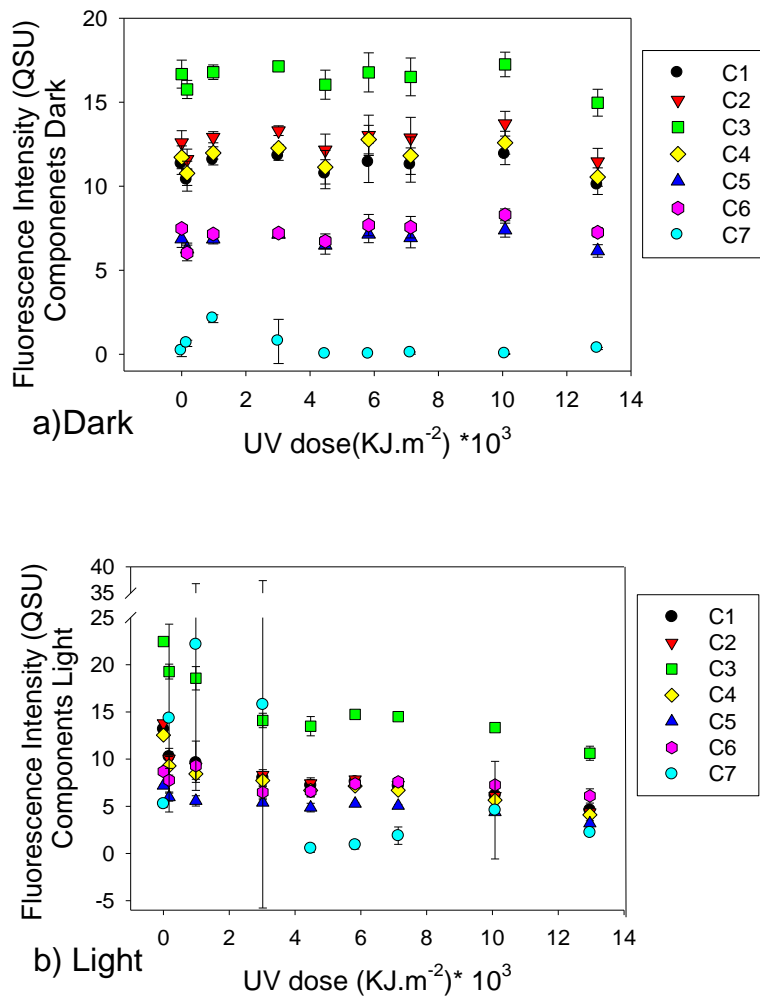


Figure 24 UV dose vs. Fluorescence Intensity of components identified by PARAFAC (a) Dark samples (b) irradiated samples.

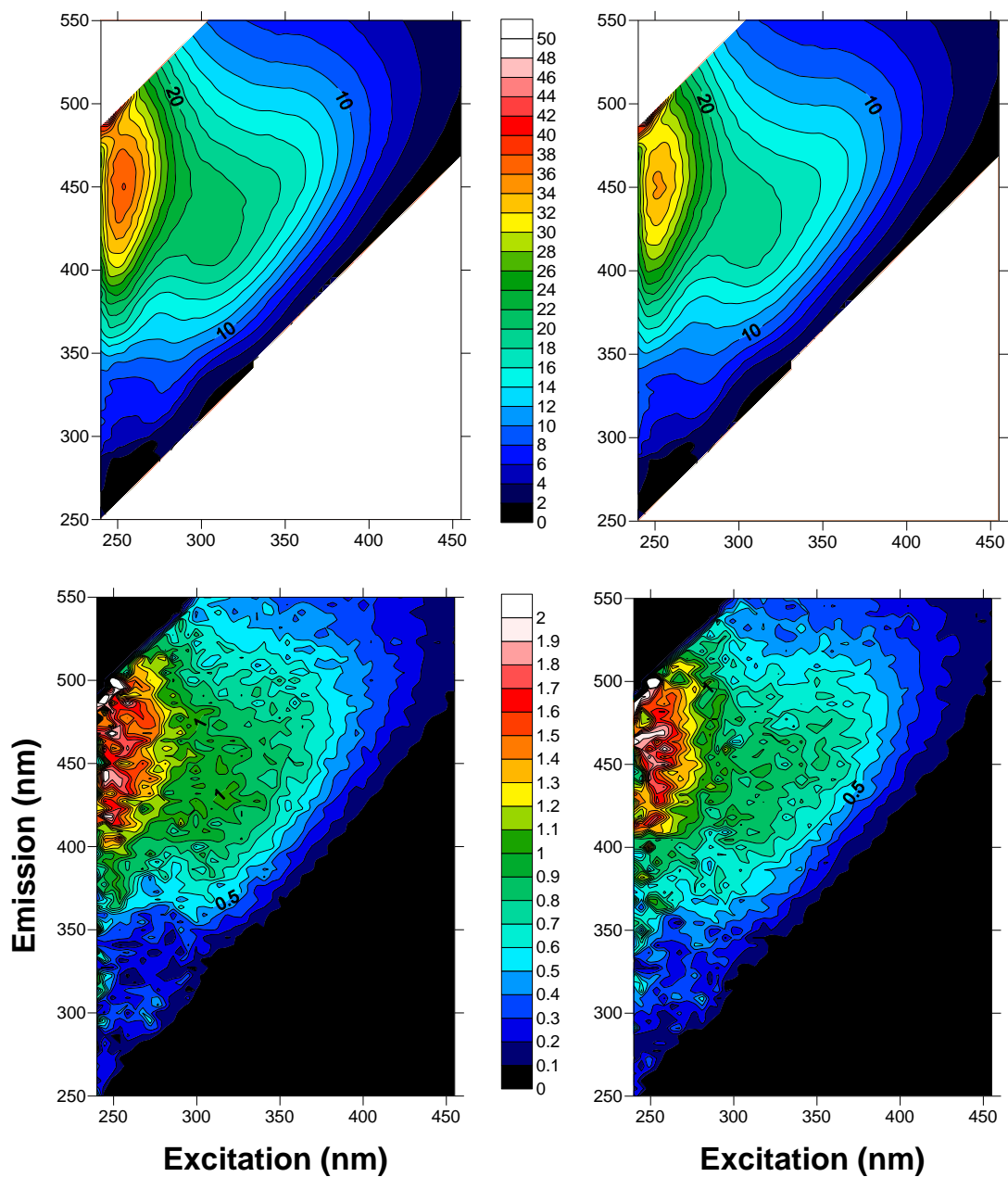


Figure 25 EEM's Average for **dark** samples in the top left (a) 0hr and top right (b) 96 hr Fluorescence Intensity in Quinine Sulfate Units (QSU) and EEM for Standard Deviation in the bottom left (c) stdev 0hr bottom right (d) stdev 96hr

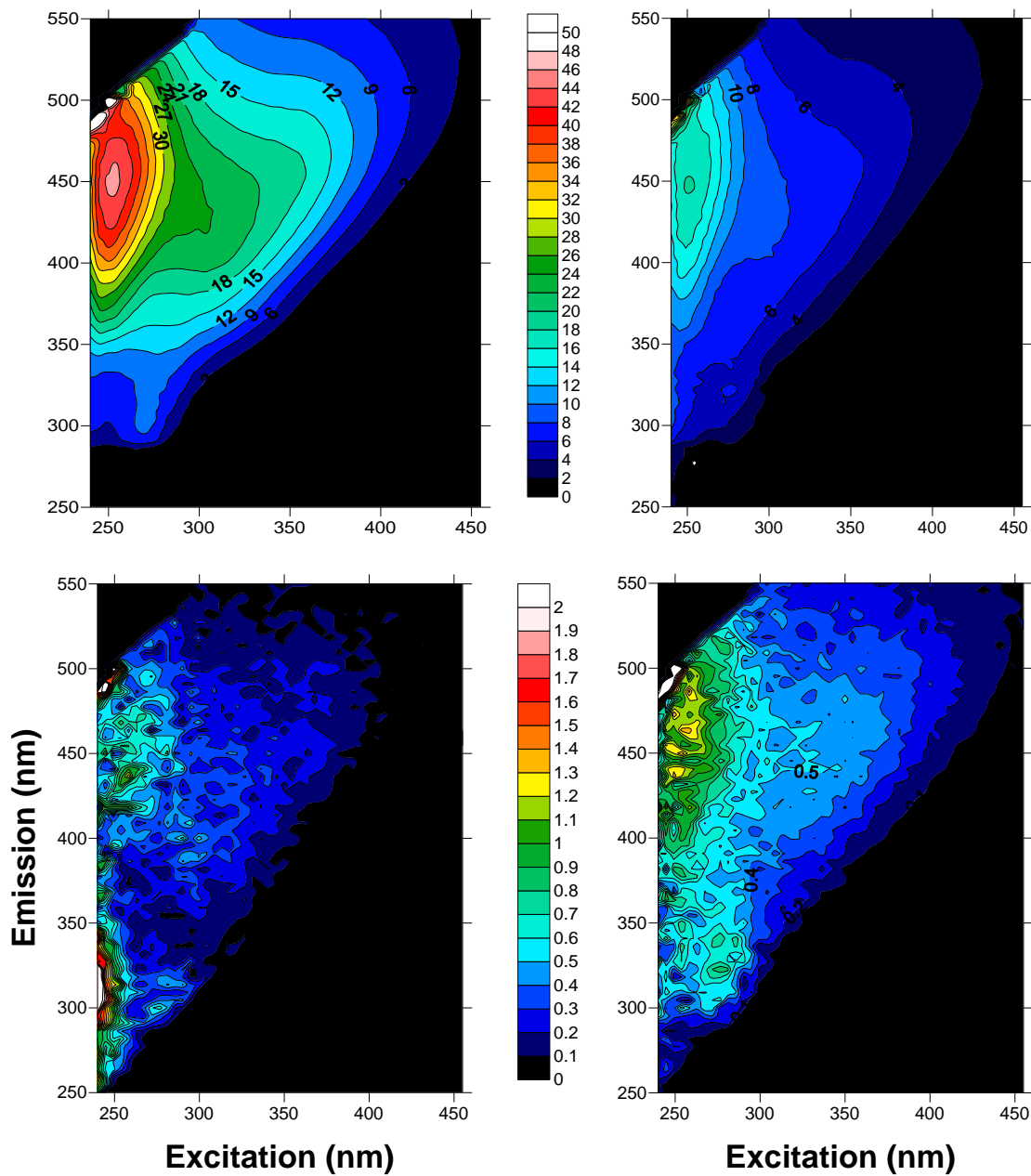


Figure 26 EEM's Average for **light** samples in the top left (a) 0hr and top right (b) 96 hr Fluorescence Intensity in Quinine Sulfate Units (QSU) and EEM for Standard Deviation in the bottom left(c) stdev 0hr bottom right (d) stdev 96hr

The values of component 4 (Region C/M) were very similar to C1 and C2. A narrow range (7 to 3) was found for component 5 during the experiment. Similarly, C6 (peak B, protein-like) presented a narrow range (8 to 6). A different pattern was observed at C7 (peak T, protein-like); F_{\max} increased from 5 to 22 in the first 9 hours and decreased with longer exposure time, with short periods of increase (Figure 24-27). A positive exponential decrease of maximum fluorescence with exposure time was observed (C1 $R^2 = 0.82$; C2 $R^2 = 0.77$; C3 $R^2 = 0.75$; C4 $R^2 = 0.77$; C5 $R^2 = 0.78$; C6 $R^2 = 0.34$; C7 $R^2 = 0.30$) (Table 8). Although fluorescence intensity and exponential decay were similar for components 1, 2, 4 and 5, they presented peaks at different excitation and emission areas with individual fluorescence spectra. Similar spectral signals were observed for components 6 and 7 (Figure 25-26). Another positive linear relationship was observed between F_{\max} and a_{350} (C1 $R^2 = 0.84$; C2 $R^2 = 0.88$; C3 $R^2 = 0.41$; C4 $R^2 = 0.87$; C5 $R^2 = 0.8$; C6 $R^2 = 0.04$; C7 $R^2 = 0.01$).

Table 8 First order kinetic for UV dose vs. PARAFAC components

Component F_{\max}						
vs.	R	R^2	SE	N	P	$f = a \cdot \exp(-b \cdot x)$
UV exp decay						
C1	0.91	0.82	1.05	9	0.0004	$y = 0.0034e^{-3E-04x}$
C2	0.89	0.77	1.26	9	0.0011	$y = 0.0035e^{-3E-04x}$
C3	0.88	0.75	1.83	9	0.0016	$y = 0.0043e^{-3E-04x}$
C4	0.89	0.77	1.12	9	0.001	$y = 0.0033e^{-3E-04x}$
C5	0.9	0.78	0.5	9	0.0009	$y = 0.0027e^{-3E-04x}$
C6	0.65	0.34	0.83	9	0.05	$y = 0.0031e^{-3E-04x}$
C7	0.62	0.3	6.56	9	0.07	

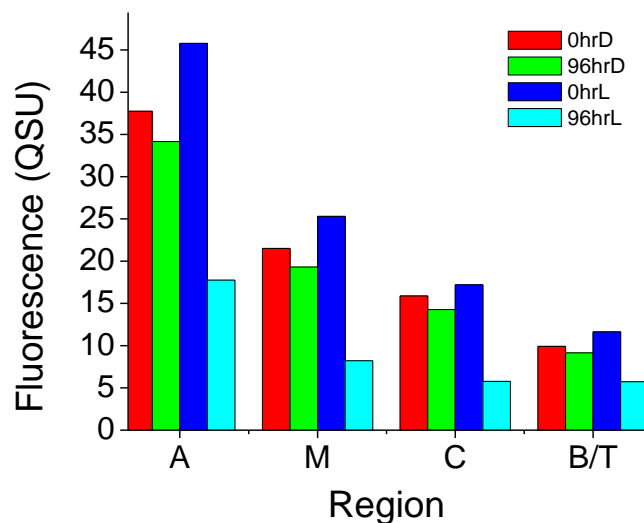


Figure 27 Fluorescence intensity of the main fluorophores (named by Coble 1996) at zero UV dose and (96hr) 8203 UV dose (KJ.m^{-2}). D = dark, L = light

Table 9 Differences between components identified by PARAFAC.

Fluorophore/ Component PARAFAC	1	2	3	4	5	6	7
1							
2							
3	LD	L					L
4			L				
5		D	LD	D			
6		D	LD				
7	D	D	LD	D			

Light (L): $F = 6.72$ $P = 0.000$ No normal data, Johnson normalization, ANOVA, Tukey's test
 Dark (D): $H = 57.81$ $P = 0.000$ Kruskal-Wallis

Photodegradation of Nitrogen Products

Total nitrogen (TN) presented a similar trend to DOC under the same environmental conditions. TN decreased exponentially with the UV dose ($R^2 = -0.92$) and had a negative tendency in the dark sample ($R^2 = -0.36$) (Figure 28). Pearson's test showed significant negative correlation with samples exposed to light ($R = -0.86$, $P = 0.003$) and non significant negative correlation with dark ($R = -0.504$, $P = 0.166$). In the first 4hr or 107 KJ.m^{-2} the TN value increased $20 \mu\text{M}$ (light) and $6 \mu\text{M}$ (dark) suggesting microbial reworking of the sample. After 8hr TN decreased $38 \mu\text{M}$ units in sunlight exposure and $39 \mu\text{M}$ in the dark sample. Both treatments presented increasing and decreasing fluctuations throughout the experiment. In the last hours TN in dark samples increased again. Meanwhile, TN values of irradiated samples continued decreasing.

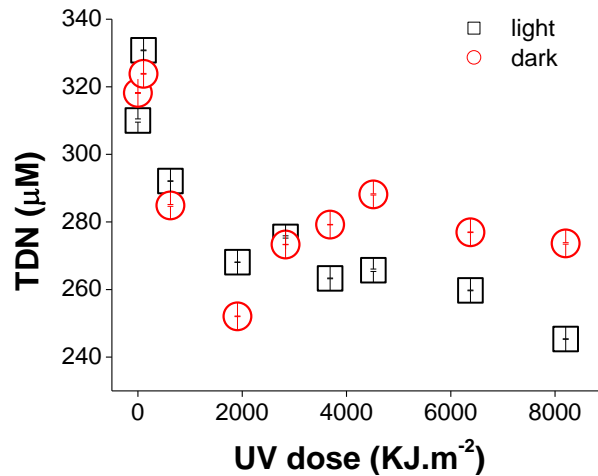


Figure 28 UV dose exposures vs. Total Dissolved Nitrogen.

NH_4^+

Polynomial Regression for UV vs. NH_4^+ was observed in the experiment [$Y = A + B1 * X + B2 * X^2$] ($Y = 2.00686 + 0.00199 X - 4.81148E-7 X^2$) ($R^2 = 0.77$, $SD = 0.66$, $n = 7$, $P = 0.05$). Slightly loose NH_4^+ concentration in the first 4 hr suggests microbial uptake of this component (Figure 29). Then the values showed NH_4^+ production in both dark and exposed samples, showing the same pattern. Pearson's test showed no significant correlation between NH_4^+ and UV dose (light, $R = -0.087$, $P = 0.852$; dark, ($R = 0.016$, $P = 0.973$).

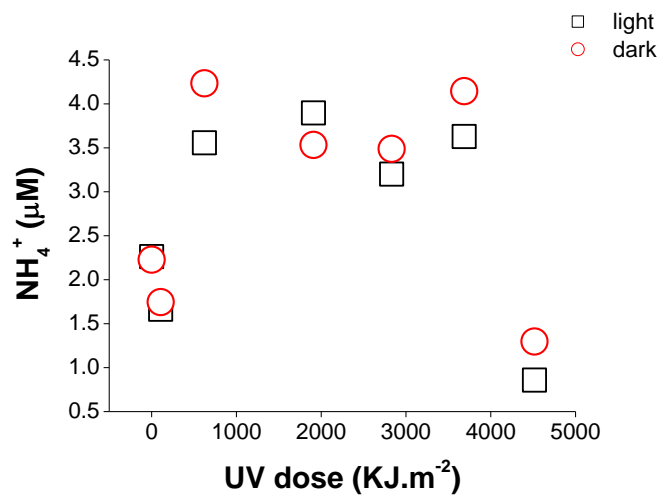


Figure 29 UV dose vs. NH_4^+ exposed to natural sunlight.

DISCUSSION

Absorption Coefficient

Mangroves are a significant source of CDOM at Jobos Bay especially during the wet season when the highest absorption values are observed in the mangrove-lined areas. A decrease is observed in waters further offshore. The maximum absorption coefficient (a_{412}) through the year concurs with the maximum precipitation on the area, and occurs within the mangrove zone. The high concentration of CDOM can be associated with terrestrial sources, salinity change and microbial or phytoplankton changes. In coastal environments, mixing of low salinity, high CDOM waters with lower CDOM seawater and CDOM photodegradation both cause changes in the optical properties (e.g. Bricaud *et al.*, 1981; Morel, 1988; Carder *et al.*, 1989; Vodacek *et al.*, 1997; Del Castillo *et al.*, 2000; in Keith *et al.*, 2001). Despite the internal consistency of our observations from month to month, the system is sufficiently heterogeneous, and CDOM absorption and spectral slope did not exhibit a clear seasonal pattern.

A low general correlation between salinity and a_{412} was observed but monthly regressions showed the influence of the dilution process in CDOM dynamics. The degree of influence of terrestrial components changed throughout the year and was mostly dependent on precipitation over the Jobos Bay watershed. We divided the study area in two zones: Inner mangrove and outer bay; but we could not distinctly separate the data by seasons (wet and dry). Precipitation in the zone is variable and alters the relation between our optical parameters. Other

major factors that may affect optical seawater properties at Jobos Bay are in situ phytoplanktonic production and organic matter photodegradation.

CDOM absorption presents a blue shift when the source changes from terrestrial to marine. This variable is useful in detecting the dominant source of CDOM in coastal and marine environments (e.g. Maie *et al.*, 2006). The samples of Barca and Canal presented a small blue shift that can be interpreted as a change from terrestrial to marine CDOM sources. Samples from Barca and Canal presented a mixture of both sources.

Slope

In agreement with other studies (e.g. Blough and Del Vecchio, 2002 and references therein), S values were larger for offshore seawaters ($\geq 0.02 \text{ nm}^{-1}$) than for coastal waters, which are influenced by river input ($0.013\text{-}0.018 \text{ nm}^{-1}$). This increase in S suggests a loss of aromaticity and a decrease in the CDOM average molecular weight in offshore waters. Recent laboratory and fieldwork indicates that photochemical bleaching can produce the same effect (Helms *et al.* 2008; Blough and Del Vecchio, 2002). Coastal margins not affected by river inputs generally show low $a_{\text{CDOM}(355)}$ ($< 0.25 \text{ m}^{-1}$), no (or little) correlation between absorption and salinity, and less seasonal variability (e.g. Blough and Del Vecchio, 2002 and references therein). In agreement, this general trend is observed at Jobos Bay with lower S values in the mangrove area and higher S out of the bay. Bay morphology and hydrology may contribute to this spatial pattern for S in Jobos Bay. Del Castillo *et al.* (1999) indicated that for Orinoco River discharge, S was independent of salinity for waters with values lower than 30. They suggested that this

independence implies there is no significant change in the optical properties and the chemical composition of the riverine organic matter within this salinity range. For Jobos Bay, plotting S versus salinity indicated that there was no dependence of S on salinities from 25 to 40. The decrease in S reported for offshore Baltic waters is explained by the presence of phytoplankton-derived CDOM further processed by bacteria and/or by photo-oxidation (e.g. Astoreca *et al.*, 2009). Low S values (0.012 nm^{-1}) similar to those were found in our mangrove zone (0.013 nm^{-1}) and have been reported for CDOM accumulated during the decaying phase of diatom cultures (e.g. Poulet, 2005 in Astoreca *et al.*, 2009). Keith *et al.* (2001) suggest that variability in S could be used as an indicator of the conditions under which accessory pigments become the primary absorbers of light in estuarine and coastal watersheds. A rather high S value (0.034 nm^{-1} (290–330 nm) was reported by Green and Blough (1994) in the Gulf of Mexico (Morel *et al.*, 2007) and a similar value was observed in this study at Barca calculating S from 200 to 690 nm.

CDOM in the mangrove area is principally of terrestrial origin. Mar Blanco is a transitional area between terrestrial and the marine organic matter sources in the bay. The absorption of light in these waters is highly dependent on CDOM. The center and the offshore areas are not as highly influenced by terrestrial CDOM as are Mar Negro, site 10 and site 9. These sites are also highly influenced by phytoplankton dynamics. From a beneficial standpoint, the strong absorption of CDOM in the UV portion of the spectrum protects phytoplankton and other biota from damaging UVB radiation (e.g. Blough & Zepp, 1990; Blough & Green, 1995; in Keith *et al.*, 2001). In the same way, this high CDOM absorption may stimulate or hinder primary production and temperature stratification (e.g. Mopper and Kieber, 2002; Kowalczyk *et*

al., 2010). The sources of CDOM can be traced through the bay but cannot be clearly identified by S and absorption parameters.

Chlorophyll

The relationship between chlorophyll a concentration and S has been applied in the Mid Atlantic Bight to assess the link between increased chlorophyll a levels and the production of *in situ* CDOM (Vodacek *et al.*, 1997 in Keith *et al.*, 2001). The present study found a strong positive correlation between chlorophyll and CDOM₄₁₂ at outer bay sites, and a low positive correlation in the mangrove enclosed areas. Correlation between CDOM optical properties and chlorophyll was used to differentiate between the products. The coefficients a_{355} and a_{412} were well correlated with chlorophyll suggesting that part of the CDOM in the area is produced by phytoplankton. Similar results were found at subtropical gyres suggesting a relationship between nutrient flux, DOM from depth and high irradiance that can generate a correlation between chlorophyll and CDOM (Siegel *et al.* 2005). At offshore waters from Bermuda (BATS), CDOM absorption did not correlate significantly with chlorophyll. However, measurements of CDOM from California and Baltic Sea were well correlated with chlorophyll (Kowalczyk, 1999; Kahru and Mitchell 2001; Blough and Del Vecchio, 2002; Nelson *et al.*, 2008). Some authors (Blough and Del Vecchio, 2002, references therein) have concluded that phytoplankton is the principal CDOM producer in offshore water but not in coastal areas. This positive relationship explains the high influence of phytoplankton/microbial production at the sampling sites suggesting a quick degradation of CDOM and efficient uptake of the molecules by phytoplankton in offshore areas. In waters with high CDOM concentration as Jobos mangrove-lined area, the

phytoplankton may use photosynthetic carotenoids (from 470 to 550 nm) having ecological implication on phytoplanktonic dynamics (Keith *et al.*, 2001). Clearly, CDOM absorption can cause overestimation of chlorophyll values using remote sensing techniques.

Photobleaching

The principal component of CDOM at the center, open or seagrass dominated areas of Jobos Bay appears to be derived from the phytoplankton and/or mangrove photodegraded matter. At local scales, *in situ* production from phytoplankton decomposition and extraction from benthic sediments may represent additional sources of CDOM (Kowalczyk, 1999; Kahru and Mitchell, 2001; Twardowski and Donaghay, 2001; Boss *et al.*, 2001). Recently, field and laboratory studies have shown that photobleaching alone is a sink of CDOM, with half-lives ranging from hundreds to thousands of hours (Vahatalo and Wetzel, 2004). Photobleaching of CDOM may not change the dissolved organic carbon concentration, but it results in an increase in the spectral slope coefficient, mainly due to relatively faster photobleaching in the UV-A (Vodacek *et al.*, 1997; Nelson *et al.*, 1998; Grzybowski, 2000; Whitehead *et al.*, 2000; Twardowski and Donaghay, 2001; Twardowski and Donaghay, 2002)

Dissolved Organic Carbon

Although the relationship between CDOM₃₅₀ and DOC can, in certain cases, be used to estimate the latter, it can be altered by the photodegradation process. This relationship is weaker in coastal regions with low river inputs (Blough and Del Vecchio, 2002) as is the Mar Negro

area. The relatively small change (18%) in DOC over a period of 8 days suggests recalcitrance and high molecular weight of the carbon contributors in the sample. DOC concentrations respond quickly to local changes in primary productivity and mineralization (Del Castillo *et al.* 1999). This study shows that DOC concentrations decrease concurrently with absorption and fluorescence index. This observation demonstrates that DOC from Mar Negro is semi-labile and moderately susceptible to photodegradation. Considering the totality of the data, the low relationship between absorption and DOC concentration in the bay point to highly recalcitrant molecules in the mangrove area and more labile matter in the open areas of the bay. $SUVA_{254}$ demonstrate the higher DOC recalcitrance in mangrove areas (MN, st9, st10). In addition, Barca presented the lowest recalcitrant DOC. Results from $SUVA_{254}$ confirm DOC recalcitrance and the photodegradation influence on DOC.

Fluorescence, photodegradation and PARAFAC

Linear regression analysis has shown that fluorescence intensity is related to a_{375} and that absorption coefficients may be inversely related to salinity (Kowalczyk *et al.*, 2005). This study at Jobos Bay showed similar results with regression analysis between a_{412} , fluorescence intensity and salinity. The fluorescence peaks, associated to terrestrial humic components, decreased when absorption decreased but the protein-like fraction decreased at a lesser degree than the others (Kowalczyk *et al.*, 2005).

The peak corresponding to tannin (280/314 as per Maie *et al.*, 2008) B/T in EEM's from Jobos Bay is affected by light exposure. The peak fluorescence intensity appears to decrease

during the transit across the bay from Mar Negro to Barca. Maie *et al.* (2008) studied the tannin degradation and concluded that light and water quality affects the transport of tannins and stimulates their polymerization. However, extensive exposure to light causes tannin depolymerization and can contribute to C and M peaks. Tannins can be eliminated in one day due to aggregation processes in high saline water, forming stable tannins-protein complexes (Maie *et al.* 2008). This processes may occur at Mar Negro, Site 9, Site 10 and Mar Blanco.

Various analyses and parameters including EEM, PARAFAC, Slope ratio(S_R), Fluorescence Index (FI) values, absorption coefficient (a) and DOC were applied to identify and asses the CDOM sources (Yamashita *et al.* 2009; Jaffe *et al.* 2008; Stedmon and Markager 2005; Kowalczuck *et al.* 2009; Kowalczuck *et al.* 2010) in Mar Negro. Photobleaching induces slope changes, as well as microbial utilization of colored dissolved organic matter (Del Vecchio and Blough, 2002; Del Vecchio and Subramaniam, 2004; Nelson *et al.* 2004). Photobleaching experiments with Mar Negro water showed significant loss of fluorescence and absorption properties. Absorbance decrease correlated positively with UV exposure (Kowalczuck *et al.*, 2005; Stedmon and Markager 2005; Zepp *et al.* 2004). At the same time, the slope and slope ratio increases show a positive correlation with UV dose, indicative of photodegradation effects on CDOM molecules (Helms *et al.*, 2008).

The fluorescence intensity of the main peaks decreased with the light exposure on this study. Analyses of EEM spectra indicated that five out of seven components decreased with decreasing absorption. The decrease of three peaks, A, M and C, with decreasing absorption may reflect changes in CDOM concentration with relatively minor changes in composition during

transport from the estuarine environment to oceanic waters (Kowalczyk *et al.*, 2005). Fluorophore A exhibited excitation maximum at 250 nm, where the solar irradiance at sea level is nil (Del Castillo *et al.*, 1999). Del Castillo *et al.* (1999) suggest that fluorophore A is not susceptible to photobleaching. However, in our experiment fluorophore A presented the mayor loss in fluorescence intensity during sunlight exposure.

The high correlation between F_{\max} of components 1, 2, 4 and 5 with a_{350} and UV dose (KJ.m^{-2}) is indicative of highly photo-labile components. Component 3 however presented a lower correlation, perhaps representing a photoproduct. Apparently, components 6 and 7 are dependent on the production or degradation of the first components. Components 1, 2 and 3 are considered terrestrial humic-like substances. Component 3 is sometimes described in the literature as a photodegradation product (Jaffe *et al.* 2008; Murphy *et al.* 2008). Component 4 was described by Stedmon and Markager (2005) as an anthropogenic agricultural source or as a microbial degradation product (Yamashita and Jaffe 2008; Stedmon and Markager 2005) as well as microbial-like derived from terrestrial source (Kowalczyk *et al.* 2009). Jobos Bay is located in an agricultural watershed. Mar Negro may thus be influenced by anthropogenic sources. Components 6 and 7 are categorized as protein-like components in the literature. Maie and collaborator (2008) working with tannins found a similar peak (280/314). Therefore, we describe these components in our samples as a protein and not as tannin.

PARAFAC results suggest that components 1, 5, 6 are the same and components 1, 3, 4 and 7 are different under light conditions. Components 1, 3 and 7 are different on dark conditions. Component 3 is not the same component as 2 in light samples. Components or

fluorophores 1, 2 and 4 are the same on Dark as are components 5 and 6. Components 1, 2 and 4 are the same in light conditions.

The model was evaluated for seven components combining light and dark samples to increase the number of samples in the model. At least 4 components are identified in Mar Negro by PARAFAC. It validated the model for 6 and 7 components under light conditions and validated the model for 5, 6 and 7 components in dark samples. The model may increase the number of components in the sample providing incorrect results.

A positive linear relationship was evident between Fluorescence Index (FI) and S_R . In addition, a regression showed a positive linear relation between S_R and FI with UV dose respectively. S_R values increased during photodegradation as has been observed elsewhere (Helms *et al.* 2008). The fluorescence index decreases with UV exposure (Cory *et al.* 2007) and observed values lower than 1.5 are consistent with fulvic acids from terrestrial sources, as occurs in large rivers in the United States (McKnight *et al.*, 2001). These tendencies in the parameters provide information about the sources and alteration processes (Yamashita *et al.* 2009) of the samples throughout the experiment.

Terrestrial components are highly influenced by photodegradation. The maximum degradation occurs during the first 12 hours. The CDOM produced in Mar Negro appears to undergo either polymerization or depolymerization by light. CDOM is an important source of carbon and nitrogen to biogeochemical cycles in the area. The proteins generated as photoproducts may be important sources sustaining nutrients dynamic. Changes in CDOM

sources and production can alter the biogeochemistry of Jobos Bay. Runoff and tidal exchange may exert considerable influence on the nutrient flux and CDOM concentrations in the bay. These changes may affect phytoplankton dynamic potentially reducing the light that penetrates in the water column. Mangroves contribute substantially to CDOM production in coastal zones with low or no river influence.

As found elsewhere (Stedmon *et al.*, 2003; Kowalczuck *et al.*, 2003; Stedmon and Markager, 2005a; Murphy *et al.*, 2008; Yamashita *et al.*, 2008; Kowalczuck *et al.*, 2010) our observations using EEM fluorescence spectroscopy indicate that CDOM composition changes substantially during transit from terrestrial sources to the open ocean. The tidal excursion in JOBANERR (the average distance traveled by a water particle during a half-tide cycle) is around 600 meters, decreasing eastward (Robles *et al.*, 2002). Considering tidal and wind effects, the mean residence time of a water mass in Jobos Bay is approximately 5.5 days (Robles *et al.*, 2002); sufficient for CDOM produced near the mangroves to be photodegraded.

NH₄⁺ and TN

In our experiments, no significant differences in ammonium production were observed between light irradiated and dark control samples. Ammonium has been shown to be photochemically produced in Orinoco river plume waters, rivers, and an estuary in southeastern USA (Morell and Corredor, 2001; Koopmans and Bronk, 2002; Smith and Benner, 2005) but not in our study. The propensity for DOM to release N photoproducts is thus likely dependent on the

source of the DOM and the light exposure history (Koopmans and Bronk, 2002). Mangrove leaves appear to be the main source of CDOM in Jobos Bay and vascular plants are known to remobilize N and P prior to leaf senescence and excision. This may explain why Jobos Bay CDOM differs from that of other locations such as the Orinoco River plume, where CDOM is presumably soil-derived and thus richer in microbially produced humic material. Meanwhile, TN presented significant differences under light conditions and no significant differences in the dark samples. It can be interpreted as a decrease in TN due to photoexposure. Sunlight exposure may affect the N cycle controlling the production of N products in a minor degree.

CONCLUSION

Slope, absorption and fluorescence can be useful as water mass tracers in the study area to identify the CDOM sources, origin and fate. The fact that the correlation of CDOM to salinity is low and that with UV dose is high, suggests that CDOM is highly influenced by photodegradation and slightly influenced by the dilution process. The components present in the bay are principally photo labile matter, as they appear to undergo photodegradation during transit through the bay. Photodegradation processes alter fluorescence intensity changing the optical properties of JOBANERR surface waters. The proteins generated as photoproducts may be important sources to sustain nutrients dynamics in the bay. EEM's and PARAFAC are valuable techniques to identify non-point sources of contamination or anthropogenic effects in Jobos Bay. The relatively small data set of EEMs in this study is representative of local and seasonal conditions, and is a good approximation of trend for the relationship between fluorescence intensities and salinity for small areas, such as Jobos Bay. Fluorescence is especially an useful

technique to identify fluorophores in DOM in clear waters with low CDOM concentrations (Kowalczuck *et al.*, 2005) and fewer factors influencing the optical properties of the waters. It is a much more sensitive technique than absorption, and provides additional information about the components present at the DOM pool.

Briefly, Jobos Bay coast is not highly influenced by freshwater and runoff. JOBANERR is characterized by : (1) high CDOM absorption decreasing towards offshore; (2) a CDOM that is not well correlated with salinity; (3) a strong correlation between CDOM and chlorophyll suggests a role of phytoplankton in the production of CDOM; (4) Photochemical process drives CDOM concentrations on the area; (5) Dilution may be a minor factor that influences CDOM optical properties at the bay, (6) a TN that is affected by photoexposure in a lesser degree and (7) a PARAFAC model that is useful to identify fluorophores and can be useful to determinate non-point pollution sources, but does not necessarily assert the correct fluorophore number.

LITERATURE CITED

- Andersson C.A., Bro R. (2000) The N-way toolbox for MATLAB. *Chemometr Intell Lab Syst* 52:1–4
- Bianchi T.S., (2007) Biogeochemistry of Estuaries. Oxford University Press.
- Blough, N.V., Del Vecchio R. (2002) Chromophoric DOM in the coastal environment, in *Biogeochemistry of Marine Dissolved Organic Matter*, edited by D. A. Hansell, and C. A. Carlson, pp. 509-546, Academic Press, San Diego.
- Brinkmann T., Sartorius D. and Frimmel F. H. (2003) Photobleaching of humic rich dissolved organic matter. *Aquat. Sci.* 65, 415–424 1015-1621/03/040415-10 DOI 10.1007/s00027-003-0670-9
- Ciotti A.M., Bricaud A. (2006) Retrievals of a size parameter for phytoplankton and spectral light absorption by colored detrital matter from water-leaving radiances at SeaWiFS channels in a continental shelf region off Brazil *Limnol. Oceanogr.: Methods* 4, 237–253
- Coble, P.G. (1996) Characterization of marine and terrestrial DOM in seawater using excitation - emission matrix spectroscopy, *Mar. Chem.*, 51, 325-346.
- Coble, P.G. (2007) Marine optical biogeochemistry: the chemistry of ocean color. *Chemical Reviews* 107 (2), 402–418.
- Coble, P.G., Schultz, C.A., Mopper, K. (1993) Fluorescence contouring analysis of DOC Intercalibration Experiment samples: a comparison of techniques. *Marine Chemistry* 41, 175-178.
- Colin A. Stedmon, Stiig Markager. (2005) Tracing the production and degradation of autochthonous fractions of dissolved organic matter by fluorescence analysis. *Limnology and Oceanography*, 50(5), 1415–1426
- Cory, R.M., and McKnight D.M. (2005) Fluorescence spectroscopy reveals ubiquitous presence of oxidized and reduced quinines in dissolved organic matter. *Environ. Sci. Technol.*, 39, 8142-8149.
- Cory, R.M., McKnight, D.M., Chin, Y.P., Miller, P., and C. L. Jaros (2007), Chemical characteristics of fulvic acids from Arctic surface waters: Microbial contributions and photochemical transformations. *J. Geophys. Res.*, 112, G04S51.
- Del Castillo C.E., Coble P.G., Morell J.M., Lopez M.L., Corredor J.E. (1999) Analysis of the optical properties of the Orinoco River plume by absorption and fluorescence spectroscopy. *Mar Chem* 66:35–51

- Del Vecchio, R., Subramaniam A. (2004) Influence of the Amazon River on the surface optical properties of the western tropical North Atlantic Ocean. *J. Geophys. Res.*, 109, C11001, doi:10.1029/2004JC002503.
- Detrés Y., Armstrong R.A., Connelly X.M. (2001) Ultraviolet induced responses in two species of climax tropical marine macrophytes. *Journal of Photochemistry and Photobiology B: Biology* 62, 55-66
- Dittmar T., Hertkorn N., Kattner G., Lara R. J. (2006) Mangroves, a major source of dissolved organic carbon to the oceans. *Global Biogeochem. Cycles*, 20, GB1012, doi:10.1029/2005GB002570.
- Dittmar T., Lara R.J., Kattner G. (2001) River or mangrove? Tracing major organic matter sources in tropical Brazilian coastal waters. *Marine Chemistry* 73, 253-271
- Helms, J. R., Jason A.S., Ritchie J.D., Minor E. C., Kieber D. J., Mopper, K. (2008) Absorption spectral slopes and slope ratios as indicators of molecular weight, source, and photobleaching of chromophoric dissolved organic matter, *Limnol. Oceanogr.*, 53, 955-969
- Hernes P.J., Benner R., Cowie G.L., Goñi M.A., Bergamaschi B.A., Hedges J.I. (2001) Tannin diagenesis in mangrove leaves from a tropical estuary: A novel molecular approach *Geochimica et Cosmochimica Acta*, Vol. 65, No. 18, pp. 3109–3122 PII S0016-7037(01)00641-X
- Holmes, R.M., Aminot A., Kerouel R., Hooker B.A., and Robertson B.J. (1999) A simple and precise method for measuring ammonium in marine and freshwater ecosystems. *Can. J. Fish. Aquat. Sci.*, 56, 1801-1808
- Jaffe' R., Boyera J.N., Lua X., Maie N., Yang C., Scully N.M., Mock S. (2004) Source characterization of dissolved organic matter in a subtropical mangrove-dominated estuary by fluorescence analysis. *Marine Chemistry* 84, 195– 210
- Keith D. J., Yoder J. A., Freeman S. A. (2001) Spatial and Temporal Distribution of Coloured Dissolved Organic Matter (CDOM) in Narragansett Bay, Rhode Island: Implications for Phytoplankton in Coastal Waters. *Estuarine, Coastal and Shelf Science* (2002) 55, 705–717doi:10.1006/ecss.2001.0922
- Koopmans D.J., Bronk D.A. (2002) Photochemical production of dissolved inorganic nitrogen and primary amines from dissolved organic nitrogen in waters of two estuaries and adjacent surficial groundwaters. *Aquatic Microbial Ecology*. 26, 295-304
- Kowalczyk P., Cooper W.J., Durako M. J. Kahn A.E., Gonsior M., Young H. (2009) Characterization of dissolved organic matter fluorescence in the South Atlantic Bight with use of PARAFAC model: Interannual variability *Marine Chemistry* 113 (2010) 182–196

- Kowalczuk P., Durako Michael J. Heather Young Amanda E. Kahn William J. Cooper Michael Gonsior. (2010) Characterization of dissolved organic matter fluorescence in the South Atlantic Bight with use of PARAFAC model: Interannual variability *Marine Chemistry* 118 (2010) 22–36 doi:10.1016/j.marchem.2009.10.002
- Kowalczuk, P., Ston-Egiert, J., Cooper W. J., Whitehead R. F., Durako M. J. (2005) Characterisation of chromophoric dissolve organic matter (CDOM) in the Baltic Sea by excitation emission matrix fluorescence spectroscopy. *Mar. Chem.* 96(3-4), 273-292.
- Kowalczuk, P., Cooper W. J., Whitehead R. F., Durako M. J., Sheldon W. (2003) Characterization of CDOM in an organic-rich river and surrounding coastal ocean in the South Atlantic Bight. *Aquatic Sciences* 65, 384–401.
- Loiselle S. A., Bracchini L., Cózar A., Dattilo A. M., Tognazzi A., Rossi C. (2009) Variability in photobleaching yields and their related impacts on optical conditions in subtropical lakes *Journal of Photochemistry and Photobiology B: Biology* Volume 95, Issue 2, 4 May 2009, Pages 129-137 doi:10.1016/j.jphotobiol.2009.02.002
- Maie N., Boyer J.N., Yang C., Jaffe´ R. (2006) Spatial, geomorphological, and seasonal variability of CDOM in estuaries of the Florida Coastal Everglades. *Hidrobiología*. 569: 135-150
- Maie, N., Parish K. J., Watanabe A., Knicker H., Benner R., Abe T., Kaiser K., and. Jaffé R. (2006) Chemical characteristics of dissolved organic nitrogen in an oligotrophic subtropical coastal ecosystem, *Geochim. Cosmochim. Acta*, 70, 4491-4506
- Maie, N., Scully N. M., Pisani O., Jaffé R. (2007), Composition of a protein-like fluorophore of dissolved organic matter in coastal wetland and estuarine ecosystems, *Water Res.*, 41, 563-570
- Maie, N., Pisani O., Jaffé R. (2008) Mangrove tannins in aquatic ecosystems: Their fate and possible influence on dissolved organic carbon and nitrogen cycling, *Limnol. Oceanogr.*, 53, 160-171
- McKnight, D.M., Boyer E. W., Westerhoff P.K., Doran P.T., Kulbe T., Andersen D. T. (2001) Spectrofluorometric characterization of dissolved organic matter for indication of precursor organic material and aromaticity, *Limnol. Oceanogr.*, 46, 38-48
- Miller R.L., Belz M., Del Castillo C, Trzaska R. (2002) Determining CDOM Absorption Spectra in Diverse Coastal Environments Using a Multiple Pathlength, Liquid Core Waveguide System. *Continental Shelf Research* Vol. 22 Issue: 9 Pages: 1301-1310

- Morell J. M. and Corredor J. E. (2001) Photomineralization of fluorescent dissolved organic matter in the Orinoco River Plume: Estimation of ammonium release. *Journal of Geophysical Research*, Vol. 106, No. C8, pages 16,807-16,813, August 15, 2001.
- Murphy, K. R., Stedmon C. A., Waite T. D, and. Ruiz G. M (2008) Distinguishing between terrestrial and autochthonous organic matter sources in marine environments using fluorescence spectroscopy, *Mar. Chem.*, 108, 40-58.
- Parlanti E., Worz K., Geoffroy L., Lamotte M.. (2000) Dissolve organic matter fluorescence spectroscopy as a tool to estimate biological activity in a coastal zone submitted to anthropogenic inputs. *Organic Geochemistry* 31:1765-1781
- Robles P.O., Field R., Laboy E.N., Capella J., González C.M. (2002) Jobos Bay Estuarine Profile: A National Estuarine Research Reserve. Revised June 2008 by Angel Dieppa, Research Coordinator.
- Santín, C., Yamashita, Y., Otero, X., Álvarez, M., Jaffé, R. (2009) Characterizing humic substances from estuarine soils and sediments by excitation-emission matrix spectroscopy and parallel factor analysis. *Biogeochemistry* Vol. 96, Num 1-3, 131-147
- Smith E.M., Benner R. (2005) Photochemical transformations of riverine dissolved organic matter: effects on estuarine bacterial metabolism and nutrient demand. *Aquatic Microbial ecology* 40: 37-50
- Stedmon, C. A., and Bro R. (2008) Characterizing dissolved organic matter fluorescence with parallel factor analysis: a tutorial, *Limnol. Oceanogr. Meth.*, 6, 572-579.
- Stedmon, C. A., Markager S., and Bro R. (2003) Tracing dissolved organic matter in aquatic environments using a new approach to fluorescence spectroscopy, *Mar. Chem.*, 82, 239-254.
- Stedmon, C. A., and Markager S. (2005a) Resolving the variability in dissolved organic matter fluorescence in a temperate estuary and its catchment using PARAFAC analysis, *Limnol. Oceanogr.*, 50, 686-697.
- Stedmon CA, Markager S (2005b) Tracing the production and degradation of autochthonous fractions of dissolved organic matter by fluorescence analysis. *Limnol Oceanogr* 50: 1415–1426
- Stedmon CA, Markager S, Bro R, Tranvik L, Kronberg L, Sla˘tis T, Martinsen W. (2007) Photochemical production of ammonium and transformation of dissolved organic matter in the Baltic Sea. *Mar Chem* 104:227–240
- Tremblay, L.B.; Dittmar, T.; Marshall, A.G.; Cooper, W.J. and Cooper, W.T. (2005) Molecular Characterization of Dissolved Organic Matter in a North Brazilian Mangrove-Fringed Estuary by FT-ICR Mass Spectrometry and Synchronous Fluorescence Spectroscopy

- (poster), 53rd Amer. Soc. Mass Spectrom. Ann. Conf. on Mass Spectrom. & Allied Topics, San Antonio, TX, June 4-9 (2005)
- Twardowski M.S., Donaghay P.L. (2002) Photobleaching of aquatic dissolved materials: absorption removal, spectral alteration, and their interrelationship. *J. Geophys. Res.*, 107(C8):6.1–6.12.
- Wurl Oliver. (2009) Practical Guidelines for the Analysis of Seawater. CRC Press, 2009 ISBN1420073060, 9781420073065 Pag.401
- Yamashita Y., Maie N., Briceño H., Jaffé R. (2010) Optical characterization of dissolved organic matter in tropical rivers of the Guayana Shield, Venezuela. *Journal of Geophys. Res. Biogeosciences* Vol. 115
- Yamashita Y., and Jaffé R. (2008) Characterizing the interactions between trace metals and dissolved organic matter using excitation-emission matrix and parallel factor analysis, *Environ. Sci. Technol.*, 42, 7374-7379.
- Yamashita, Y., and Tanoue E. (2003) Chemical characterization of protein-like fluorophores in DOM in relation to aromatic amino acids, *Mar. Chem.*, 82, 255-271.
- Yamashita Y., Jaffé R., Maie N., and Tanoue E (2008) Assessing the dynamics of dissolved organic matter (DOM) in coastal environments by excitation and emission matrix fluorescence and parallel factor analysis (EEM-PARAFAC), *Limnol. Oceanogr.*, 53, 1900-1908.
- Zepp R.G., Callaghan T.V., Erickson D.J. (1998) Effects of enhanced solar ultraviolet radiation on biogeochemical cycles. *Journal of Photochemistry and Photobiology: Biology* 46 69–82
- Zhao, Wenxi Cao, Guifen Wang, Dingtian Yang, Yuezhong Yang, Zhaohua Sun, Wen Zhou, Shaojun Liang. (2009) The variations in optical properties of CDOM throughout an algal bloom event *Estuarine, Coastal Shelf Science* 82 (2009) 225–232 doi:10.1016/j.ecss.2009.01.007
- Zitello, A.G., Whitall D.R., Dieppa A., Christensen J.D., Monaco M.E., Rohmann S.O. (2008) Characterizing Jobos Bay, Puerto Rico: A Watershed Modeling Analysis and Monitoring Plan. *NOAA Technical Memorandum NOS NCCOS* 76. 81 p

Appendix 1 Site Description

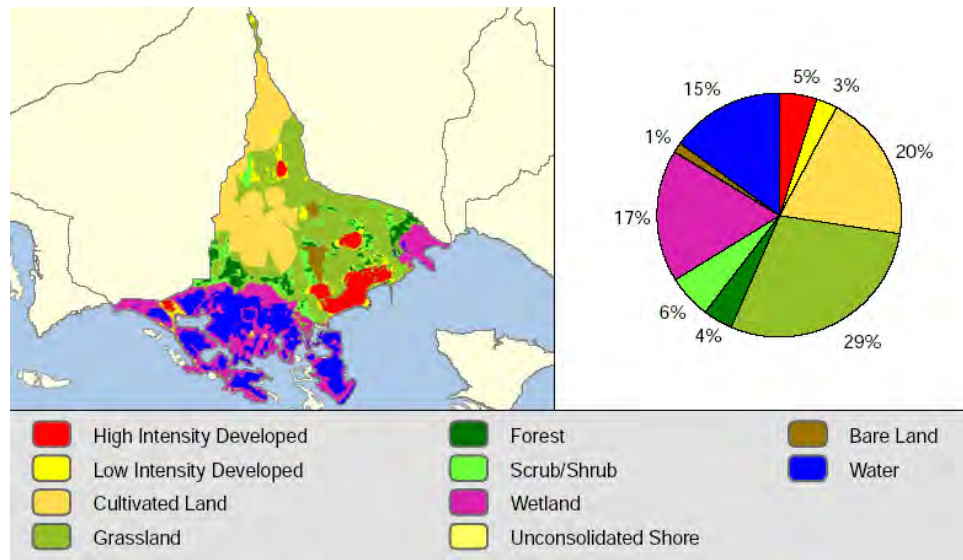


Figure 1 Spatial distribution and percent coverage of Central Aguirre land cover categories (Zitello *et al.*, 2008).

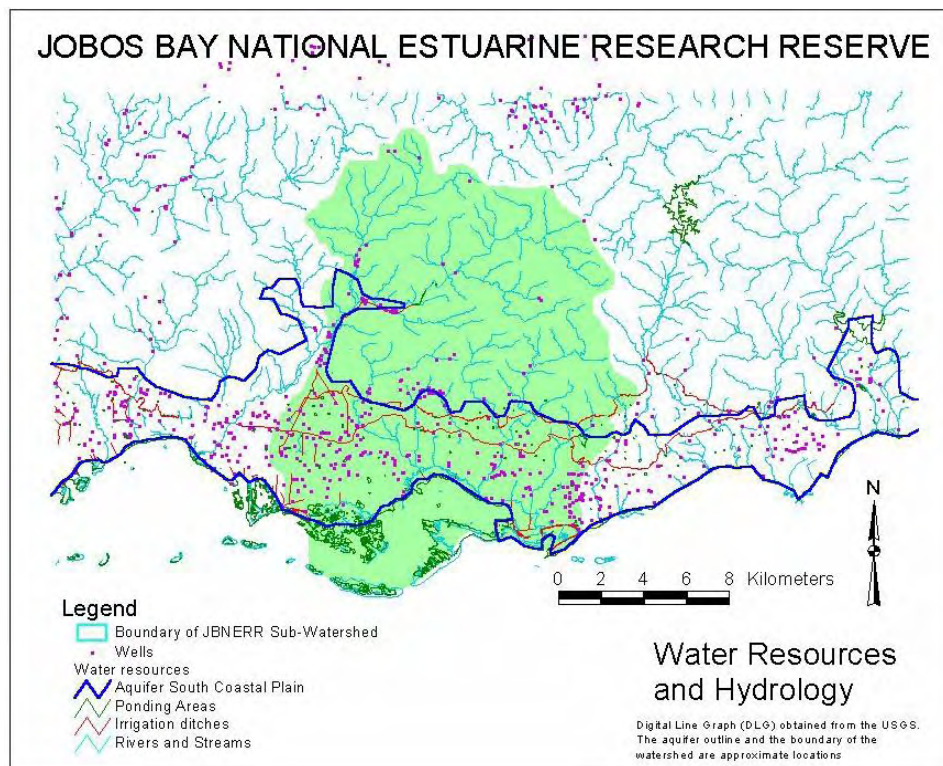


Figure 2 Water Resources and Hydrology for JOBANERR (Robles *et al.*, 2002)

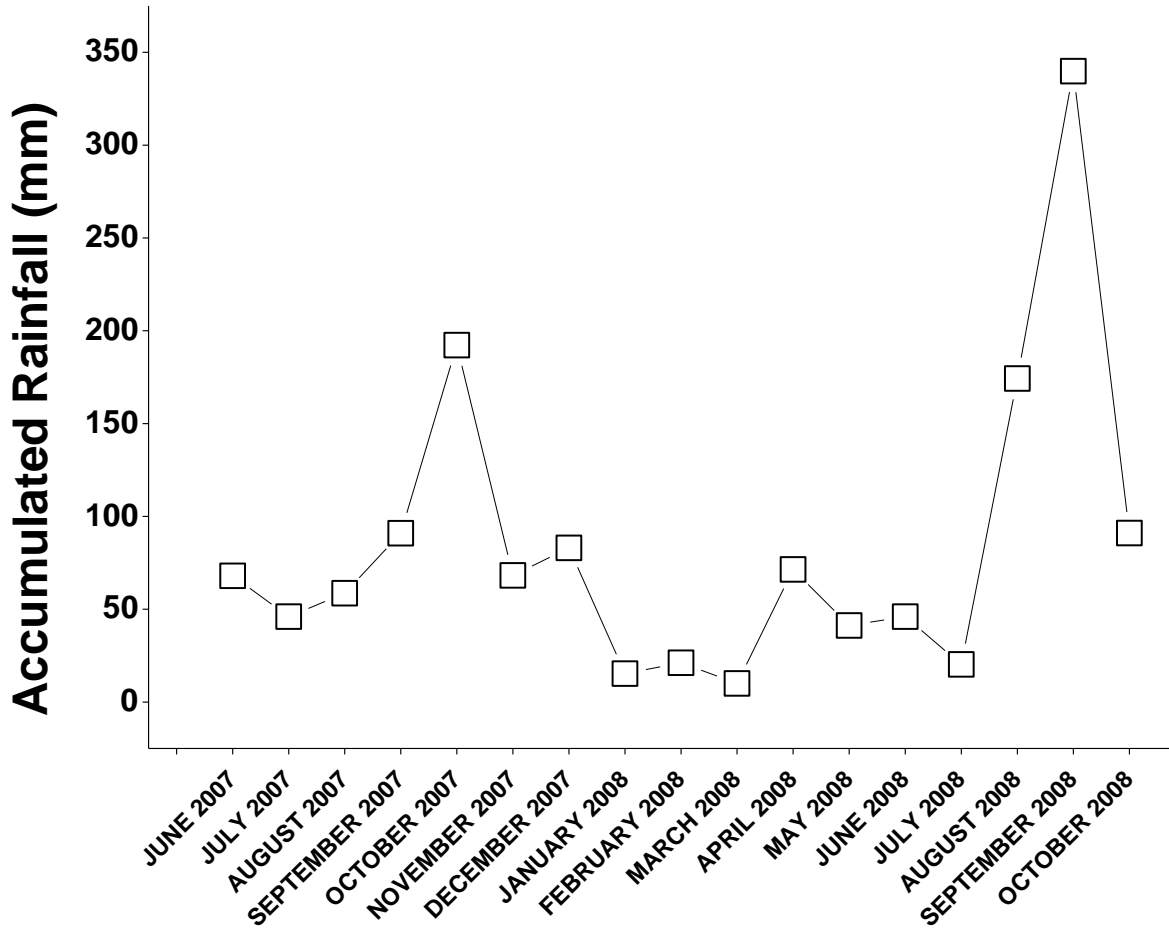


Figure 3 Accumulated rainfalls for Jobs Bay watershed on sampling.

Appendix 2

Data by sampling site and sampling date.

Absorption coefficient in m^{-1} at 412 nm, 254 nm and 355 nm.

Salinity

Chlorophyll ($\mu g/L$)

Dissolved Organic Carbon (DOC) (μM)

Site/Date	a(m^{-1}) 412	a 254	a 355	Salinity	chlorophyll ($\mu g/L$)	DOC (μM)
Barca						
July 2007	0.06	3.20	0.16	35.30	0.10	
September 2007	0.09	3.40	1.13	35.31		
October 2007	0.05	1.51	0.15	35.22	0.19	162
December 3, 2007	0.04	1.65	0.13	34.94	0.34	264
December 18, 2007	0.07	1.65	0.16	34.69	0.71	
January 2008	0.03	1.35	0.08	35.38	0.24	154
March 3, 2008	0.06	1.31	0.11	35.97	0.27	195
March 28, 2008	0.04	1.34	0.11	36.62	0.27	138
April 2008	0.06	1.68	0.16	36.22	0.26	182
June 3, 2008	0.02	1.24	0.06	37.07	1.07	325
June 30, 2008	0.06	1.19	0.13	36.22	0.56	452
August 21, 2008	0.06	2.05	0.15	34.49	0.17	730
September 2008	0.27	3.76	0.66	33.47	2.05	375
average	0.07	1.95	0.24	35.45	0.52	298
Canal						
	a(m^{-1}) 412	a 254	a 355	Salinity	chlorophyll ($\mu g/L$)	DOC (μM)
July 2007	0.22	3.20	0.57	35.41	0.05	
September 2007	0.73	3.38	2.56	35.38		
October 2007	0.17	3.07	0.46	35.25		157
December 3, 2007	0.14	2.58	0.38	35.10	1.08	211
December 18, 2007	0.14	2.12	0.34	34.65	0.77	
January 2008	0.13	2.40	0.33	34.87	0.68	158
March 3, 2008	0.12	2.17	0.30	36.14	0.55	237
March 28, 2008	0.07	1.63	0.18	36.60	0.31	202
April 2008	0.10	1.84	0.26	36.45	0.44	178
June 3, 2008	0.11	2.29	0.31	36.10	0.37	173
June 30, 2008	0.15	2.36	0.38	36.27	0.48	695
August 21, 2008	0.12	2.51	0.32	34.76	0.52	142
September 2008	0.52	6.31	1.28	32.05	2.90	362
average	0.21	2.76	0.59	35.31	0.74	251

Appendix 2

Data by sampling site and sampling date.

Absorption coefficient in m^{-1} at 412 nm, 254 nm and 355 nm.

Salinity

Chlorophyll ($\mu g/L$)

Dissolved Organic Carbon (DOC) (μM)

Mar Blanco	a(m^{-1}) 412	a 254	a 355	Salinity	chlorophyll ($\mu g/L$)	DOC (μM)
January 2007	0.28			34.48		
July 2007	0.39	2.24	1.02	24.98		
September 2007	1.66	2.40	4.46	35.47		
October 2007	0.53	6.75	1.41	35.26	1.25	170
December 3, 2007	0.23	3.68	0.61	35.17	1.26	276
December 18, 2007	0.42	5.38	1.08	34.53	1.99	
January 2008	0.28	4.13	0.74	34.48	1.71	227
March 3, 2008	0.26	3.75	0.66	36.00	1.00	311
March 28, 2008	0.30	4.25	0.78	36.98	1.28	269
April 2008	0.30	4.39	0.79	36.68	0.65	
June 3, 2008	0.26	3.66	0.63	36.15	1.15	631
June 30, 2008	0.31	4.00	0.77	36.60	0.84	711
August 21, 2008	0.36	5.25	0.88	34.88	1.28	302
September 2008	0.57	6.75	1.41	32.79	2.79	202
average	0.44	4.36	1.17	34.60	1.38	344
Mar Negro	a(m^{-1}) 412	a 254	a 355	Salinity	chlorophyll ($\mu g/L$)	DOC (μM)
January 2007	1.87	3.85	6.44	38.40		
July 2007	1.95	10.75	4.86	45.78	0.12	
September 2007	11.52	10.81	27.30	37.36		
October 2007	3.70	42.47	9.05	35.42	2.88	466
December 3, 2007	3.06	36.86	7.69	34.73	4.21	907
December 18, 2007	3.34	41.68	8.53		5.10	
January 2008	1.87	25.92	4.94	38.40	1.23	358
March 3, 2008	1.18	16.66	3.04	38.33	2.09	
March 28, 2008	1.19	16.68	3.09	39.43	2.88	262
April 2008	1.31	18.67	3.45		2.09	252
June 3, 2008	1.45			39.52	3.97	
June 30, 2008	1.46	19.23	3.72	41.74	3.40	726
August 21, 2008	1.46	40.97	8.36	32.12	5.90	685
September 2008	5.37	55.00	13.02	8.52	23.52	438
average	2.91	26.12	7.96	35.81	4.78	512

Appendix 2

Data by sampling site and sampling date.

Absorption coefficient in m^{-1} at 412 nm, 254 nm and 355 nm.

Salinity

Chlorophyll ($\mu g/L$)

Dissolved Organic Carbon (DOC) (μM)

St9	a(m^{-1}) 412	a 254	a 355	Salinity	chlorophyll ($\mu g/L$)	DOC (μM)
January 2007	0.97	1.97	3.51	36.78		
July 2007	1.30	5.93	3.01	36.48	0.17	
September 2007	6.07	6.04	13.97	36.18		
October 2007	1.62	16.90	3.88	35.07	5.50	376
December 3, 2007	1.23	13.71	3.00	--	2.77	481
December 18, 2007	1.76	40.64	4.27	31.59	3.52	
January 2008	0.97	11.27	2.39	36.78	1.74	289
March 3, 2008	1.02	11.80	2.49	37.88	5.26	270
March 28, 2008	1.19	14.54	2.96	38.33	11.60	284
April 2008	1.32	15.52	3.31	38.24	10.38	199
June 3, 2008	1.58	0.77	3.73	37.41	5.40	822
June 30, 2008	1.54	14.70	3.57	37.73	5.85	393
August 21, 2008	2.54	27.50	6.14	34.49	10.56	629
September 2008	2.14	20.48	4.93	30.70	8.72	367
average	1.80	14.41	4.37	35.97	5.95	411
St10	a(m^{-1}) 412	a 254	a 355	Salinity	chlorophyll ($\mu g/L$)	DOC (μM)
January 2007	1.06	2.45	4.17	36.08		
July 2007	1.12	4.58	2.77	36.96	0.12	
September 2007	0.12	5.42	1.20	36.66		
October 2007	2.02	81.59	3.42	36.05	--	
December 3, 2007	2.64	30.74	6.59	34.87	3.98	631
December 18, 2007	2.82	33.38	7.10		2.60	
January 2008	1.06	13.83	2.72	36.08	2.12	246
March 3, 2008	0.80	10.98	2.03	37.32	1.30	363
March 28, 2008						
April 2008				38.01	1.65	288
June 3, 2008	1.06	13.00	2.58	37.33	1.34	314
June 30, 2008	0.96	11.44	2.37		1.13	418
August 21, 2008	2.05	23.98	5.08	33.43	2.37	621
September 2008	2.84	27.73	6.74	25.05	14.64	225
average	1.55	21.59	3.90	35.26	3.13	388

Appendix 2

Data by sampling site and sampling date.

Absorption coefficient in m^{-1} at 412 nm, 254 nm and 355 nm.

Salinity

Chlorophyll ($\mu g/L$)

Dissolved Organic Carbon (DOC) (μM)

St19	a(m^{-1}) 412	a 254	a 355	Salinity	chlorophyll ($\mu g/L$)	DOC (μM)
January 2007	0.17	3.44	0.40	35.47		
July 2007	0.19	3.41	0.50	35.58		
September 2007	0.69	3.57	2.36	36.09		
October 2007	0.21	3.30	0.55	35.22	0.53	418
December 3, 2007	0.17	2.66	0.43	--	0.61	679
December 18, 2007	0.19	2.66	0.47	34.60	0.83	
January 2008	0.17	2.58	0.41	35.47	0.60	402
March 3, 2008	0.13	2.16	0.31	36.18	0.38	167
March 28, 2008	0.14	2.36	0.36	36.76	0.67	293
April 2008	0.17	2.60	0.44	36.41	0.37	
June 3, 2008	0.11	2.17	0.25	36.08	0.45	681
June 30, 2008	0.19	2.81	0.47	36.32	0.59	223
August 21, 2008	0.21	2.97	0.51	34.48	0.42	392
September 2008	0.23	2.99	0.52	30.48	5.78	427
average	0.21	2.83	0.57	35.32	1.02	409
St20	a(m^{-1}) 412	a 254	a 355	Salinity	chlorophyll ($\mu g/L$)	DOC (μM)
January 2007	0.12	8.94	0.21	35.53		
July 2007	0.15	3.24	0.46	35.42		
September 2007	0.44	3.36	1.63	35.99		
October 2007	0.13	1.77	0.29	31.05	0.16	128
December 3, 2007	0.09	1.77	0.24	--	0.11	237
December 18, 2007	0.10	1.58	0.25	34.64	0.63	
January 2008	0.12	2.17	0.30	35.53	0.49	264
March 3, 2008	0.09	1.58	0.21	36.04	0.26	123
March 28, 2008	0.10	1.58	0.27	36.60	0.18	234
April 2008	0.09	1.66	0.23	36.09	0.29	273
June 3, 2008	0.10	1.79	0.26	36.15	0.17	429
June 30, 2008	0.09	1.59	0.24	36.08	0.26	153
August 21, 2008	0.13	2.26	0.34	34.49	0.14	649
September 2008	0.17	2.56	0.43	33.46	1.06	365
average	0.14	2.56	0.38	35.16	0.34	286

Appendix 2

Data by sampling site and sampling date.

Absorption coefficient in m^{-1} at 412 nm, 254 nm and 355 nm.

Salinity

Chlorophyll ($\mu g/L$)

Dissolved Organic Carbon (DOC) (μM)

Centro Bahia	a(m^{-1}) 412	a 254	a 355	Salinity	chlorophyll ($\mu g/L$)	DOC (μM)
March 28, 2008	0.13	1.71	0.25	36.73	0.31	294
April 2008	0.13	2.04	0.24	37.09		116
June 3, 2008	0.15	1.95	0.40	35.87	0.49	252
June 30, 2008	0.16	2.03	0.30	36.13	0.41	154
August 21, 2008	0.14	2.42	0.29	34.72	0.39	308
September 2008	0.30	4.34	0.76	32.66	5.20	354
average	0.17	2.42	0.37	35.53	1.36	
Punta Rodeo	a(m^{-1}) 412	a 254	a 355	Salinity	chlorophyll ($\mu g/L$)	DOC (μM)
April 2008	0.20	3.23	0.53	36.27	0.59	
June 3, 2008	0.16	2.94	0.42	36.61	1.18	
June 30, 2008	0.23	3.61	0.58	36.50	1.20	
August 21, 2008	0.26	4.23	0.65	34.97	0.94	
September 2008	0.33	4.57	0.84	32.09	4.30	
average	0.24	3.71	0.60	35.29	1.65	
Playita	a(m^{-1}) 412	a 254	a 355	Salinity	chlorophyll ($\mu g/L$)	DOC (μM)
June 3, 2008	0.17	2.88	0.44	36.98		
June 30, 2008	0.23	3.55	0.59	36.63	1.40	
August 21, 2008	0.15	2.59	0.37	34.68	0.62	
September 2008	0.23	3.36	0.58	33.12	2.10	
average	0.20	3.09	0.49	35.35	1.37	

APPENDIX 3 Table of Characteristics of the seven components derived from photodegradation experiment by Parallel Factor Analysis (PARAFAC)

Table. Characteristics of the seven components derived from photodegradation experiment by PARAFAC.					
Component	Excitation Maximum (nm)	Emission Maximum (nm)	Component Region	Description and probable source by references	Possible Characterization
1	295(250)	382-450	M	Terrestrial humic-like Component 3: <250 (385) / 504 (Ref 1) Component 3: 295/398 (Ref 2) P1: 310 (<260) / 414 (Ref 4) GSL2d: 300 / 462 GSL7d: 300/446 (Ref 5) Component 6: 325 (<260) / 385 (Ref 6) Component 1: 305 (<260) / 428 (Ref 7) Component 1: <260 (305) / 438 (Ref 8) Component 1: <260 (315) / 447 (Ref 9) Component 3: <260 (305) / 416 (Ref 10)	terrestrial autochthonous humic-like terrestrial humic-like/anthropogenic M Peak/photodegradation process humic-like terrestrial humic-like fulvic acid type terrestrial humic-like terrestrial humic-like/fulvic acid type
2	265(365)	463	A/C	Ubiquitous Humic-like Component 4: <250 (360) / 440 (Ref 1) Component 5: 345 / 434 (Ref 2) P8: <260 (355) / 434 (Ref 4) GSL1d: <260 / 466; GSL2d: <260 / 462 (Ref 5) Component 5: 265 (380) / 462 (Ref 7) Component 4: 370 (<260) / 440 (Ref 9) Component 1: <260 (345) / 462 (Ref 10)	terrestrial autochthonous humic-like terrestrial humic-like A Peak/photodegradation process microbial humic-like microbial reduced quinone-like(Cory and McKnight) ubiquitous humic-like

APPENDIX 3 Table of Characteristics of the seven components derived from photodegradation experiment by Parallel Factor Analysis (PARAFAC)

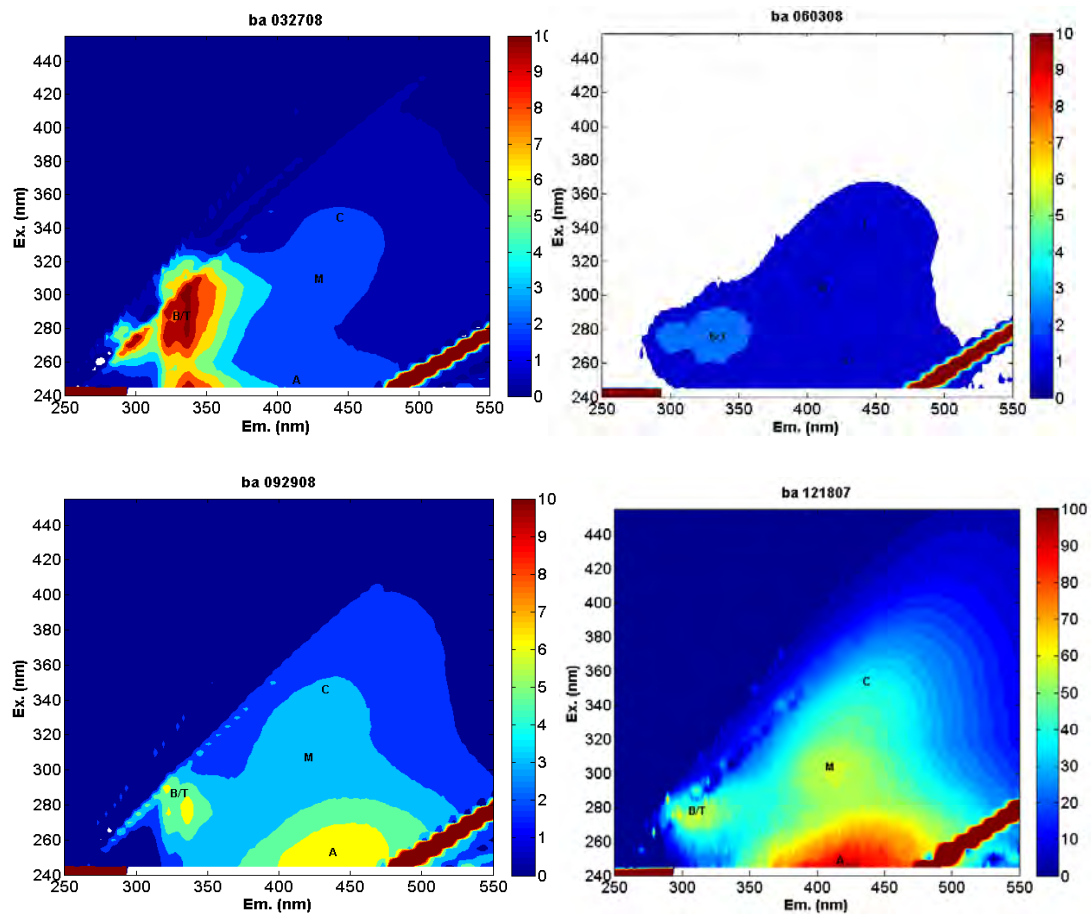
3	250	464	A	<p>Terrestrial humic-like/degradation of the peak A</p> <p>Component 1: <250 / 448 (Ref 1)</p> <p>Component 1: <240 (355) / 476 (Ref 2)</p> <p>Component 2: 250 / 420 (Ref 3)</p> <p>Component 9: <240 / 422 (Ref 4)</p> <p>GSL1d: <260 / 468 GSL2d: <260 / 466 (Ref 5)</p> <p>GSL7d: <260 / 462 GSD7d: <260 / 470 (Ref 5)</p> <p>Component 1: <260 / 458 (Ref 6)</p> <p>Component 3: <260 / 448 (Ref 7)</p> <p>Component 2: <250 / 454 (Ref 10)</p>	<p>terrestrial humic-like</p> <p>terrestrial humic-like</p> <p>photochemical product of terrestrial organic matter</p> <p>A peak/ photodegradation process</p> <p>A peak/ photodegradation process</p> <p>terrestrial humic-like</p> <p>terrestrial humic-like</p> <p>terrestrial humic-like; probably photo-oxidized products</p>
4	330(250)	415	C/M	<p>Marine humic like/ Microbial product of photodegradation process</p> <p>Component 6: <250 (320) / 400 (Ref 1)</p> <p>Component 2: 240 (355) / 398 (Ref 2)</p> <p>Component 3: 250 (310) / 400 (Ref 3)</p> <p>P1: 310 (<260) / 414 (Ref 4)</p> <p>Component 4: 305 (<260) / 378 (Ref 7)</p> <p>Component 3: <260 (<315) / 421 (Ref 9)</p> <p>Component 6: 325 / 406 (Ref 10)</p>	<p>anthropogenic/wastewater DOM/agricultural animal waste or fertilizer</p> <p>microbial degradation</p> <p>marine/terrestrial, possible microbial reprocessing</p> <p>terrestrial humic-like/anthropogenic</p> <p>microbial humic-like</p> <p>marine humic</p> <p>ubiquitous humic-like/probably degradation or modification of C3</p>
5	285(405)	515		<p>Autochthonous Humic-like</p> <p>Component 2: <250 (385) / 504 (Ref 1)</p> <p>Component 7: 420 (275) / 488 (Ref 2)</p> <p>Component 4 : 270 (390) / 508 (Ref 3)</p> <p>P3: <260 (380) / 498 (Ref 4)</p> <p>Component 2: <260 (340, 405) / >500 (Ref 7)</p> <p>Component 2: 256 (385) / >500 (Ref 8)</p> <p>Component 5: 275 (405) / >500 (Ref 10)</p>	<p>terrestrial autochthonous humic-like</p> <p>terrestrial humic-like</p> <p>terrestrial humic-like</p> <p>similar to terrestrial humic-like</p> <p>humic-acid type</p> <p>terrestrial humic-like</p>

APPENDIX 3 Table of Characteristics of the seven components derived from photodegradation experiment by Parallel Factor Analysis (PARAFAC)

6	275	324	B	<p>tyrosine like</p> <p>Component 8: 275 / 304 (Ref 1)</p> <p>Component 4: 275 / 306 (338) (Ref 2)</p> <p>Component 5: 270 / 332 (Ref 3)</p> <p>P6: 275 / 318 (Ref 4)</p> <p>GSD1d: 275 / 303 (Ref 5)</p> <p>Component 4: 280/ 318 (Ref 6)</p> <p>Component 7: 295 / 340 (Ref 7)</p> <p>Component 4: 275 / 304 (Ref 8)</p> <p>Component 5: (Ref 9)</p> <p>Component 7: 275 / 326 (Ref 10)</p>	<p>autochthonous/tyrosine-like</p> <p>protein-like</p> <p>amino-acids free bound in protein</p> <p>amino-acids free bound in protein</p> <p>protein-like</p> <p>tryptophan-like</p> <p>tryptophan-like</p> <p>tyrosine-like</p> <p>tryptophan-like</p> <p>tyrosine-like</p>
7	270(310)	294	T	<p>tryptophan-like</p> <p>Component 7: 280 / 344 (Ref 1)</p> <p>Component 6: 280 / 338 (Ref 2)</p> <p>P5: 270 / 310 (Ref 4)</p> <p>Component 7: 270 / 299 (Ref 6)</p> <p>Component 8: 275 / 324 (Ref 7)</p> <p>Component 8: 300 / 342 (Ref 10)</p>	<p>autochthonous/tryptophan-like</p> <p>tryptophan-like</p> <p>tyrosine like</p> <p>tyrosine-like/ degradation process may be important for dynamics</p> <p>tyrosine-like</p> <p>tryptophan-like</p>
<p>Component region by Coble (1996).</p> <p>Ref 1. Stedmon and Markager a(2005); Ref 2 Stedmon and Markager b(2005); Ref 3 Kowalczyk <i>et al.</i> (2009); Ref 4 Murphy <i>et al.</i> (2008); Ref 5 Jaffe <i>et al.</i> (2008); Ref 6 Yamashita <i>et al.</i> (2008); Ref 7 Yamashita and Jaffe (2008); Ref 8 Santin <i>et al.</i> (2009); Ref 9 Yamashita <i>et al.</i> (2010); Ref 10 Florida Coastal Everglade model (Yamashita, Personal.Com. 2009)</p> <p>Secondary peak on brackets.</p>					

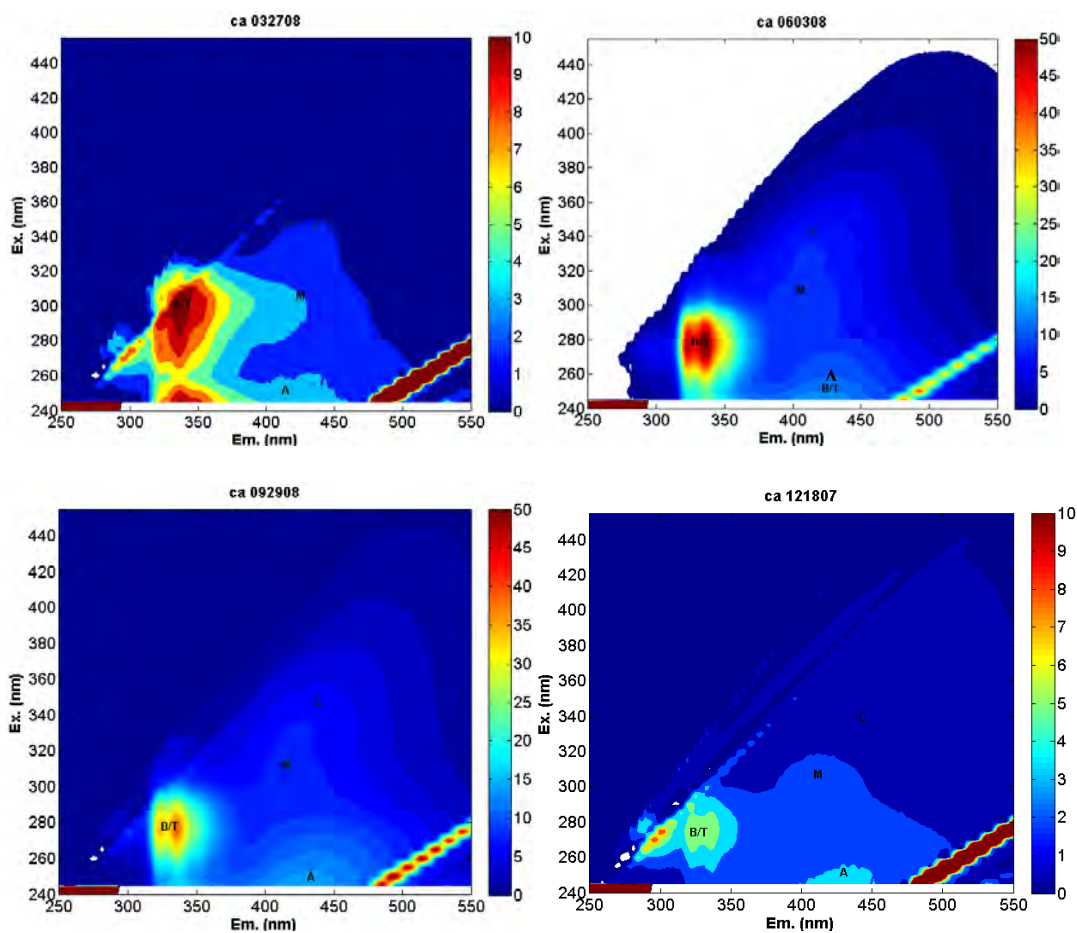
Appendix 4 Excitation Emission Matrices (EEM) for Barca - Ba, Canal - Ca, Mar Blanco - MB, Mar Negro - MN and Site 20 – St20 for 4 months (December 2007, March 2008, June 2008 and September 2008) identified with the main fluorophores named by Coble (1996). The color scale is in Quinine Sulfate Units (QSU).

Barca



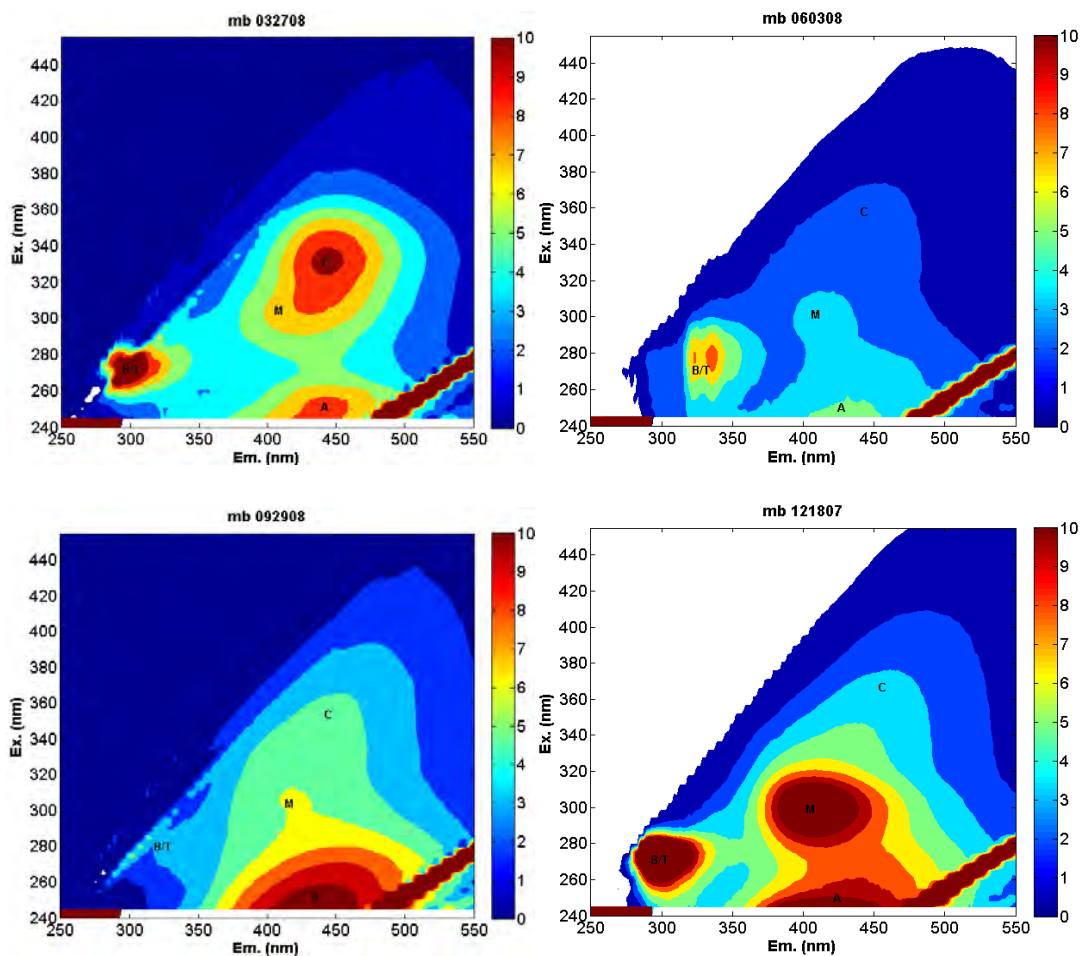
Appendix 4 Excitation Emission Matrices (EEM) for Barca - Ba, Canal - Ca, Mar Blanco - MB, Mar Negro - MN and Site 20 – St20 for 4 months (December 2007, March 2008, June 2008 and September 2008) identified with the main fluorophores named by Coble (1996). The color scale is in Quinine Sulfate Units (QSU).

Canal



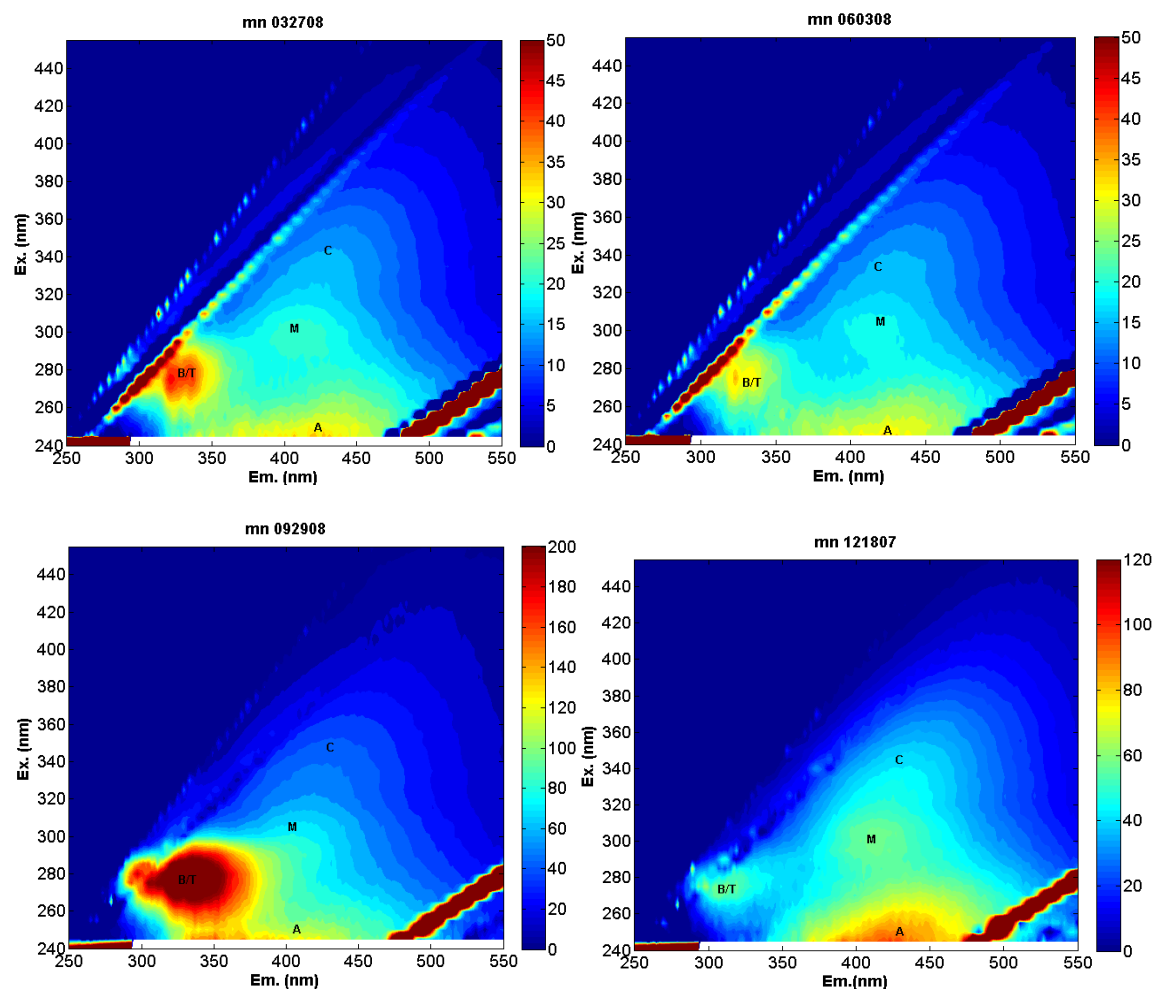
Appendix 4 Excitation Emission Matrices (EEM) for Barca - Ba, Canal - Ca, Mar Blanco - MB, Mar Negro - MN and Site 20 – St20 for 4 months (December 2007, March 2008, June 2008 and September 2008) identified with the main fluorophores named by Coble (1996). The color scale is in Quinine Sulfate Units (QSU).

Mar Blanco



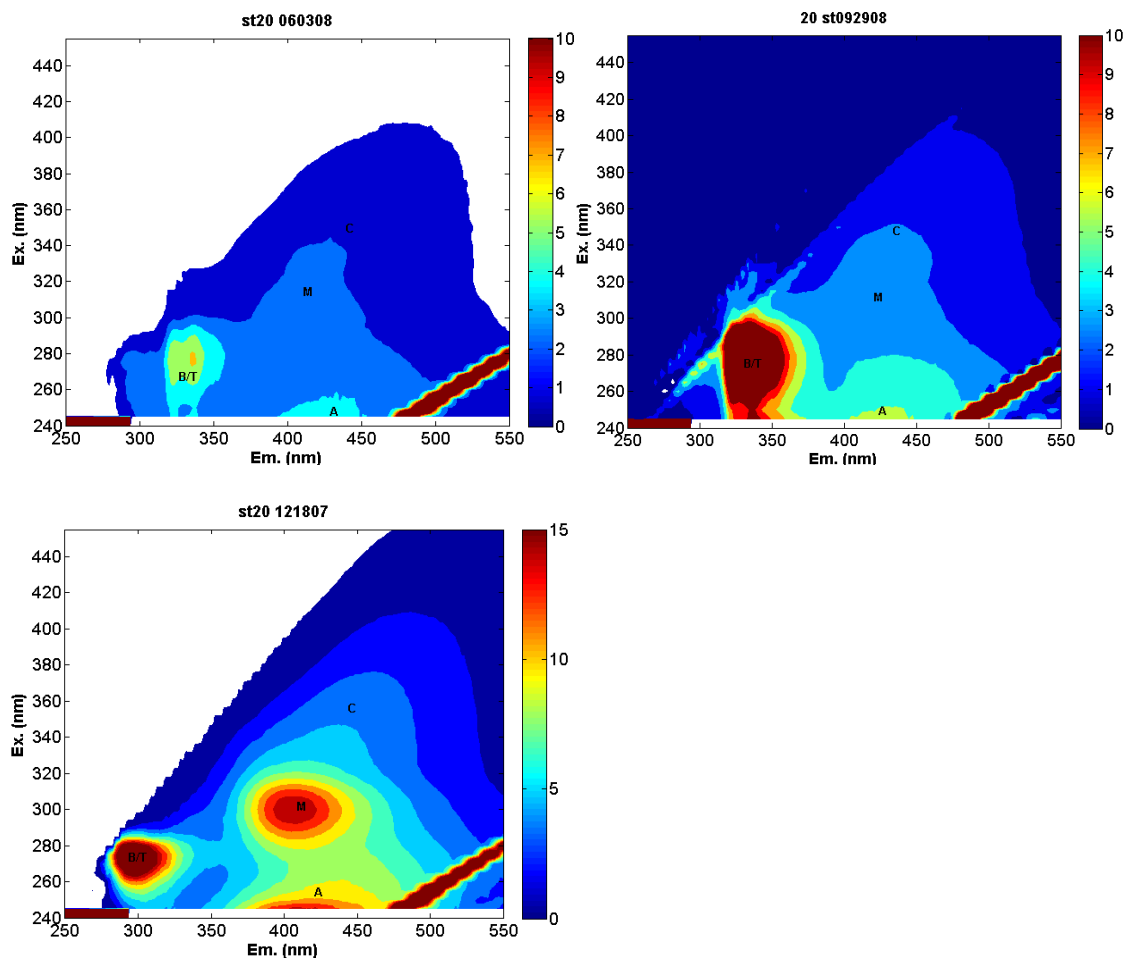
Appendix 4 Excitation Emission Matrices (EEM) for Barca - Ba, Canal - Ca, Mar Blanco - MB, Mar Negro - MN and Site 20 – St20 for 4 months (December 2007, March 2008, June 2008 and September 2008) identified with the main fluorophores named by Coble (1996). The color scale is in Quinine Sulfate Units (QSU).

Mar Negro



Appendix 4 Excitation Emission Matrices (EEM) for Barca - Ba, Canal - Ca, Mar Blanco - MB, Mar Negro - MN and Site 20 – St20 for 4 months (December 2007, March 2008, June 2008 and September 2008) identified with the main fluorophores named by Coble (1996). The color scale is in Quinine Sulfate Units (QSU).

Site 20



APPENDIX 5 ATTACHMENT

Spatial distribution of CDOM in Jobos Bay National Estuarine Research Reserve (JOBANERR). Images provided by Puerto Rico Department of Natural and Environmental Resources and developed by Orthophoto production in Puerto Rico and adjacent islands, St Louis District, US Army Corps of Engineers.

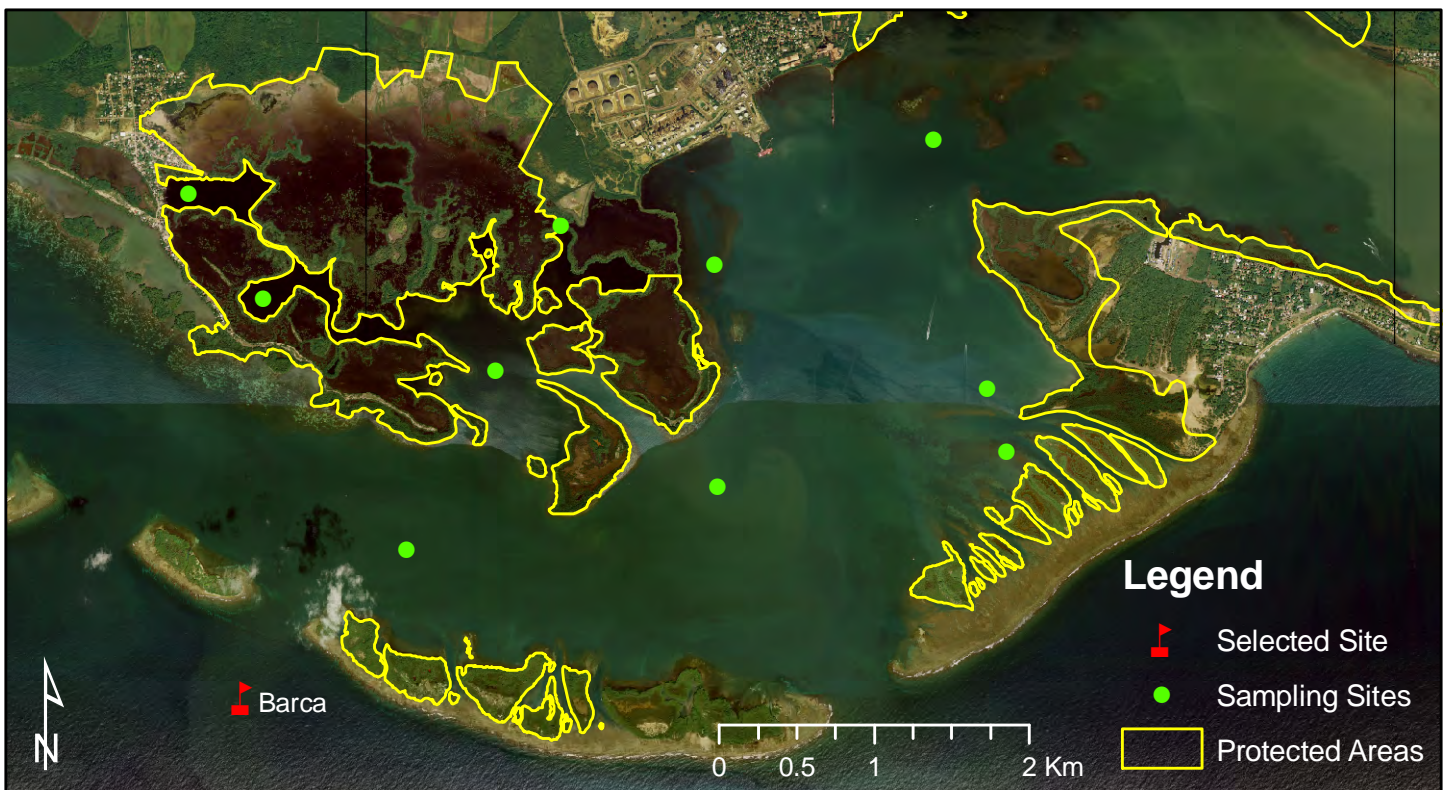
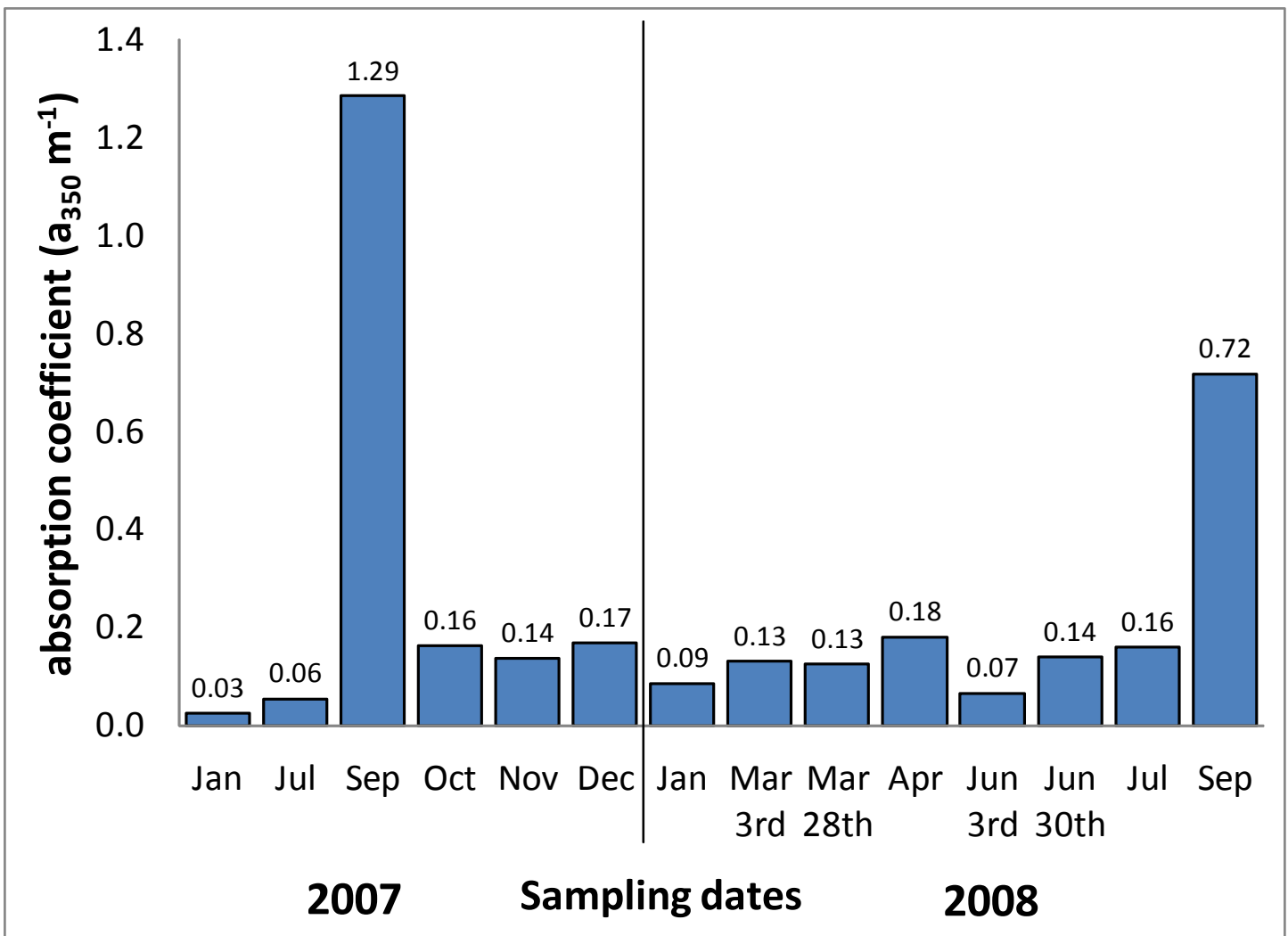


Fig. 1 Absorption coefficient of chromophoric dissolved organic matter (CDOM $a_{350} \text{ m}^{-1}$) at sampling site Barca.

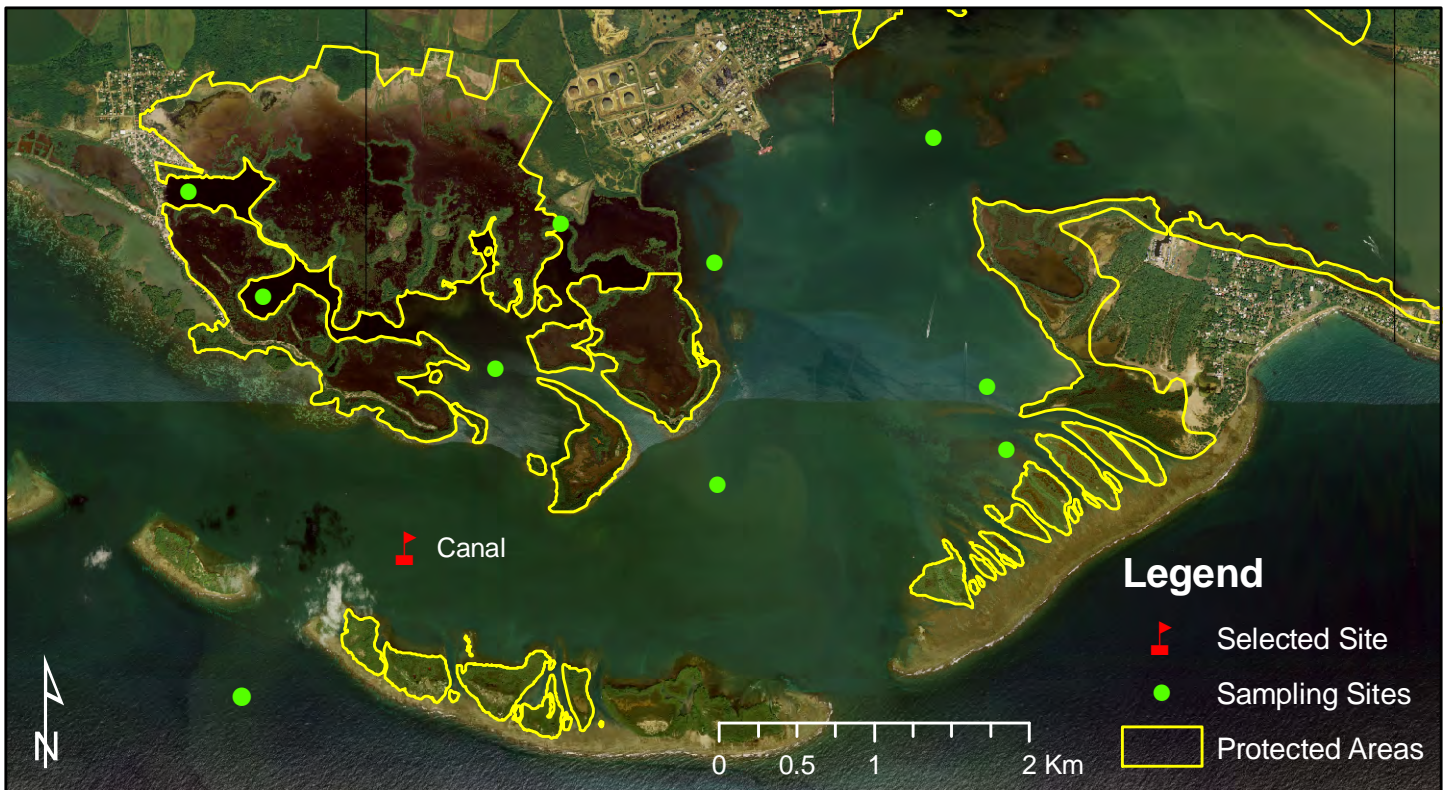
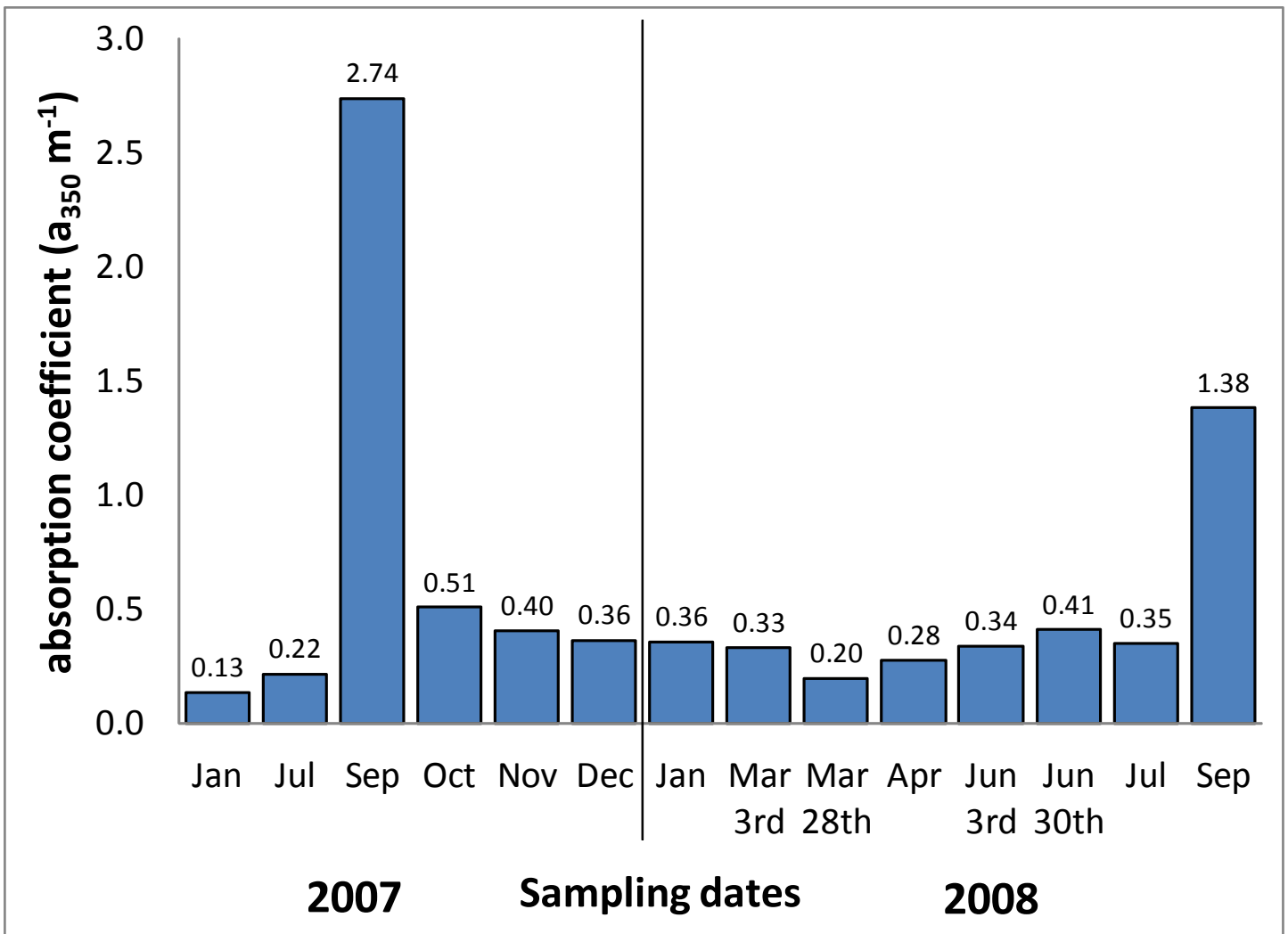


Fig. 2 Absorption coefficient of chromophoric dissolved organic matter (CDOM $a_{350} \text{ m}^{-1}$) at sampling site Canal.

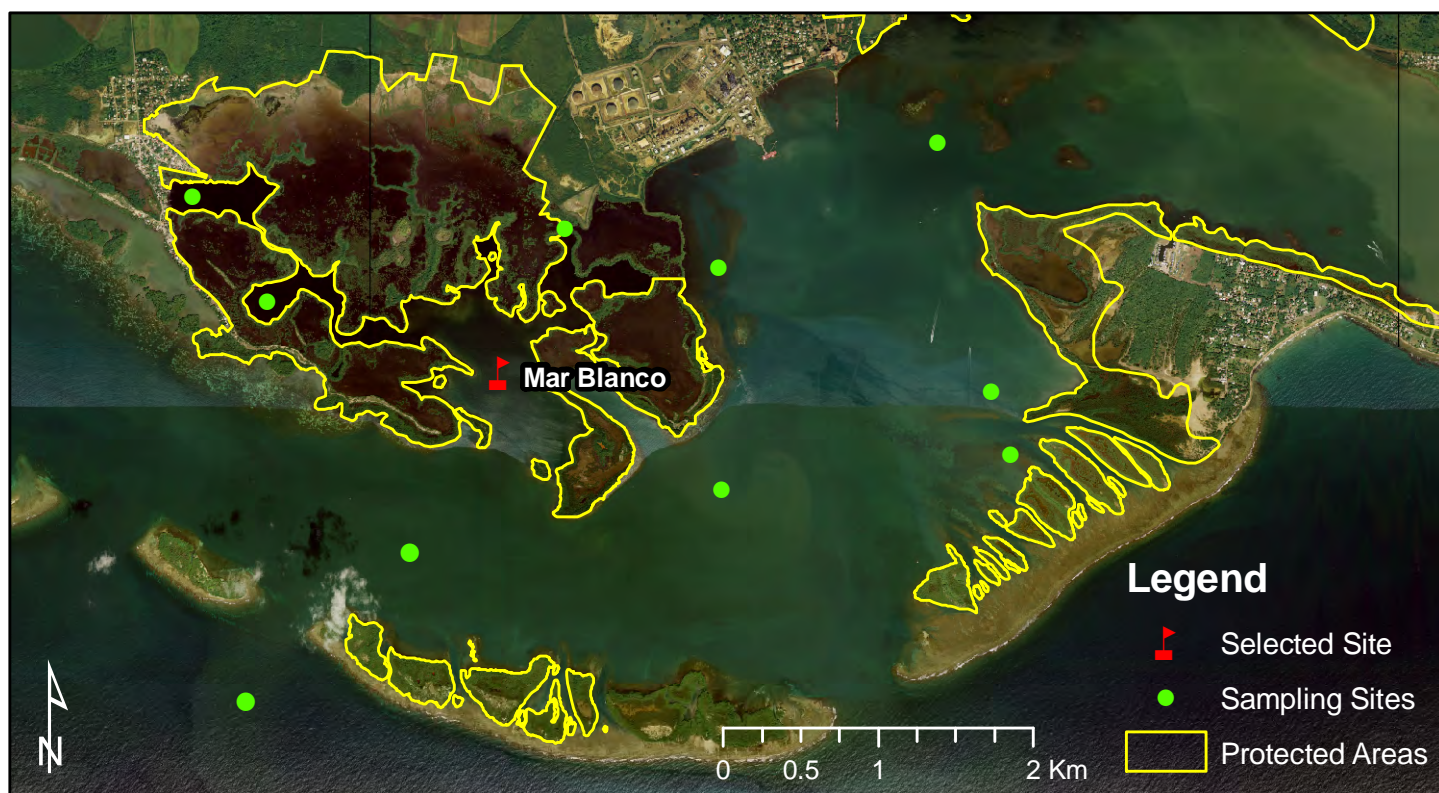
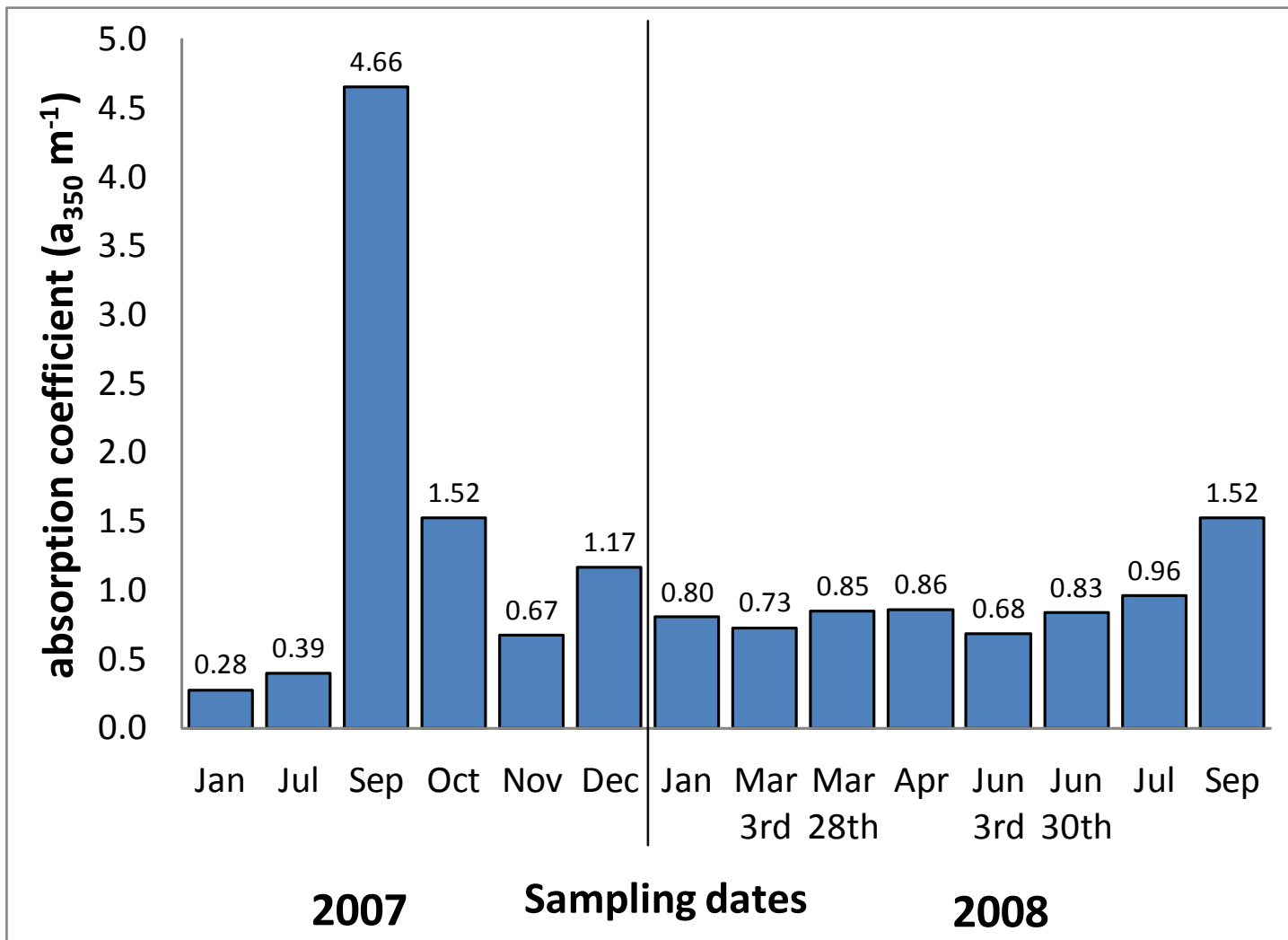


Fig. 3 Absorption coefficient of chromophoric dissolved organic matter (CDOM $a_{350} \text{ m}^{-1}$) at sampling site Mar Blanco.

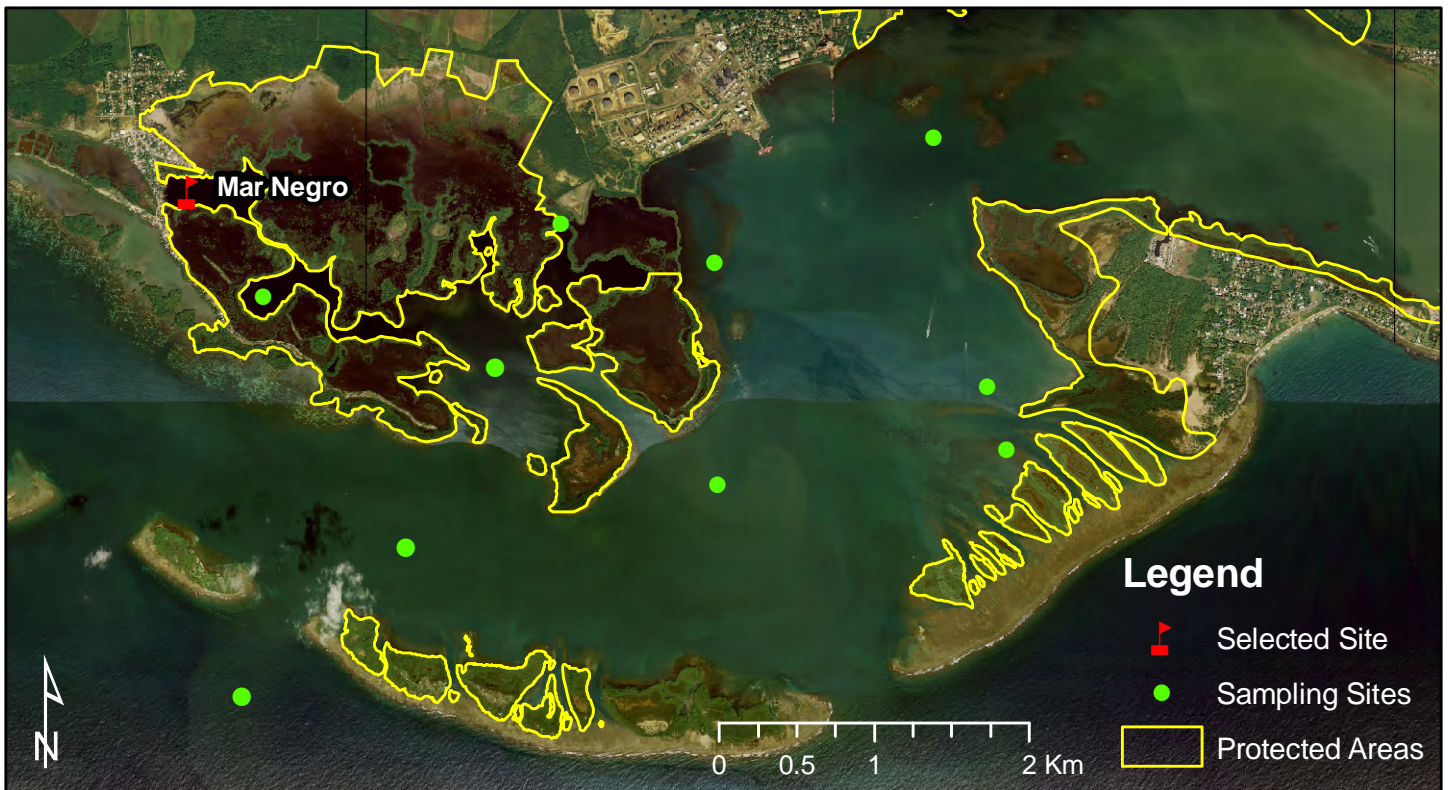
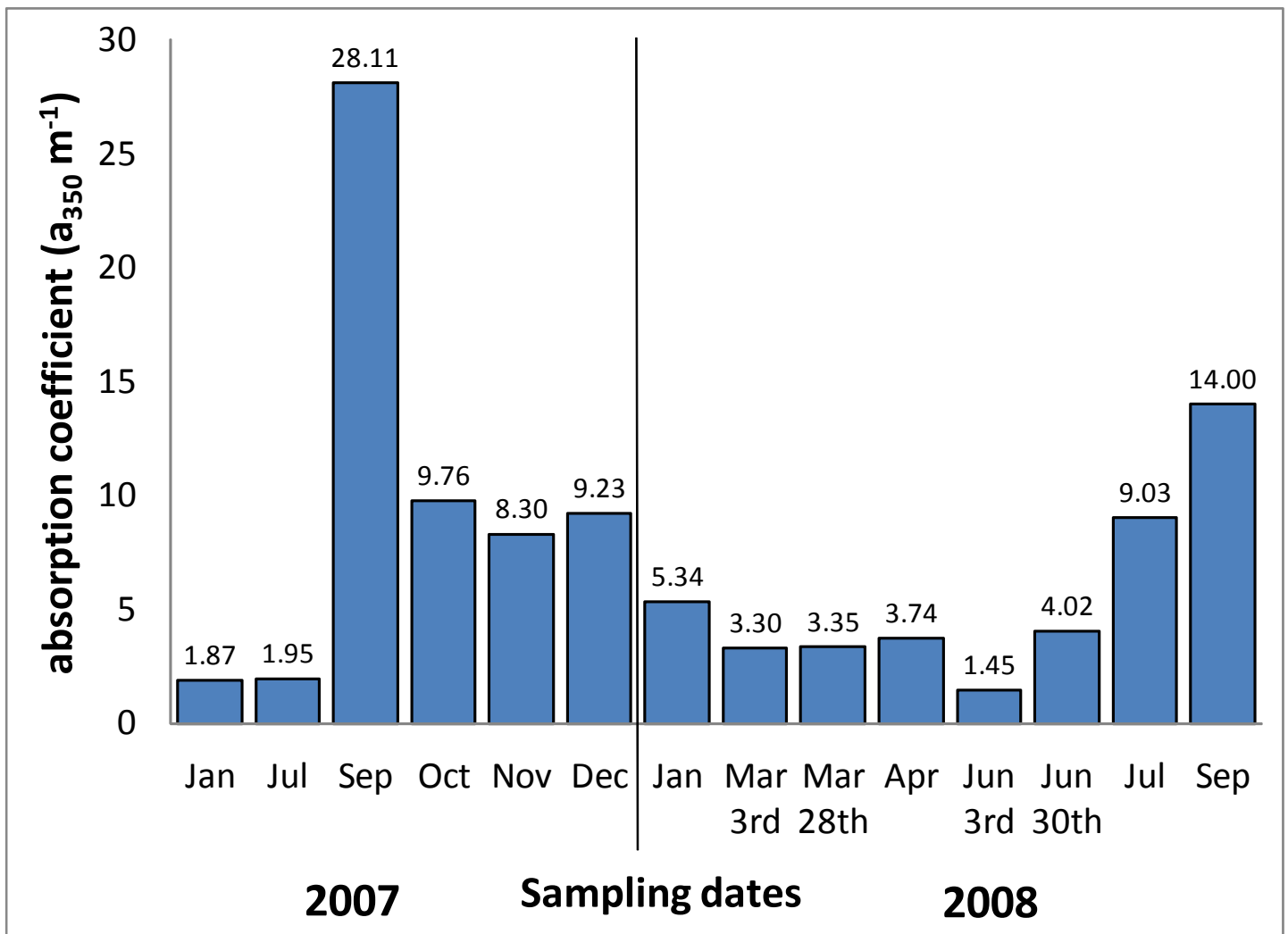


Fig. 4 Absorption coefficient of chromophoric dissolved organic matter (CDOM $a_{350} \text{ m}^{-1}$) at sampling site Mar Negro.

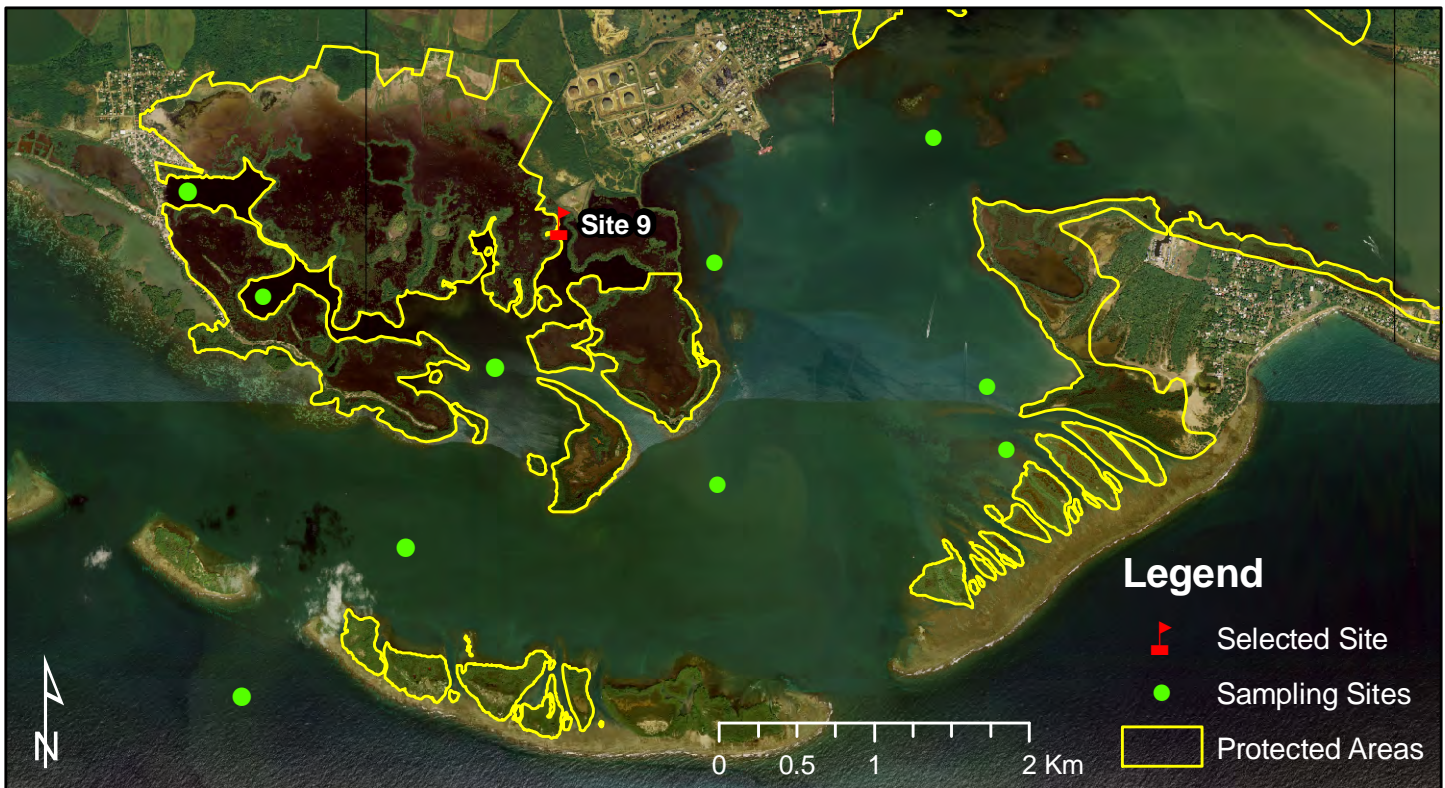
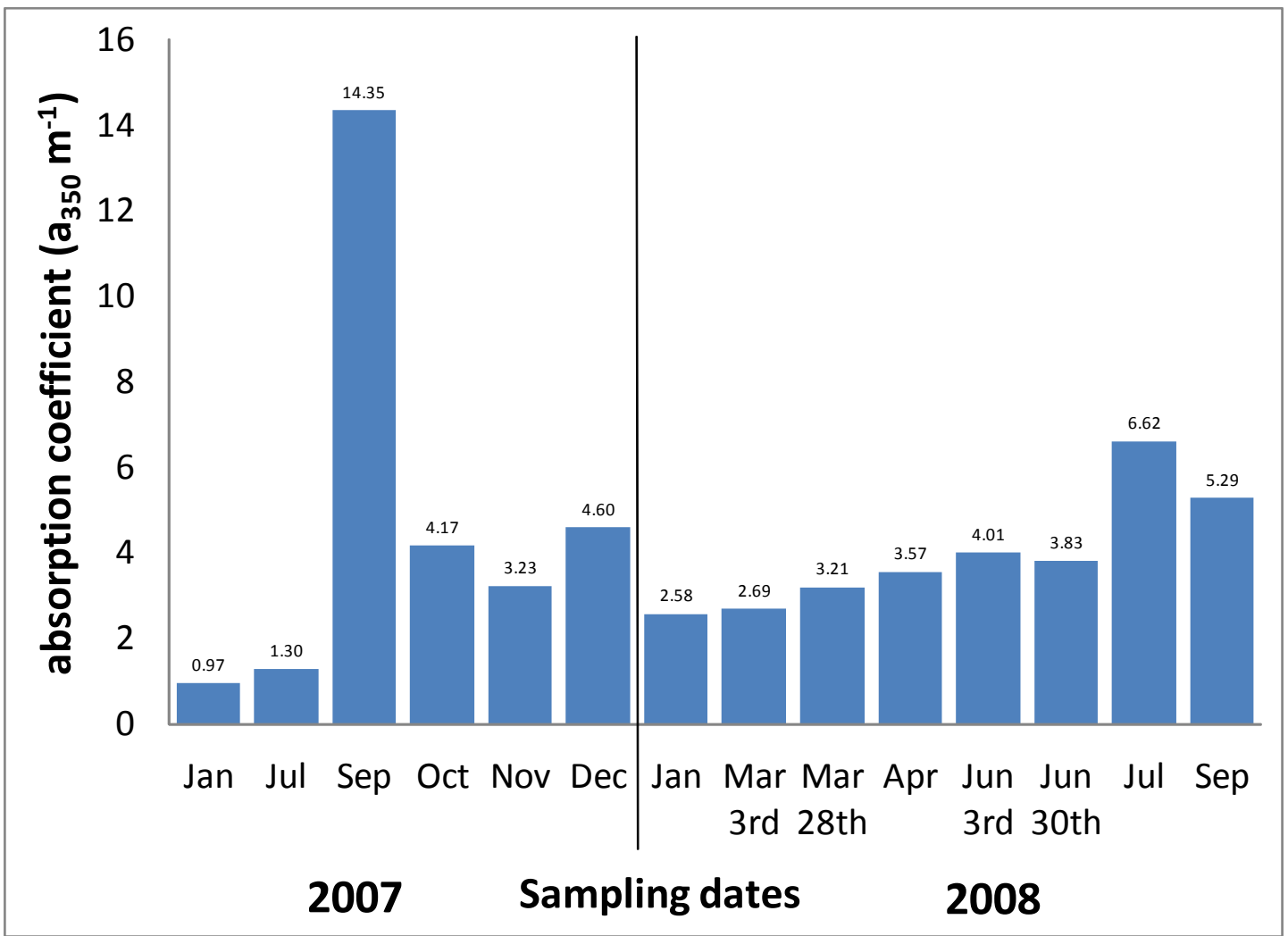


Fig. 5 Absorption coefficient of chromophoric dissolved organic matter (CDOM $a_{350} \text{ m}^{-1}$) at sampling site number 9.

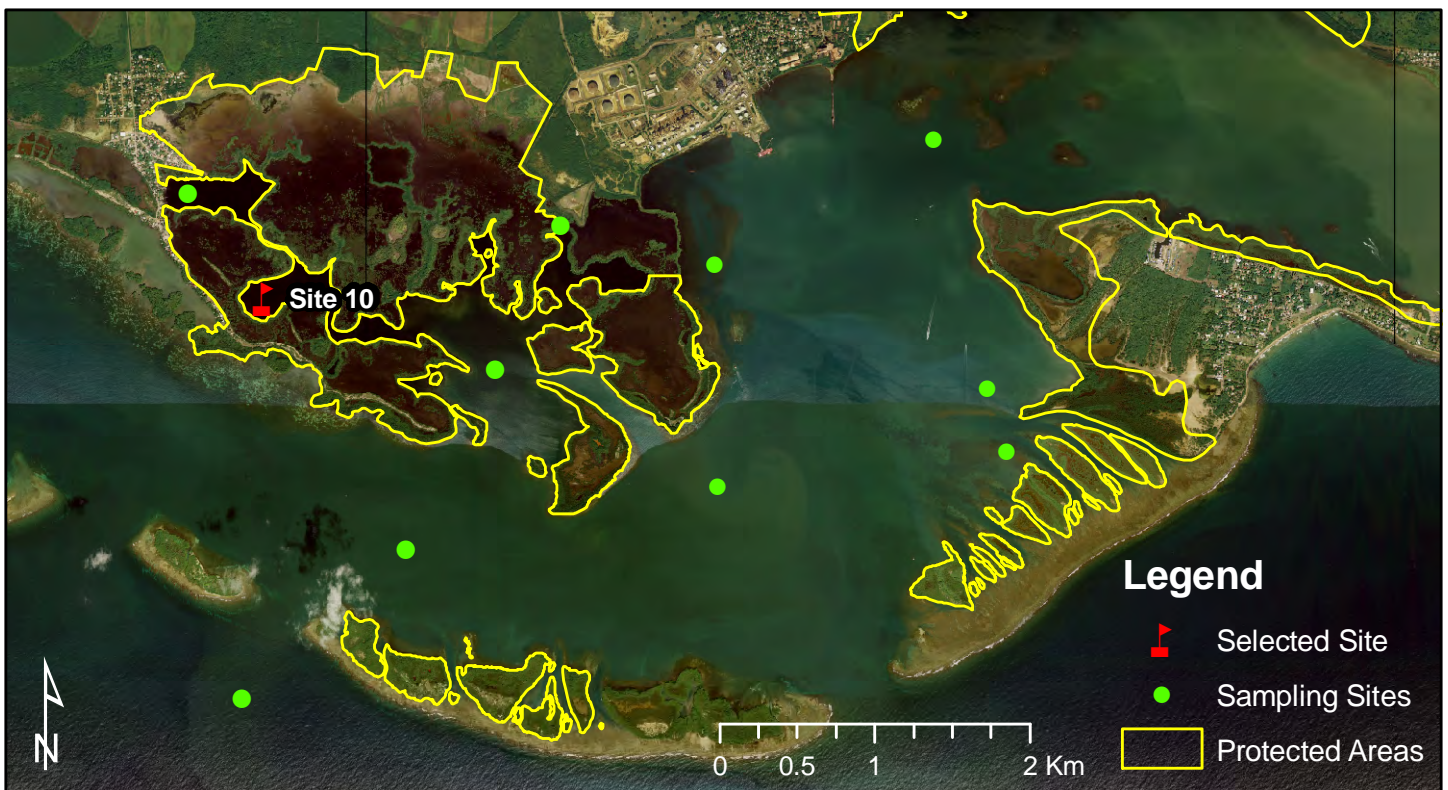
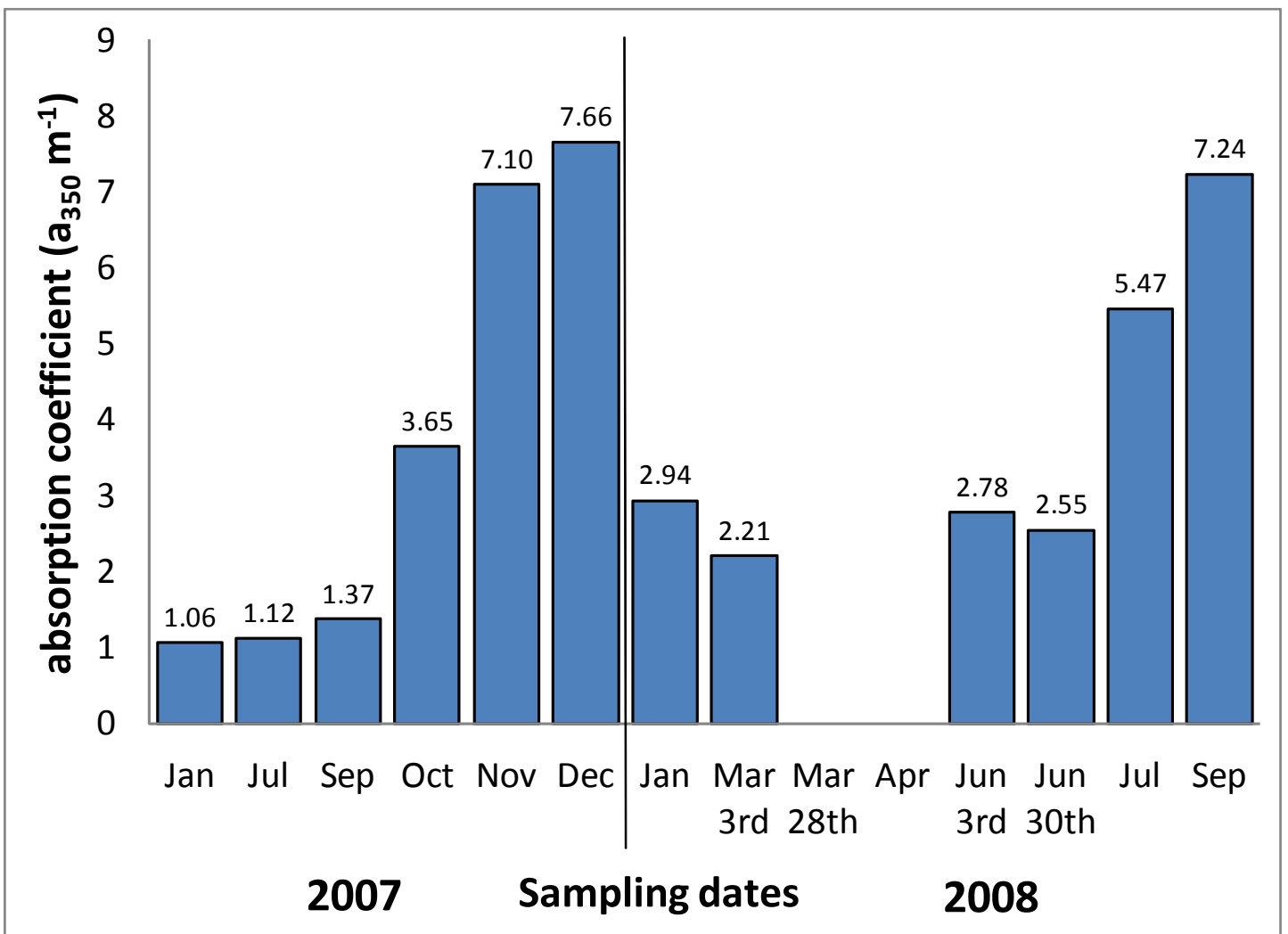


Fig. 6 Absorption coefficient of chromophoric dissolved organic matter (CDOM $a_{350} \text{ m}^{-1}$) at sampling site number 10.

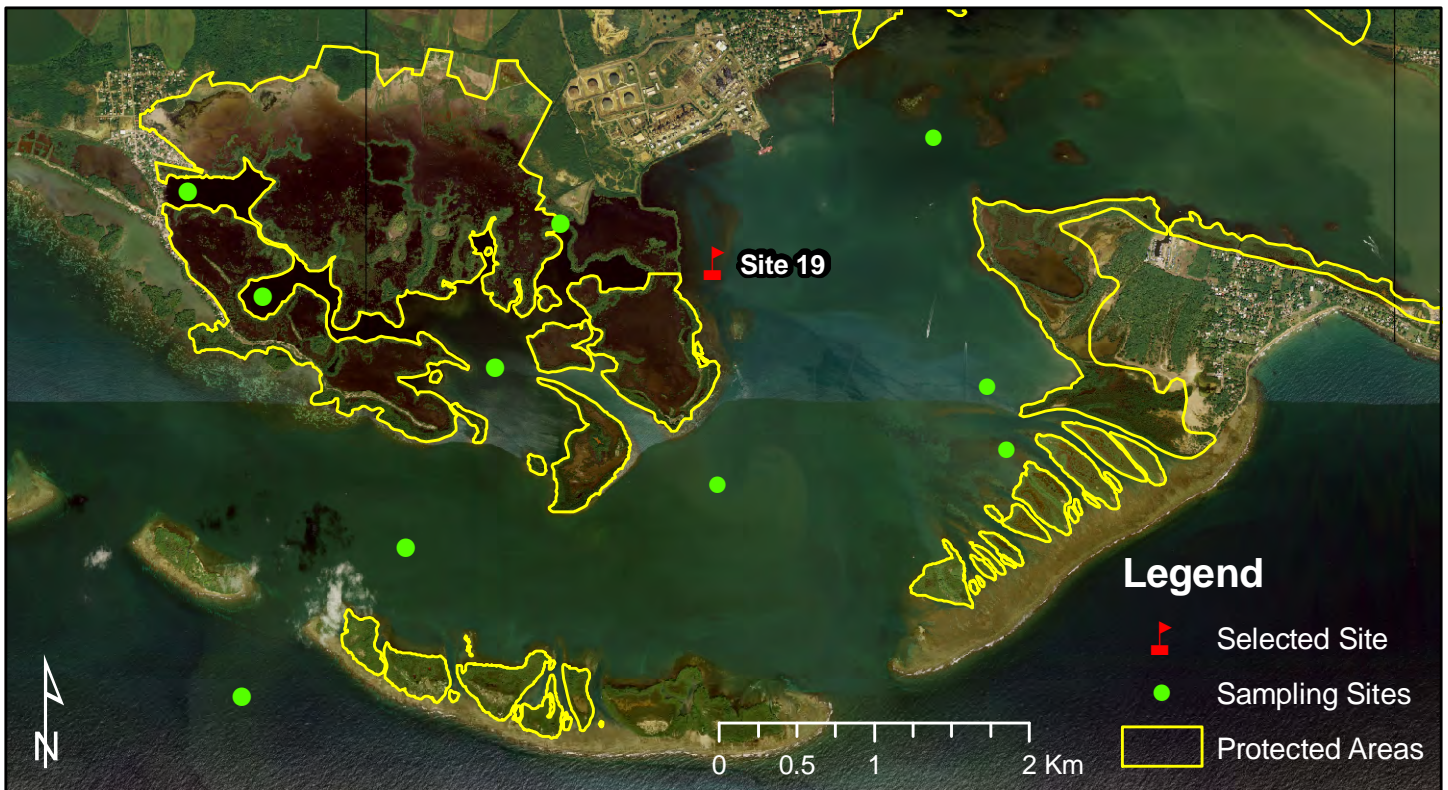
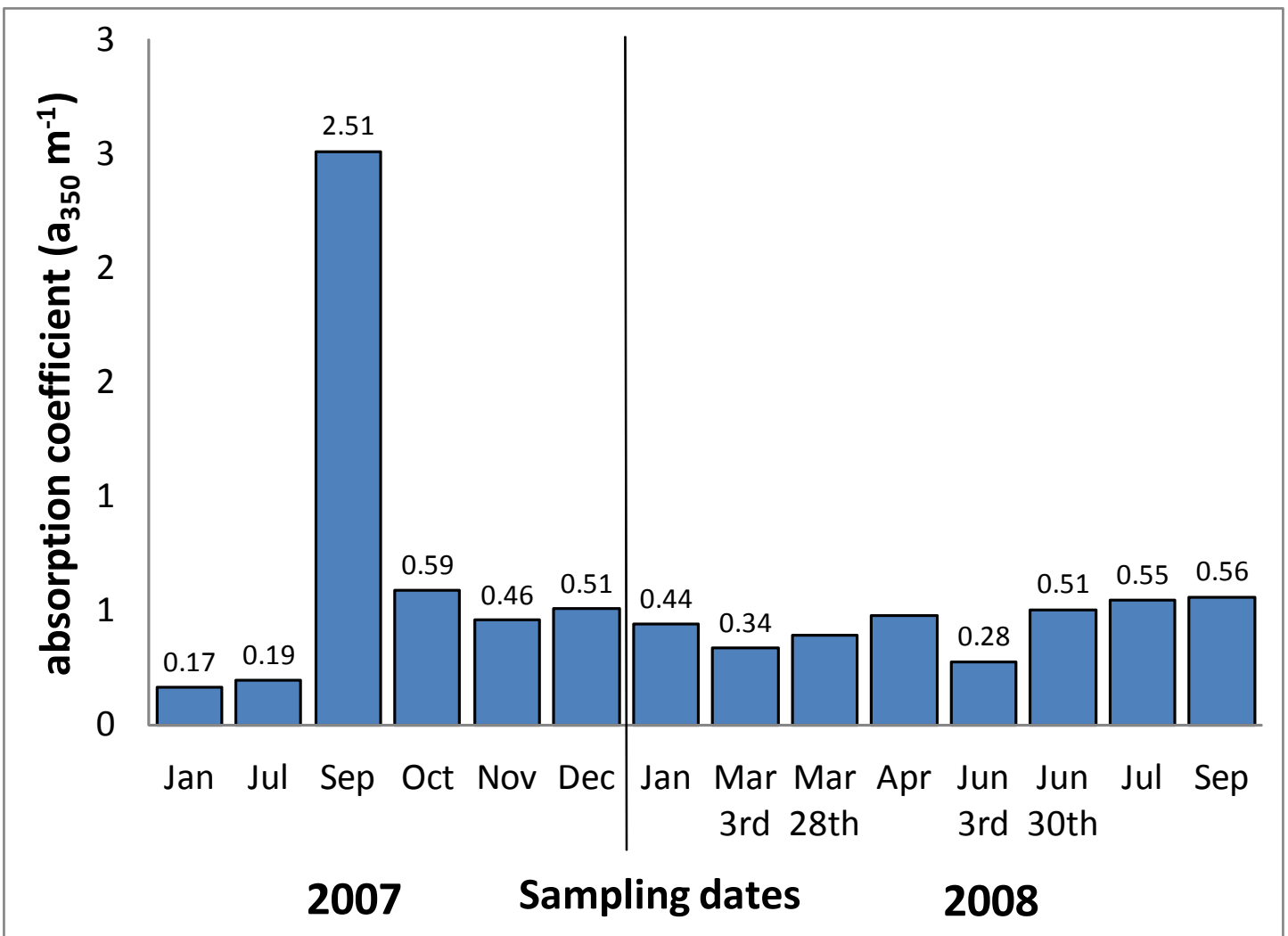


Fig. 7 Absorption coefficient of chromophoric dissolved organic matter (CDOM $a_{350} \text{ m}^{-1}$) at sampling site number 19.

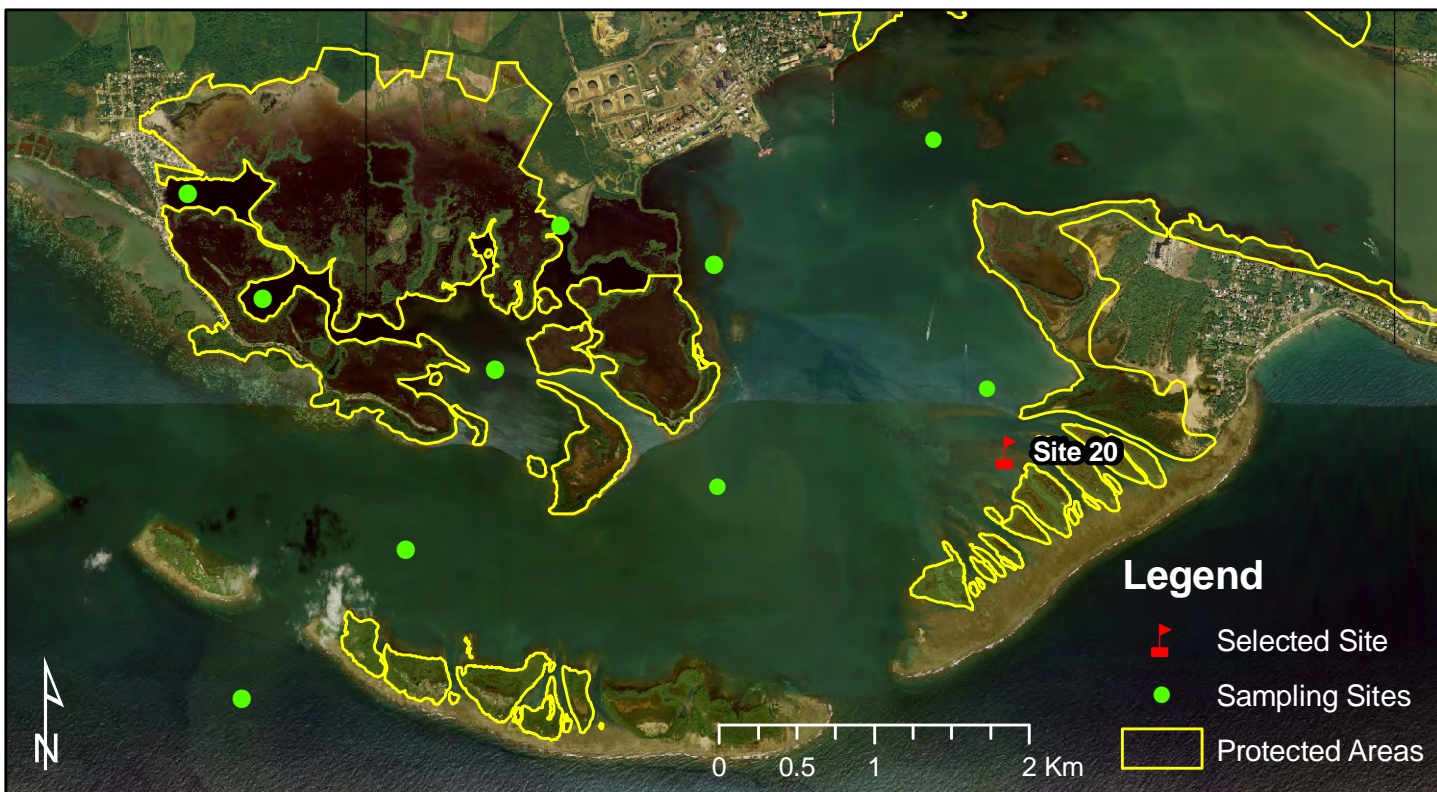
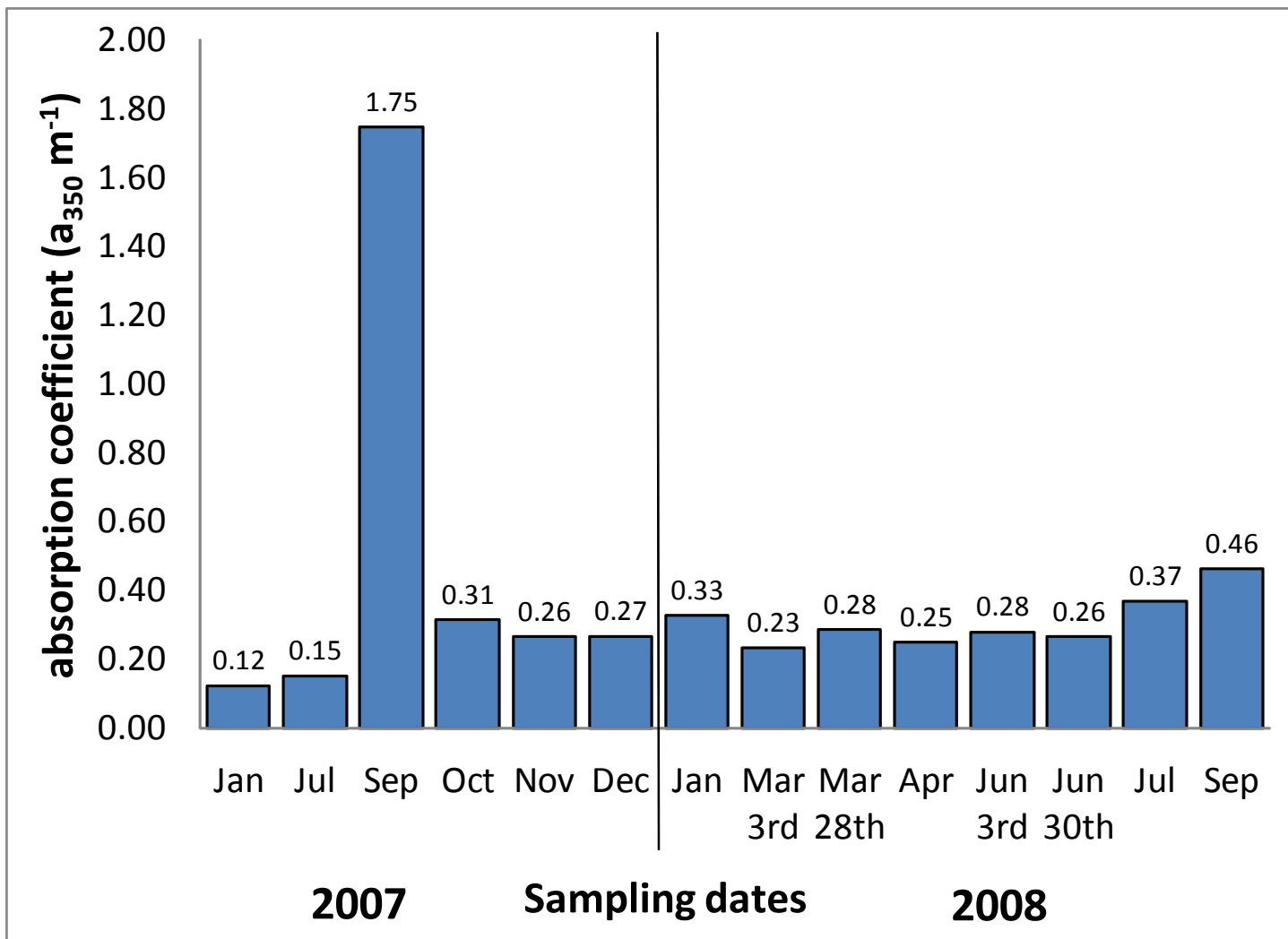


Fig. 8 Absorption coefficient of chromophoric dissolved organic matter (CDOM $a_{350} \text{ m}^{-1}$) at sampling site number 20.

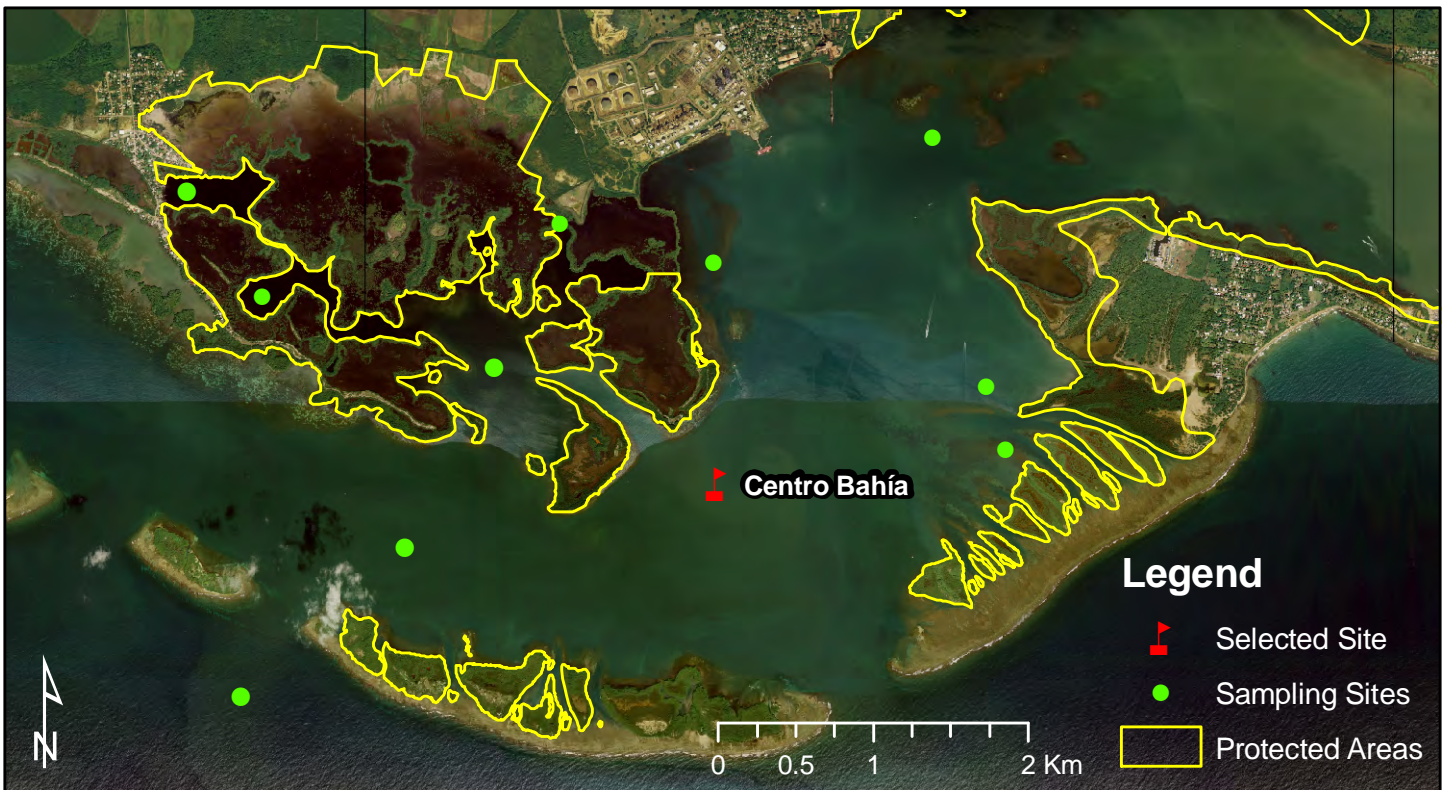
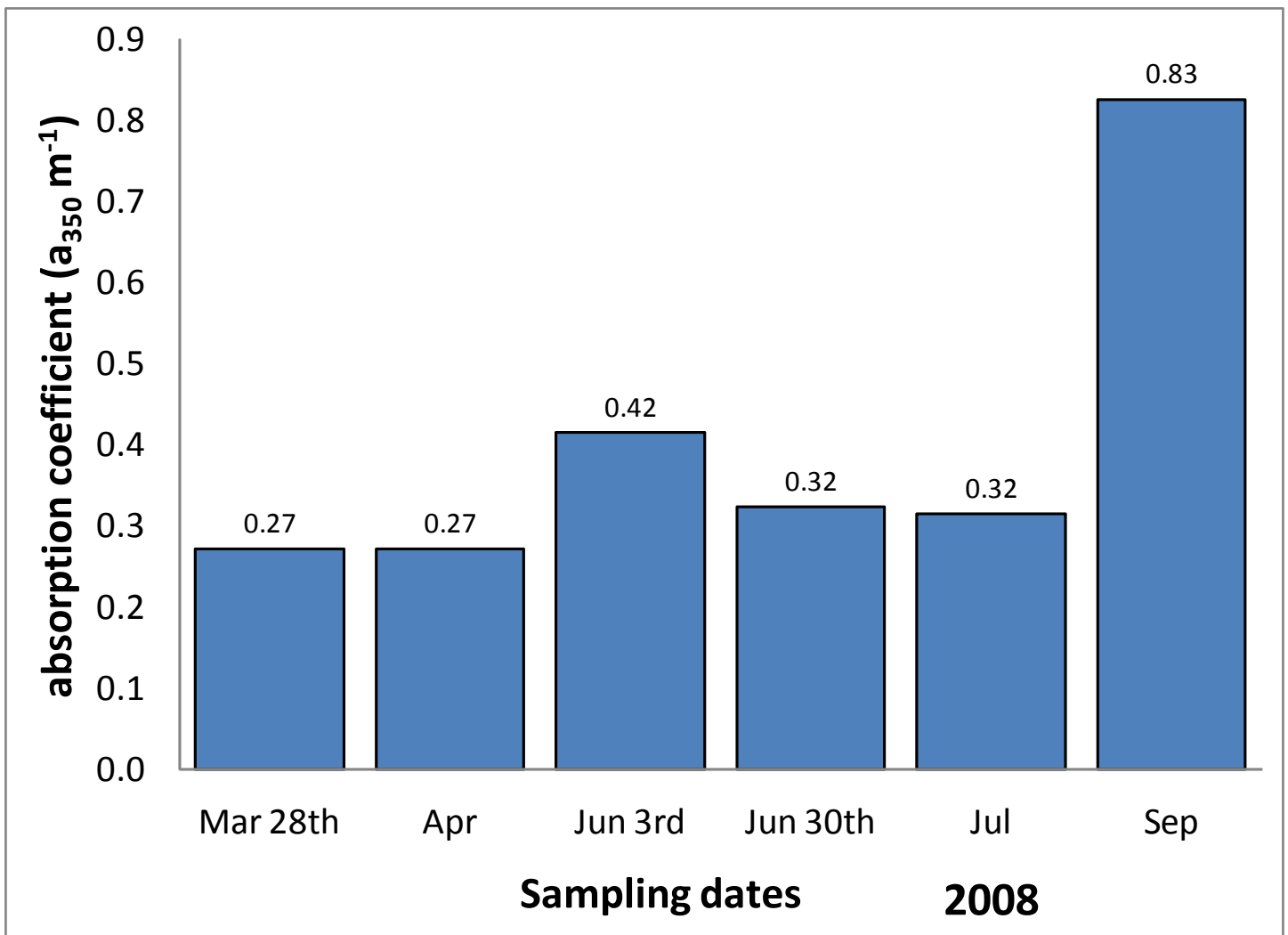


Fig. 9 Absorption coefficient of chromophoric dissolved organic matter (CDOM $a_{350} \text{ m}^{-1}$) at sampling site Centro Bahía.

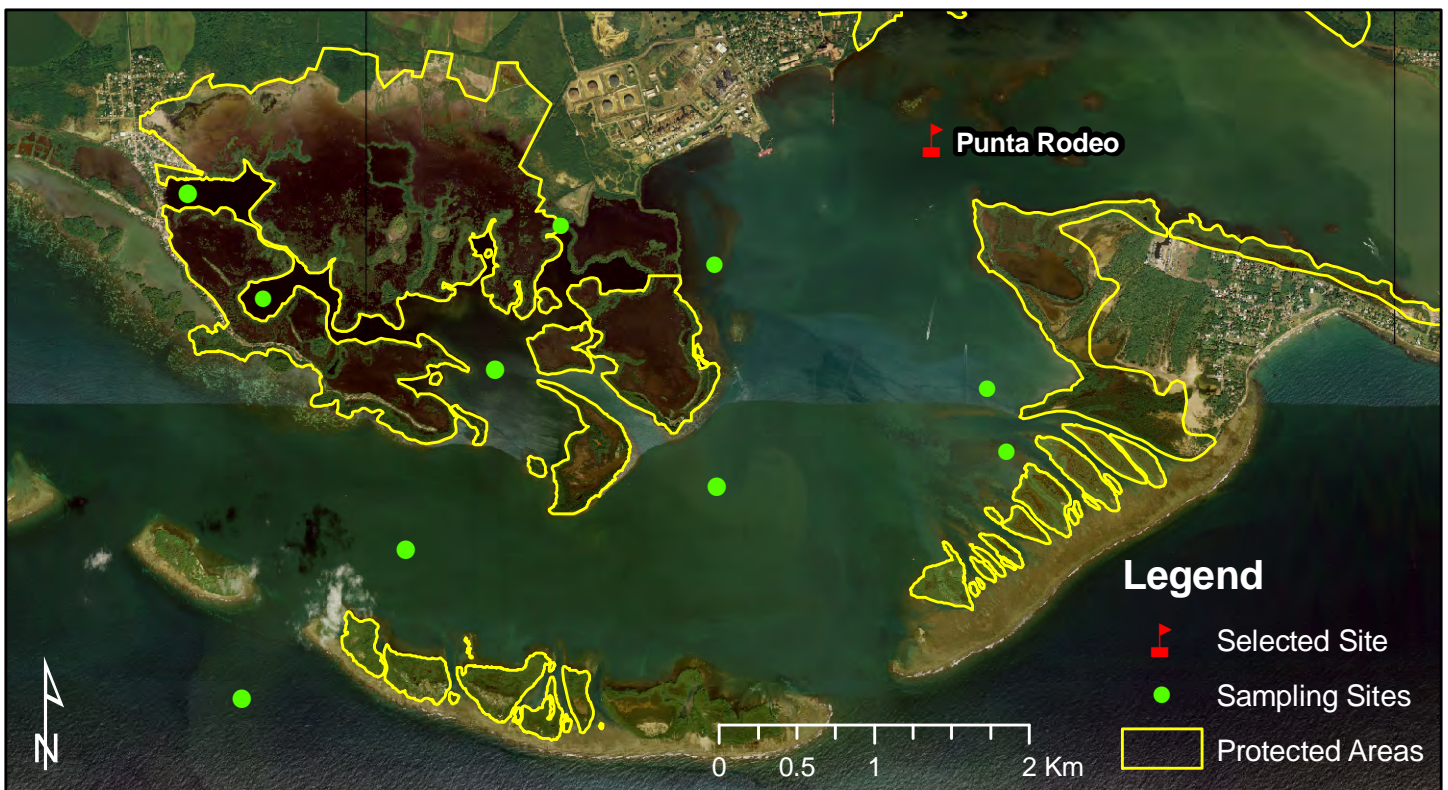
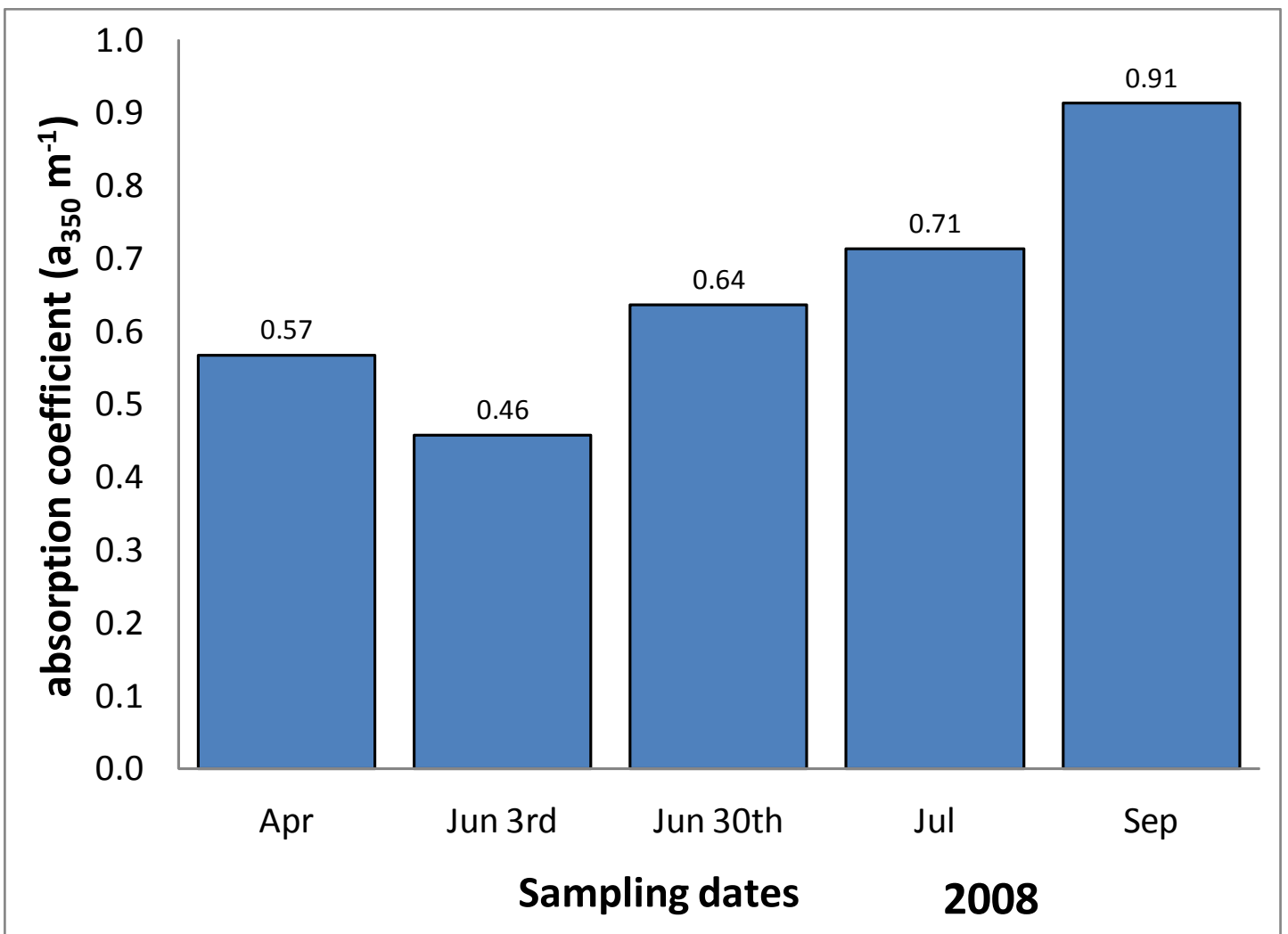


Fig. 10 Absorption coefficient of chromophoric dissolved organic matter (CDOM $a_{350} \text{ m}^{-1}$) at sampling site Punta Rodeo.

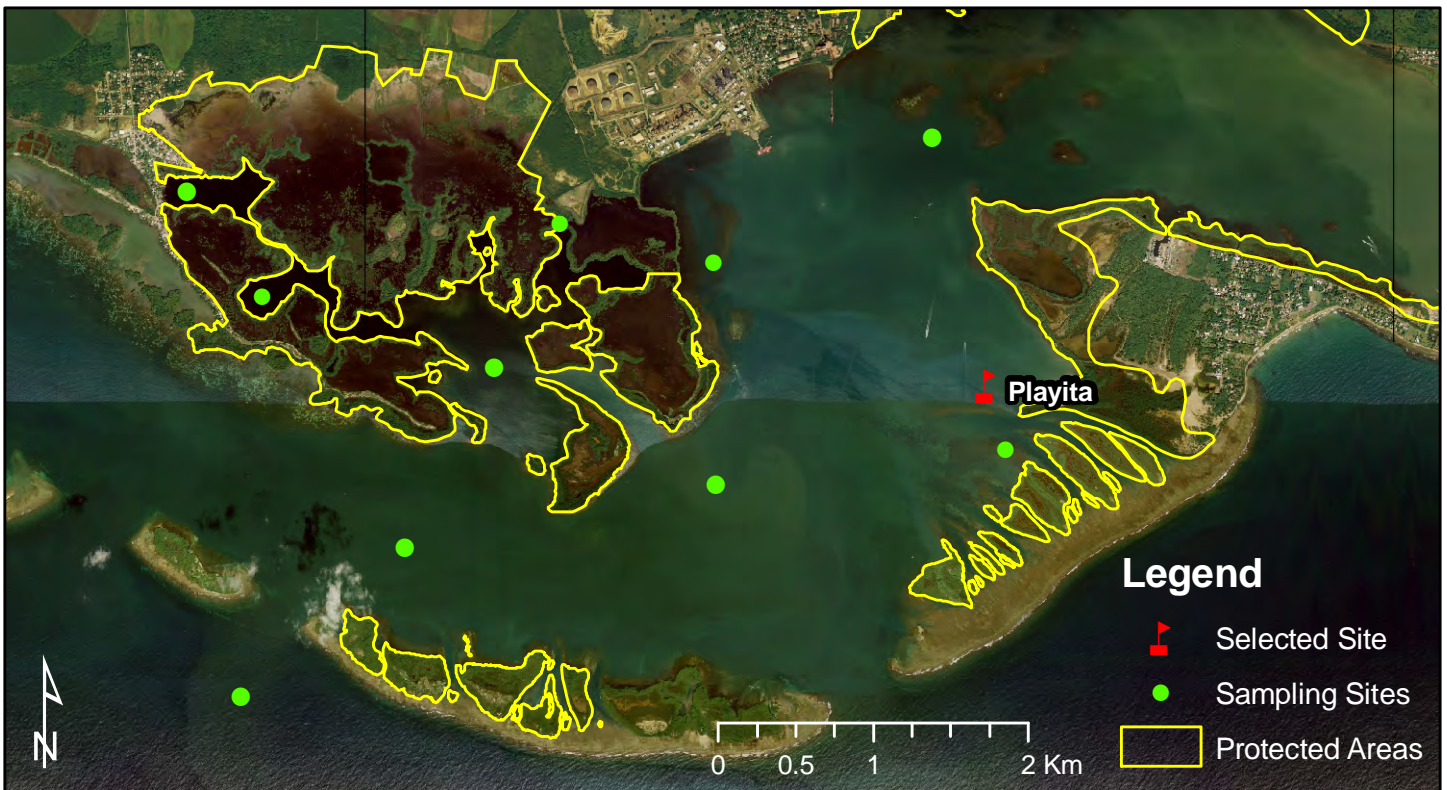
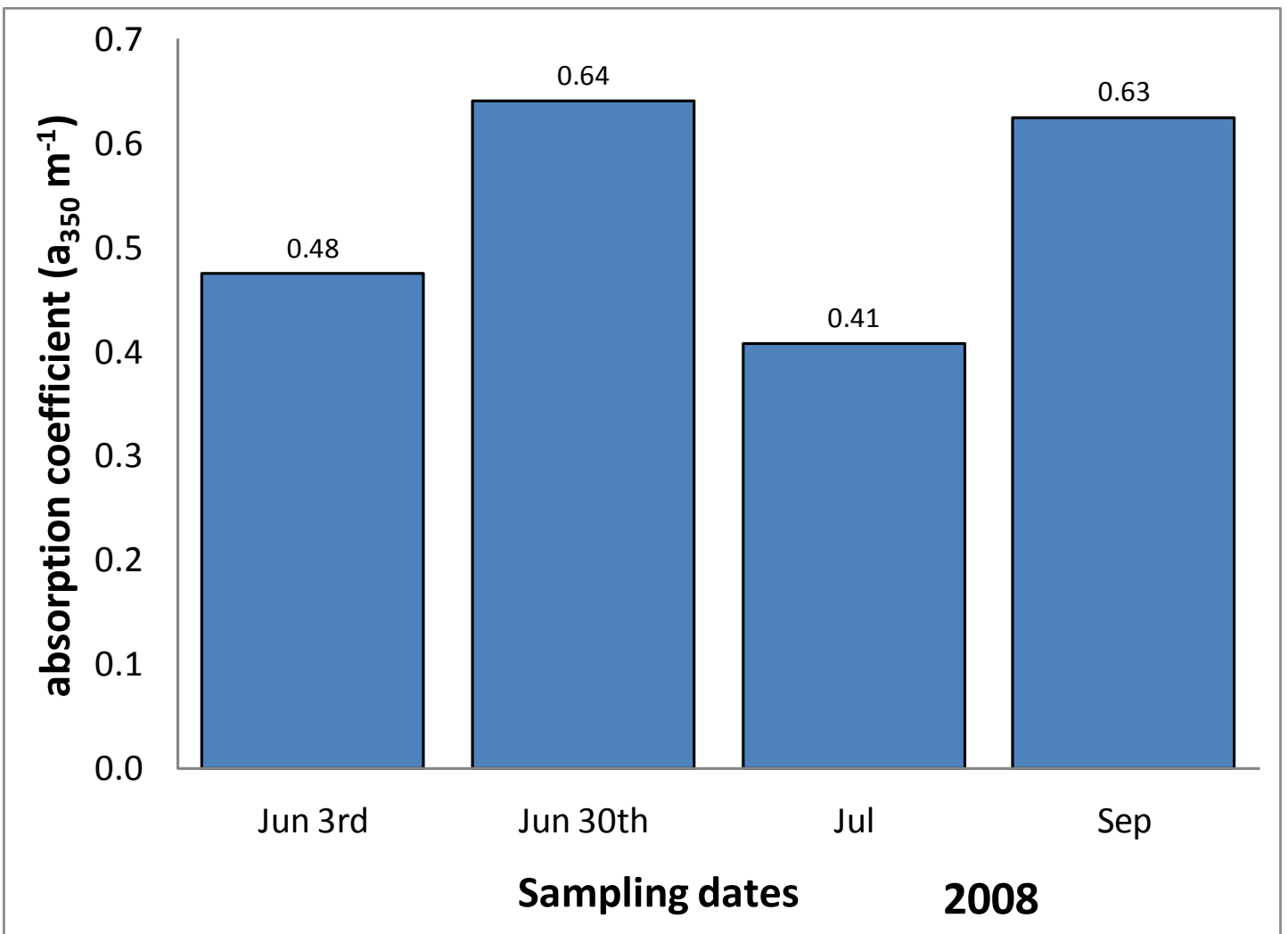


Fig. 11 Absorption coefficient of chromophoric dissolved organic matter (CDOM $a_{350} \text{ m}^{-1}$) at sampling site Playita.

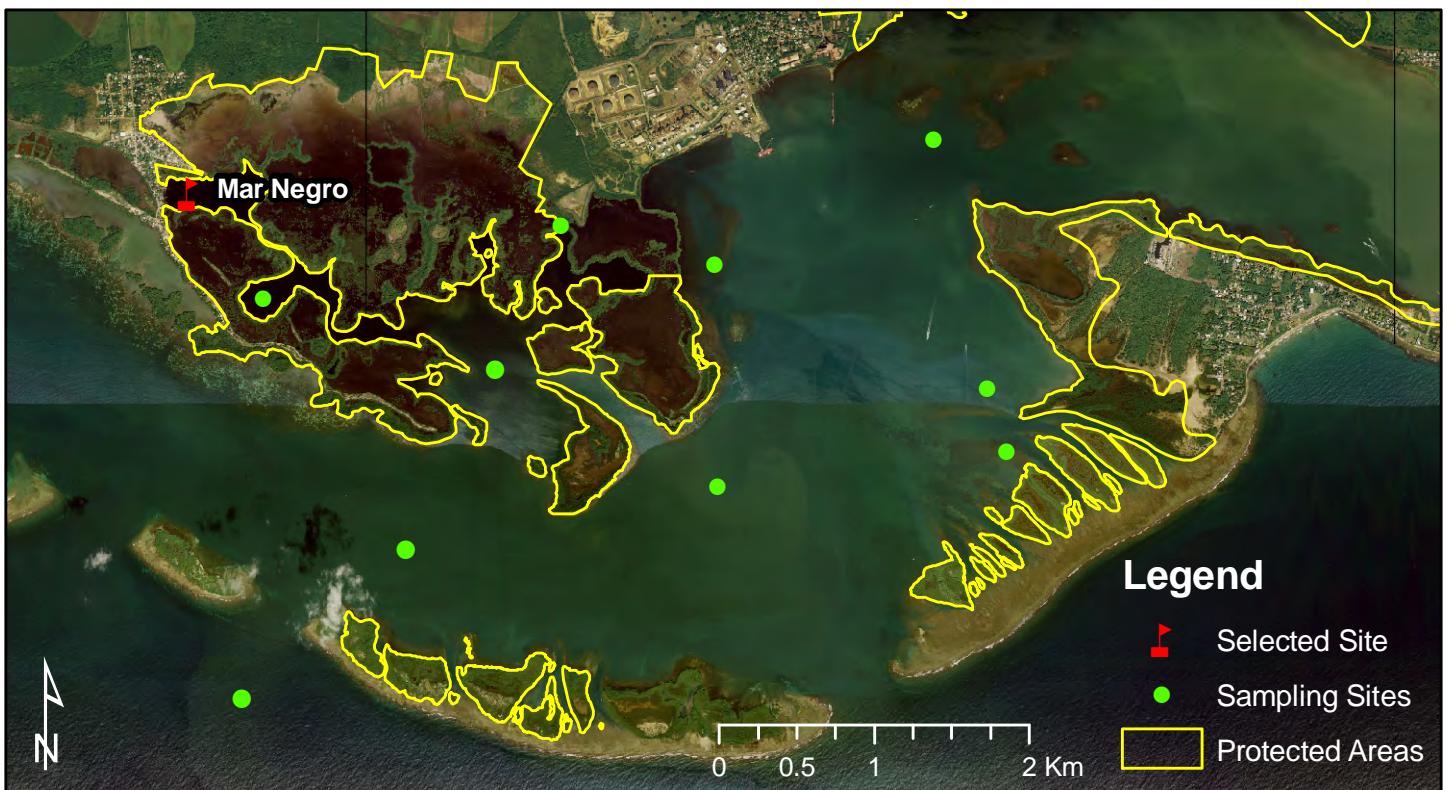
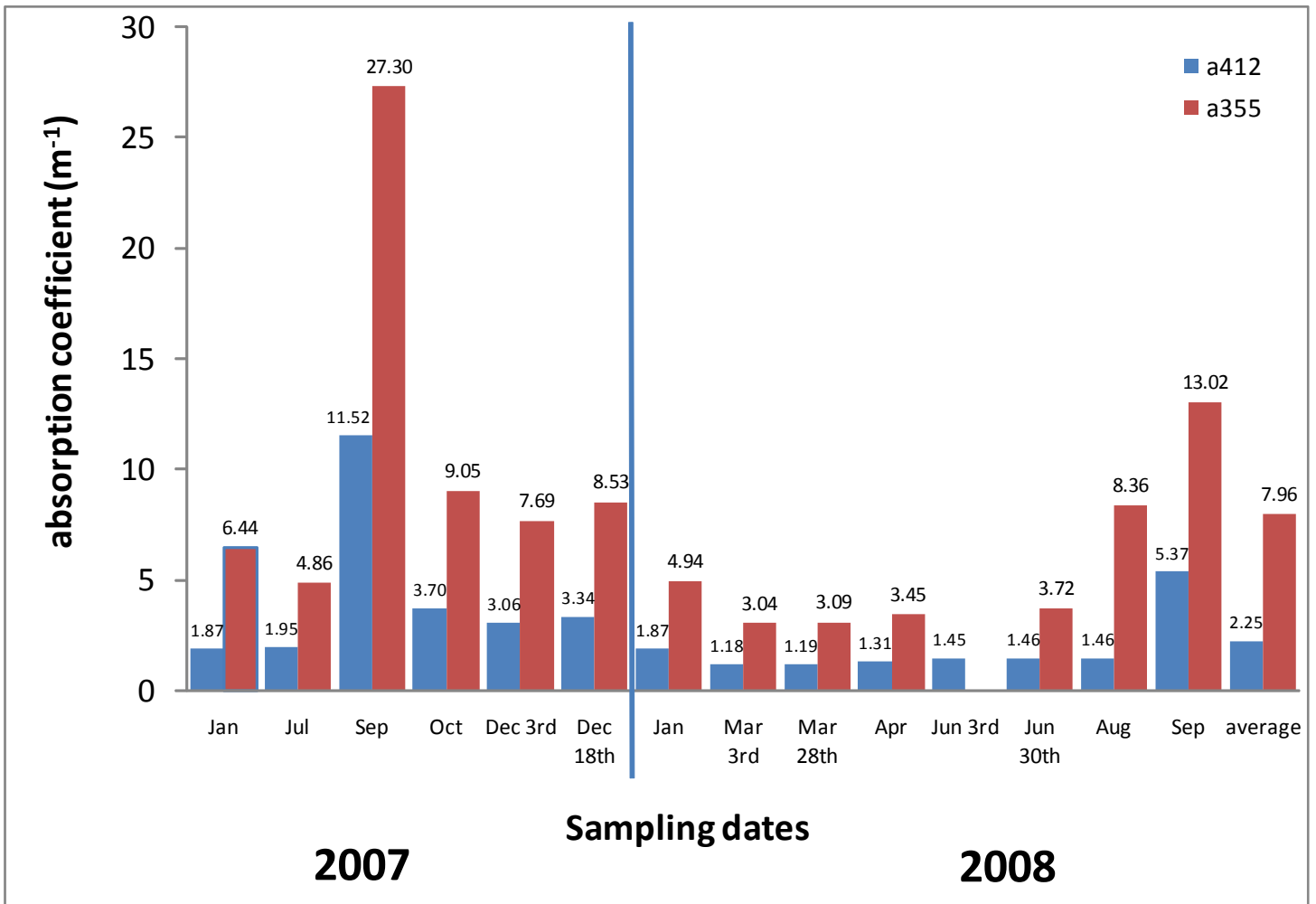


Fig. 12 Absorption coefficient of chromophoric dissolved organic matter (CDOM $a_{412} \text{ m}^{-1}$ and $a_{355} \text{ m}^{-1}$) at sampling site Mar Negro.

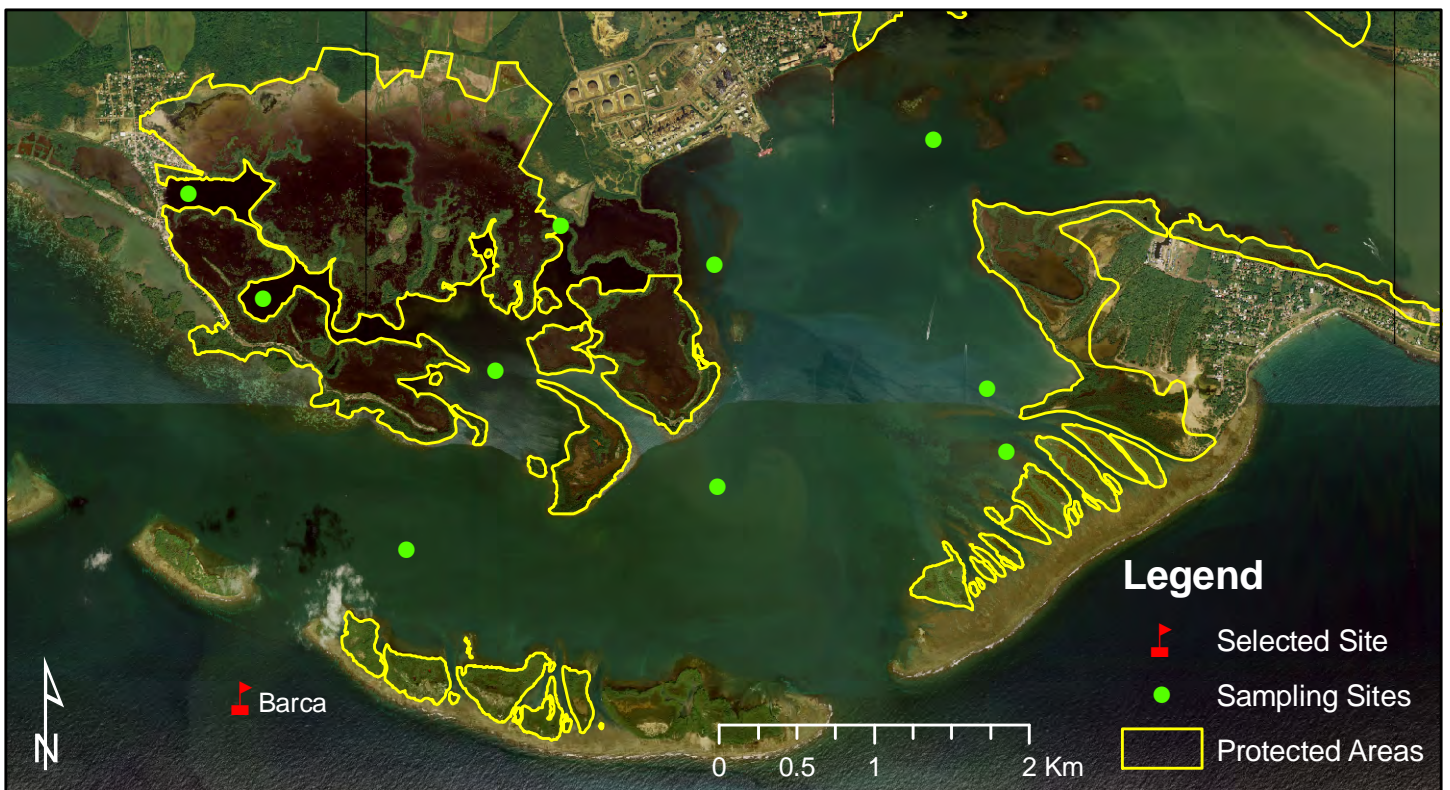
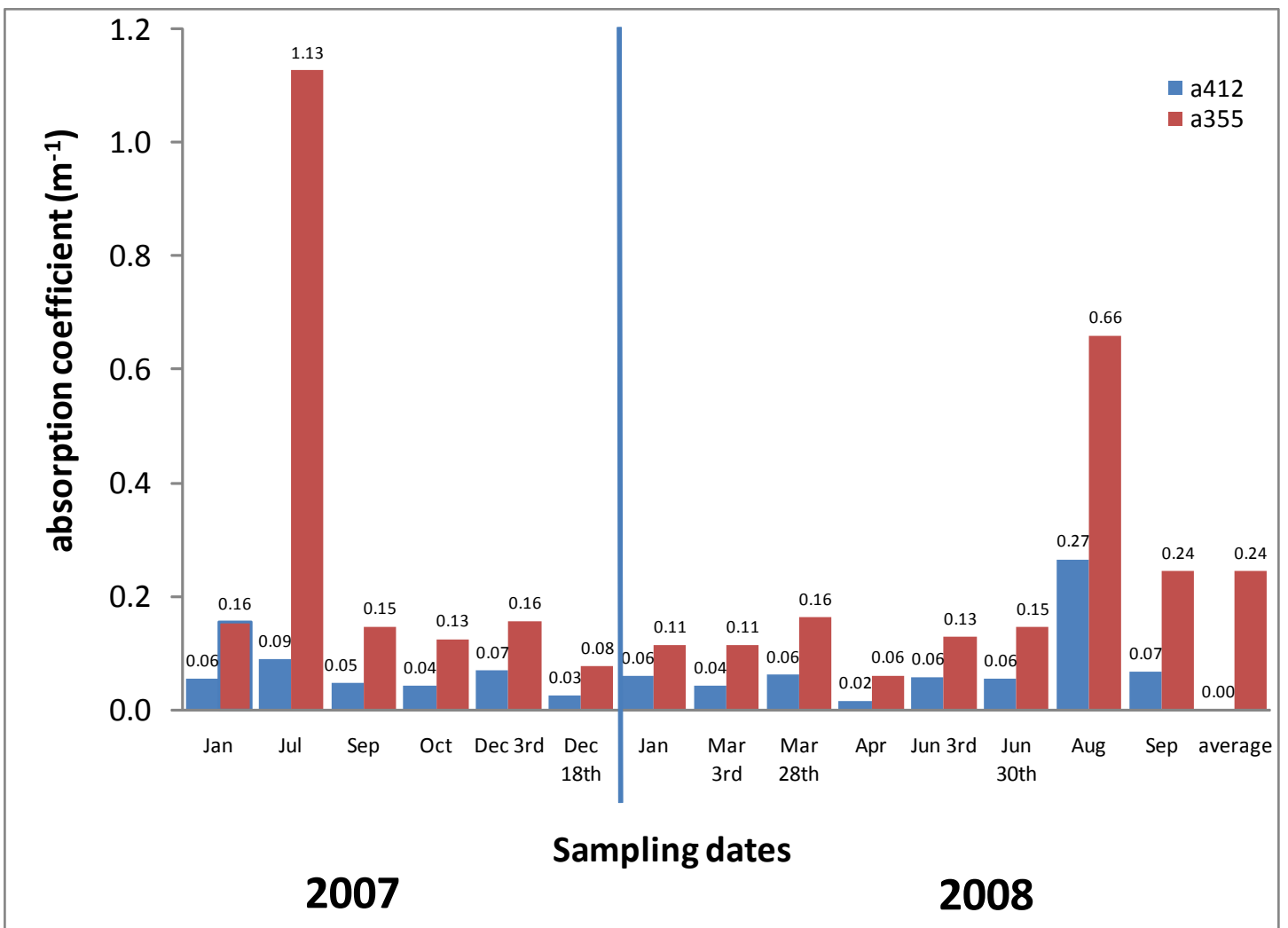


Fig. 13 Absorption coefficient of chromophoric dissolved organic matter (CDOM a_{412} m^{-1} and a_{355} m^{-1}) at sampling site Barca.

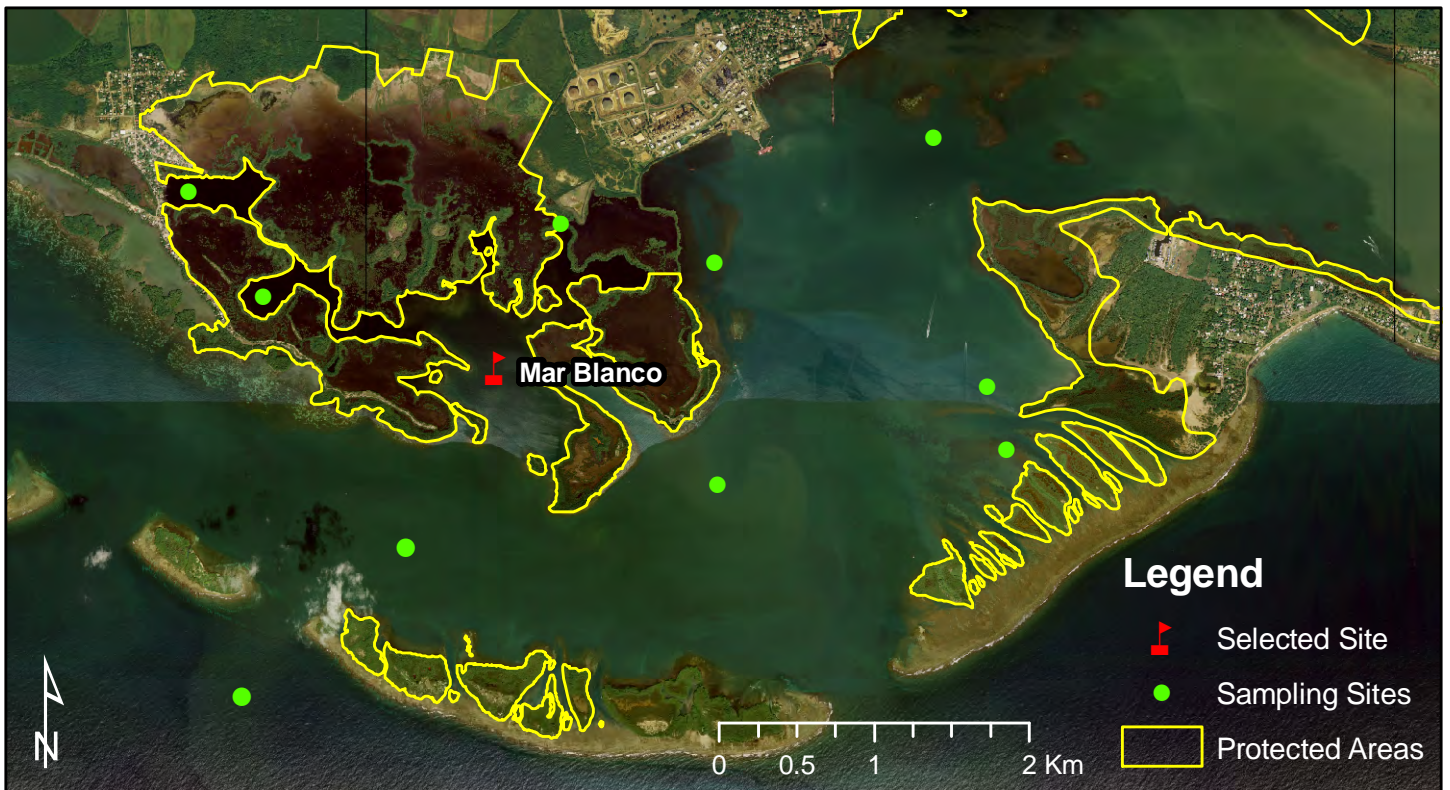
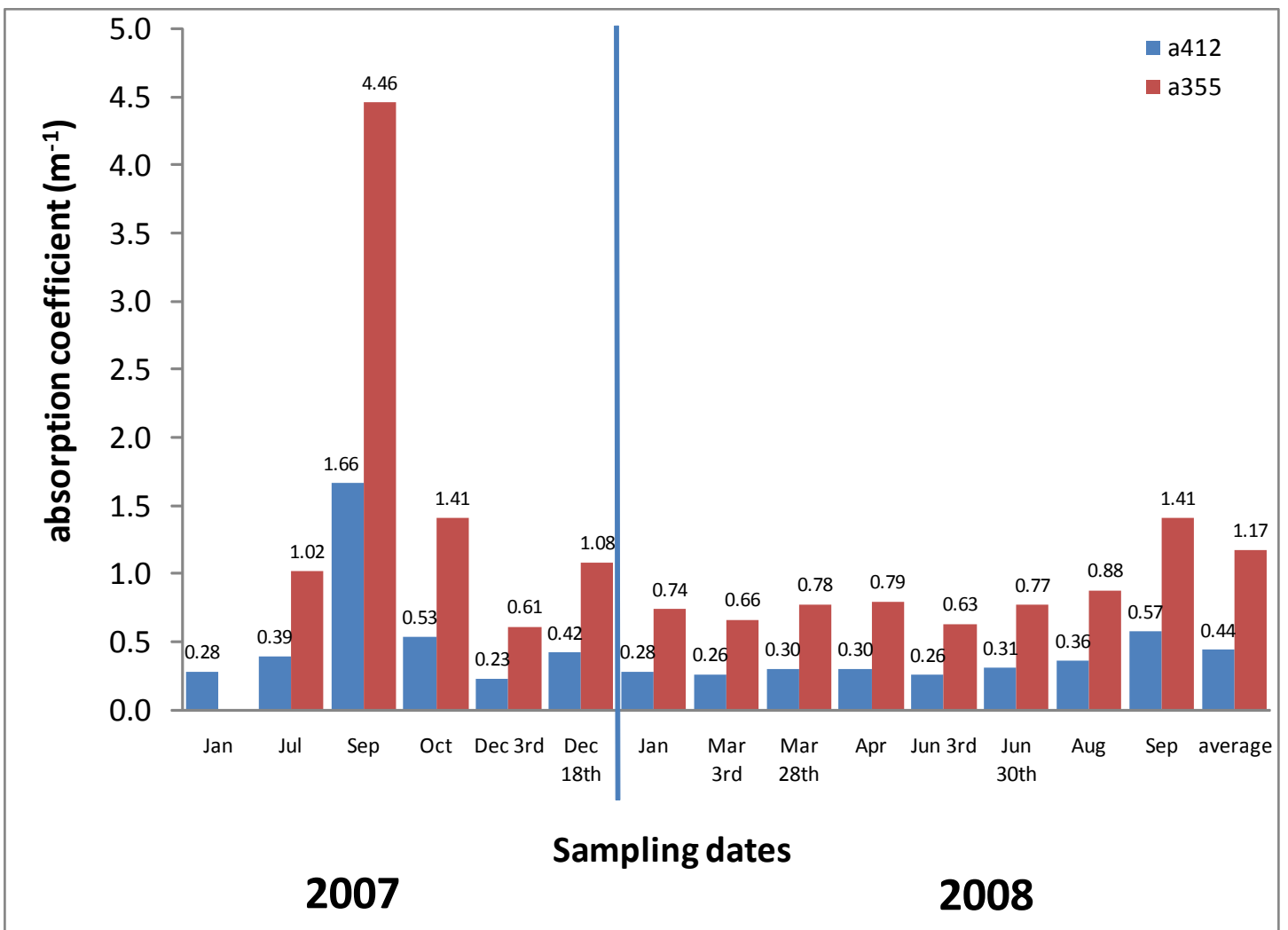


Fig. 14 Absorption coefficient of chromophoric dissolved organic matter (CDOM $a_{412} \text{ m}^{-1}$ and $a_{355} \text{ m}^{-1}$) at sampling site Mar Mar Blanco.

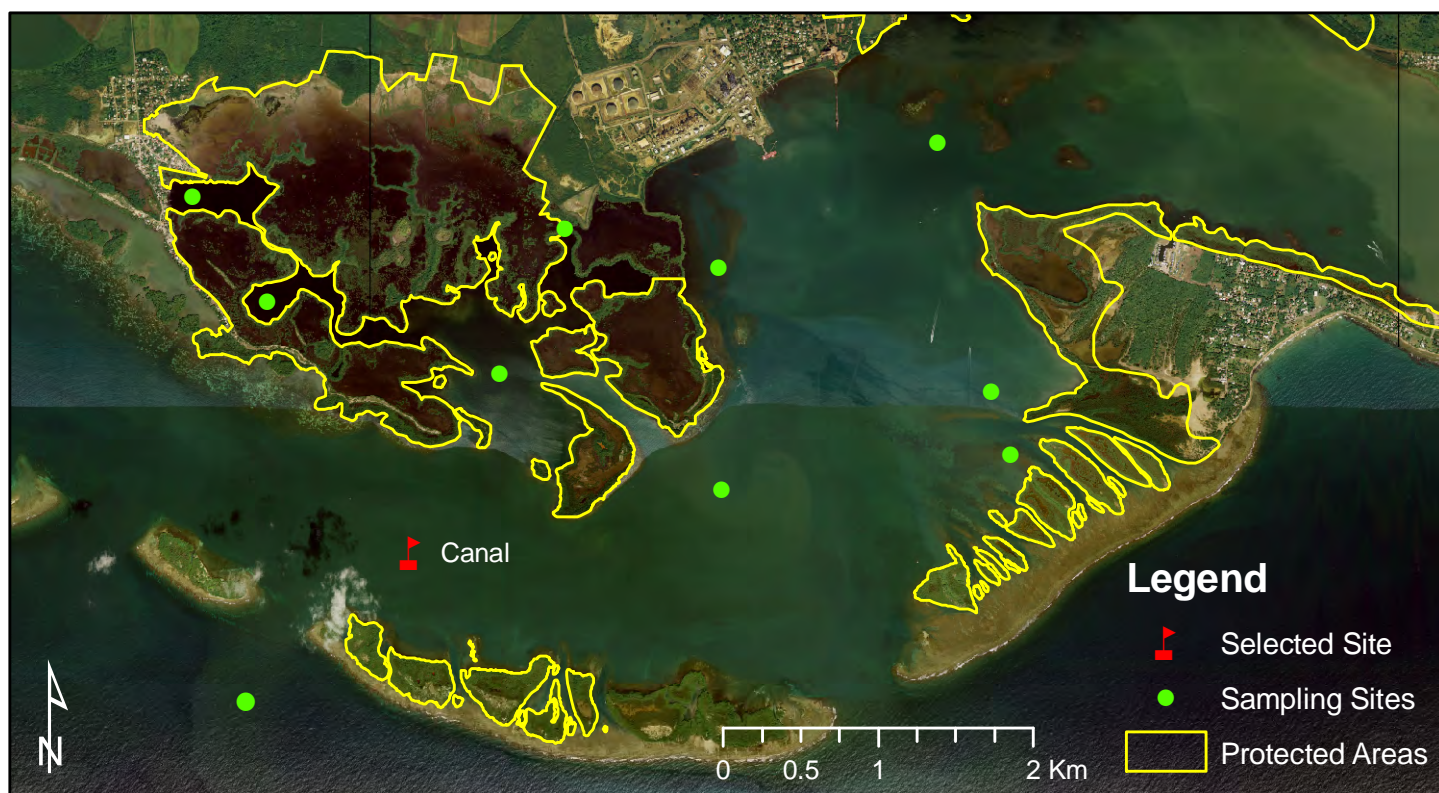
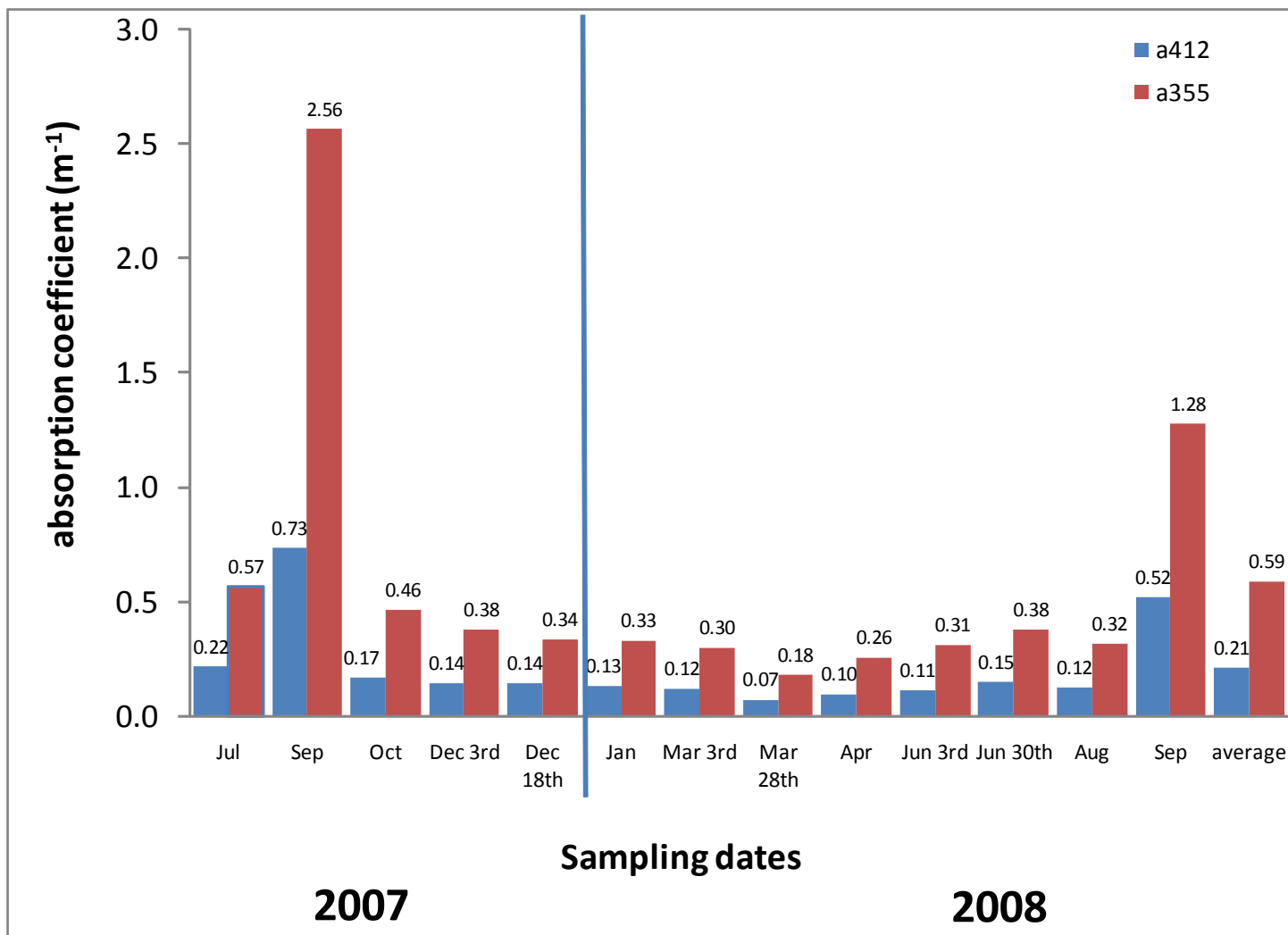


Fig. 15 Absorption coefficient of chromophoric dissolved organic matter (CDOM $a_{412} m^{-1}$ and $a_{355} m^{-1}$) at sampling site Canal.